X-320-66-353

NASA TM X-55640

THE VIBRATION RESPONSE OF AN ORBITING GEOPHYSICAL OBSERVATORY SPACECRAFT FULL-SCALE STRUCTURAL MODEL TO A SIMULATED LAUNCH ACOUSTIC ENVIRONMENT

AUGUST 1966

GODDARD SPACE FLIGHT CENTER

GREENBELT, MD.

X-320-66-353

THE VIBRATION RESPONSE OF AN ORBITING GEOPHYSICAL OBSERVATORY SPACECRAFT FULL-SCALE STRUCTURAL MODEL TO A SIMULATED LAUNCH ACOUSTIC ENVIRONMENT

By

Paul J. Alfonsi
Test and Evaluation Division
Systems Reliability Directorate

August 1966

GODDARD SPACE FLIGHT CENTER
Greenbelt, Maryland

THE VIBRATION RESPONSE OF AN ORBITING GEOPHYSICAL OBSERVATORY SPACECRAFT FULL-SCALE STRUCTURAL MODEL TO A SIMULATED LAUNCH ACOUSTIC ENVIRONMENT

Prepared by: Paul J. Alfonsi
Structural Dynamics Branch
Test and Evaluation Division

Reviewed by: William R. Forlifer
Assistant Head, Structural Dynamics Branch

Approved by: John H. Boeckel
Associate Chief, Test and Evaluation Division

TEST PROGRAM STATUS

This is the final report on the Orbiting Geophysical Observatory Structural Model acoustic test program; this report presents analysis of all acquired data.

Authorization
Test and Evaluation Division Charge No.: 321-S-70-04

THE VIBRATION RESPONSE OF AN ORBITING GEOPHYSICAL OBSERVATORY SPACECRAFT FULL-SCALE STRUCTURAL MODEL TO A SIMULATED LAUNCH ACOUSTIC ENVIRONMENT

by

Paul J. Alfonsi
Goddard Space Flight Center

SUMMARY

The Orbiting Geophysical Observatory (OGO) acoustic test was accomplished during the period from January through March of 1964 at Langley Research Center, Virginia. In essence, the test item was an assemblage of a full-scale structural model of the OGO spacecraft, a flight-type shroud, and the forward equipment rack portion of an Agena B vehicle. The test article was subjected to a simulated launch acoustic environment which was generated by the Langley 9 × 6 thermal structures wind tunnel. Vibration transducers were attached at pertinent locations on the spacecraft and adjacent structure, and the responses resulting from acoustic excitation were recorded on magnetic tape. Tape recordings were also made of microphone data pertinent to the acoustic environment. A total of 205 channels of data was acquired.

This report presents a detailed discussion of the test program and a detailed analysis of all acquired data.

CONTENTS

THE VIBRATION RESPONSE OF AN ORBITING GEOPHYSICAL OBSERVATORY SPACECRAFT FULL-SCALE STRUCTURAL MODEL TO A SIMULATED LAUNCH ACOUSTIC ENVIRONMENT

by

Paul J. Alfonsi
Goddard Space Flight Center

1. INTRODUCTION

The Orbiting Geophysical Observatory (OGO), Figure 1, was developed as part of a step-by-step science program to gain further knowledge of the earth and its environment so that optimum exploration of the universe can be accomplished. The OGO versatility as an observatory-type spacecraft allows it to be launched from several different boosters and to accommodate up to 50 different experiments on each mission.

The main body of the OGO spacecraft is a box-like structure approximately $3 \times 3 \times 6$ feet with projecting panels, gas jets, antennas, and experiments. Two sides of the main body are hinged to provide interior access as shown in Figure 2. Scientific experiments are mounted on the inside of these doors and on extendible booms with subsystems mounted on shelves and walls within the structure. Electrical power is supplied by a pair of large solar panels. Coarse orientation is achieved by cold gas jets and fine positioning by means of a set of reaction wheels. For geophysical missions, the spacecraft carries a number of external experiment packages. Experiments of high sensitivity or special orientation angle requirements are mounted on booms projecting from the spacecraft box. Solar-oriented experiments are located on each solar paddle while orbit plane experiments are continuously oriented parallel to the orbital plane. Figure 3 shows the spacecraft launch configuration.

During the launch phase, a spacecraft is subjected to random vibration with a broad frequency spectrum from about 5 cps to more than 10 kc. The source of this input is complex, resulting from a combination of effects such as: wind gust loading, booster engine vibrations, rocket engine noise at launch, and aerodynamic turbulence occurring during the region of transonic flight and maximum dynamic pressure. The lower frequency environment (up to about 250 cps) is the result of both launch vehicle modal excitation, structurally coupled to the spacecraft, and acoustic excitation of the spacecraft and adjacent structure.

Higher frequency vibration is generated by the engine and its components. However, most of this energy is attenuated by the mechanical filtering characteristics of the vehicle structure and, therefore, is not present at the spacecraft mounting interface. The primary cause of high-frequency (above 250 cps) vibration input to the spacecraft is direct acoustic excitation of the spacecraft and adjacent structure. Presently, there are no proven analytical methods for determining the coupling effects and response of a complex structure which is subjected to random acoustic loading.

The major objective of the test program was to experimentally determine the spectra and levels of vibration in the OGO spacecraft, resulting from a simulated launch acoustic environment. Another objective was to obtain shroud transmission loss characteristics on which the amount of acoustic energy directly impinging upon the spacecraft is dependent.

This report presents a description of the test program and a detailed analysis of all data acquired during the test. Appendix A presents data channel allocations, type and location of transducers, and overall rms response of vibration channels. Appendix B contains a power spectral density analysis of all vibration data.

2. DISCUSSION

ACOUSTIC ENVIRONMENT

The acoustic environment to which a spacecraft is subjected at launch is best described as a "hemispheric free field." The sound field is hemispheric rather than spherical, due to the bounding effect of the ground surface. Prior to the selection of a test site for the OGO assemblage, a number of acoustic test facilities was investigated. The large size of the test specimen (approximately 5 feet in diameter and 22 feet long) and the desired "hemispheric free field" acoustic conditions eliminated most operational facilities and, therefore, dictated a choice of the sound field produced by the Langley Research Center's (LRC) 9- × 6-foot thermal-structures tunnel.

The 9- × 6-foot thermal-structures tunnel (Figure 4) is a "blowdown" facility. Air, contained at high pressures in large storage vessels, is released or "blown down" to a lower pressure at which it is used. The air passes through a heat exchanger that is capable of raising the stagnation temperature to 1120°R; then through a supersonic nozzle into a test section where structural models are normally located. The air then passes through a diffuser section and is exhausted into the atmosphere at supersonic velocities. The tunnel run time is limited by the air storage volume to a maximum of about 45 seconds. The run time is further dependent upon the operating temperature requirements.

The LRC 9×6 tunnel exhaust jet develops an equivalent thrust of 475,000 pounds and radiates acoustic power in excess of 3 million acoustic watts (reference 1). The large amount of acoustic power radiated and the natural "hemispheric free field" characteristics of the sound field made it a very suitable test area for the OGO acoustic test. The facility had been previously used for acoustic testing of large specimens, including the Mercury Spaceflight Capsule (reference 2); therefore, data pertinent to sound field characteristics were available. In addition, a study of the near and far sound field characteristics had been performed and results published in reference 3.

The intensity and spectral content of the 9 × 6 tunnel sound field can be varied to some extent by adjustments of the operating parameters of the tunnel. Further, a particular set of test conditions may be achieved by suitable placement of the specimen within the sound field. The sound field is projected over a large unobstructed area which provides a natural dissipation of the sound and a variation with location of the levels and spectra.

For the OGO acoustic test, LRC personnel used data from previous tunnel runs to select a general location for the test article and then performed additional surveys within this area. An analysis of this survey data revealed a location where the acoustic conditions satisfied the required levels (within specified tolerances).

It was further desired to simulate the condition of "wave coincidence" in the Agena skin surfaces, allowing maximum transmission of acoustic energy. The coincidence frequency was calculated to be 1000 cps with a 90-degree angle of incidence (usually referred to as grazing incidence). To establish this condition, it was necessary to determine the location of the "apparent source" of the energy in the 1000-cps region. In a jet, where turbulent mixing of gases occur, noise is generated by the shearing action of high-velocity gases with respect to the quiescent surrounding atmosphere. The higher frequency spectra are generated in the proximity of the exhaust nozzle while lower frequency energy is developed several diameters downstream. A survey was performed at the determined test location using a directional microphone mounted on a turntable. The microphone response and angular location were recorded on magnetic tape during a tunnel blowdown. The data were then analyzed using a 200-cps-bandwidth filter with a center frequency of 1000 cps, and the response versus angular displacement was plotted. The angle at which the maximum response was generated was determined, providing the azimuth to the "apparent 1000-cps source." The test assemblage was oriented along this azimuth.

The test specifications presented in Table 1 were derived from predicted and launch data from booster vehicles similar to those planned for OGO flights.

The spectrum reflected an increase in the high-frequency spectra level to encompass both the launch and maximum dynamic pressure conditions.

The specified exposure time was 3 minutes. Naturally, because of the "blow-down" operation of the wind tunnel, continuous test runs of this duration are not possible. It was therefore decided to accrue the required exposure time by means of six 30-second runs.

A "high-level" exposure of 153-db overall sound pressure level with the same spectral distribution (as the previous runs) was planned to obtain data on the linearity of the vibration response. The high-level runs also simulated the environment anticipated from a thrust-augmented-type booster vehicle. The duration of the high-level run was 30 seconds.

TEST SPECIMEN

Several configurations of the OGO spacecraft and adjacent structure were considered in an effort to select one providing the most realistic dynamic characteristics. The resulting configuration was an assembly of the structural model of the OGO spacecraft, a ballasted Agena forward equipment rack, and a flight-type shroud.

The OGO structural model was complete with mockup appendages, solar paddles, and mass/center of gravity models of interior equipments. A total of six solar cell modules, each containing 112 cells, were attached to the solar paddles at locations of anticipated maximum deflection or acceleration. The modules were not flight acceptable and were included only as a minor objective to determine possible gross damage. Flight-type interstage fittings and a Marmon-type band were used to attach the structural model to the Agena forward equipment rack section.

The forward equipment rack is the upper portion of the Agena vehicle above the tank section. It is a section about 4 feet long and contains a truss network on which the guidance and control equipments are mounted. The interstage fittings or trusses are attached directly to the top of the forward equipment rack as is the shroud attachment ring. Mass and center-of-gravity mockups of all major internal equipments were attached at appropriate locations within the Agena section.

Since the planned flight vehicles are approximately 90 feet long and provide considerable attenuation to flanking acoustic transmission, a suitable closure was required for the aft end of the Agena section. Naturally, to establish realistic simulation conditions, the aft closure structure was required to provide

about the same attenuation characteristics as the omitted portion of the booster structure. The average transmission loss of the closure plate was specified to be at least 35 db with no less than 30 db at 250 cps. (These decibel (db) notations are re: 0.0002 microbar, as are all others within this report.) A "sandwich construction" panel of sand between 1/4-inch steel plates spaced 1 inch apart was selected. Due to the panel's high damping and surface density, an average transmission loss of 44 db (calculated) and approximately 48-db transmission loss (calculated) at 250 cps was provided.

A flight-type shroud with appropriate thermal insulation was included as a part of the test assembly to provide realistic attenuation of the acoustic environment. Shroud-handling restrictions, in addition to handling and buildup requirements of the other parts of the test specimen, dictated a vertical assembly procedure. The test configuration required horizontal orientation of the test specimen for mounting on a flat bed trailer. Therefore, the specimen was built up on a tiltable fixture that allowed the entire assembly to be rotated 90 degrees into a horizontal position, when completely assembled. Figure 5 shows the specimen mounted on the tilt fixture with one-half of the shroud in position.

As previously mentioned, the entire assembly was mounted on a flat bed cargo trailer (Figure 6) to provide mobility and to enable interior storage during inclement weather conditions and periods of nontest. The assembly was supported at four locations incorporating vibration isolators to provide for the specimen a mounting natural frequency less than 15 cps. The purpose of the isolation system was to reject all but airborne energy inputs to the test specimen.

INSTRUMENTATION

The vibrational responses at some 90 experiment and other pertinent locations on the spacecraft and appendages were sensed by piezoelectric accelerometers. The accelerometers were oriented along the orthogonal axes of the spacecraft, or, in the case of obliquely mounted experiments, along the orthogonal axes of the particular experiment. In addition to these, 14 locations were monitored on interstage fittings and other locations within the Agena section.

Microphones were used to determine the acoustic environment within the spacecraft between the spacecraft and shroud and the exterior to the shroud. Acoustic measurements were also taken inside and outside the Agena section. External microphone locations are illustrated in Figure 7.

A total of 205 measurements was recorded during the test. Of these, about one-fourth were acoustic measurements and three-fourths were vibration response measurements. All data were recorded on two 14-channel tape recorders

in conjunction with a five-channel constant band multiplex system providing a total of 32 recording channels. The tape recorders and all necessary signal conditioning equipments were installed in an instrumentation van that was located approximately 300 feet from the test specimen (Figure 4).

The requirement to obtain information from about 190 locations with 32 available magnetic tape recording channels necessitated classification of the data into seven groups. The first was a group of six "reference" transducers which were recorded during each test run. The remainder was divided into six groups, each group being recorded during one test run only.

The reference transducer group was also recorded during the "high-level" run. In addition, transducers which indicated large responses from "quick-look" inspections of low-level test data or at apparent "critical" locations were recorded during the high-level runs.

TEST PROCEDURE

During periods of nontesting, the trailer-mounted test assembly was housed in the shop area of the 9 × 6 thermal structures tunnel. The test sequence was initiated with transportation of the specimen assembly to the test site where it was positioned at the determined location and orientation. The transducers which were monitored during the particular run were connected and a system calibration was performed. In the case of all accelerometers, calibrations were accomplished by "insert-voltage" techniques. Accessible microphones were pressure-calibrated by means of an acoustic calibration device which applied a known sound pressure level at a particular frequency. Inaccessible internal microphones were calibrated prior to installation at the completion of the test.

Upon verification of the operation of appropriate instrumentation channels, the area was cleared of personnel and secured; then the tunnel was activated. The period between runs, necessary for recharging the tunnel air storage vessels, was utilized for quick-look at the acquired data and preparation for subsequent runs.

The initial directional survey dictated an orientation of the test assembly depicted as position 1 of Figure 8 with tunnel operating parameters of 130 psia and 300°F. Four 30-second test runs were performed with this orientation. On the fifth run, data from microphones on the +X (downstream) side revealed an asymmetric distribution of acoustic loading about the specimen. A quick-look at the data showed that the overall level at this location was about 5.5 db low. A later spectrum analysis indicated a rolloff of the entire spectrum above the second octave. An analysis of the response of four circumferentially deployed

microphones during run 5 is plotted in Figure 9. This figure clearly illustrates the problem. The apparent cause of this discrepancy was acoustic shading by the test assembly of the downstream side from all but the low-frequency energy, which is developed several diameters downstream of the exhaust.

A resurvey of the sound field was performed; it proved that the specimen was incorrectly oriented. The correct orientation was found to be that of position 2 of Figure 8. An examination of the details of the first directional survey indicated two likely causes of the misorientation. One factor was an overdeviation of a portion of the recorded data which allowed loss of the data peaks on part of the directional survey. The other contributing factor was an apparent error in microphone orientation caused by tolerance buildup (backlash) in the gears of the turntable drive mechanism.

The test specimen was located at position 2 of Figure 8, and run 5 was repeated and designated 5B. The tunnel operating parameters during run 5B were 130 psia and 300°F. An analysis of the microphone data acquired is presented in Figure 10 and clearly demonstrates a symmetric distribution of acoustic loading about the test article.

Since four runs had been performed in the misoriented position and the asymmetric loading conditions were considered undesirable for the test program, it was decided to rerun the complete test in the correct orientation. The "misoriented" runs were designated the "A" series and the correctly oriented ones were therefore designated the "B" series.

Although the initial plan specified six 30-second runs, the exposure time for the "B" series was reduced to provide six 15-second runs. The factors considered in the reduction of the test time included exposure time of the shroud during the misoriented runs. Since the shroud was a backup flight unit, excessive exposure to acoustic energy was undesirable. Further, 15 seconds of magnetic tape data of the structural vibration response was deemed adequate from an analysis standpoint. This allowed accomplishment of three test runs per day and expedited the program without compromising on the amount of acquired data.

The resurvey of the sound field was also used to determine a location at which the requirements of the high-level run could be accomplished. This is shown as position 3 of Figure 8. The tunnel operating parameters during the high-level runs were 300°F and 150 psia, and the exposure time was 30 seconds.

3. TEST RESULTS

GENERAL

Appendix A shows the tape recorder channel allocations, the transducer manufacturer and model designation, location and orientation, and overall response levels. Table 2 lists 11 locations, referred to as test plan locations c through m. Initially, 224 data channels were available from the seven test runs; however, a pretest checkout eliminated two multiplex channels per run (total of 14 channels) due to excessive oscillator/discriminator noise. During the course of the test, five channels were lost due to defective cabling so that a total of 205 channels was recorded.

Detailed analysis of all data further eliminated 20 channels due primarily to low-carrier amplitude which is undetectable during cursory data edit. The net result was acquisition of usable data from 185 of the 205 possible data channels or 90-percent recovery of the recorded data which is considered very good for a field operation of this magnitude.

Power-spectral-density analyses were performed on all vibration channels and the resulting acceleration spectral density plots are presented in Appendix B. The analysis was performed utilizing a Technical Products Corporation model 627 analyzer with the following effective square filter bandwidths (B_w) and filter scan rates (R_s):

20-300 cps	B_w = 2.94 cps	R_s = .14 cps/sec
300-1000 cps	B_w = 6.2 cps	R_s = .31 cps/sec
1000-5000 cps	B_w = 25 cps	R_s = 2.0 cps/sec

The reason for utilizing three ranges of analysis was to maintain the same degree of resolution at all frequencies and to optimize analysis time.

All acoustic data were analyzed in octave bands by means of a General Radio type 1550A octave band analyzer. These analyses for exterior microphones are presented in Figures 10, 11, and 12. Octave band analyses of interior microphone responses are presented in Figures 13 through 15.

Probability density analyses of representative vibration and acoustic data channels were accomplished utilizing a Bruel and Kjaer model 160 probability density analyzer. These curves are shown in Figures 16 through 19 for the locations indicated. They are indicative of a "normal" (Gaussian) amplitude distribution for both the acoustic input and vibration response data.

ACOUSTIC ENVIRONMENT

Prior to the test, some concern was voiced about the repeatability of the sound field generated by the LRC 9 × 6 thermal structures tunnel. This was justifiable since, because of the large number of data points involved, the data were acquired from a total of seven test runs. Substantial variation would have complicated any direct comparison of response data acquired from subsequent runs. The maximum and minimum variation in octave band levels recorded at the reference microphone location during all six of the B series runs are plotted in Figure 20. As indicated, the repeatability of the sound field was excellent with no more than 1 db variation in these data from all low-level runs. The repeatability is further verified by the response of accelerometers which were monitored during all runs. These accelerometers were located at the base of the interstage fitting on the Agena ring. As indicated in Table 3, the response at this location was virtually the same for each of the low-level runs. Figure 10 shows that, in general, the applied spectrum was within the required limits.

As anticipated, acoustic loading over the 22-foot length of the test assembly varied somewhat but not sufficiently from the specified tolerances to cause concern. Figure 7 illustrates the microphone locations. The specification levels were established in the plane of location II. At this location, as presented in Figure 10, the measured circumferential distribution of acoustic loading was uniform with ±2 db with the exception of the first octave of the top microphone (II-B). This microphone indicated about 3-db lower than the others at this location. This was probably the result of a shaded ground reflection path.

The distribution of acoustic energy around the forward and aft ends of the test assembly (locations I and III) are presented in Figures 11 and 12, respectively. The general spectrum shape, as shown, remained about the same, fore and aft. However, the high-frequency portion was somewhat higher at locations closer to the tunnel centerline than might be expected. Even so, the data exhibit uniformity within ±2 db.

Figure 20 shows the high-level-run spectrum. The overall level was 153 db, about 3 db higher than the low-level runs. It is interesting to note that the difference was attained by a general increase in the spectrum of about 3 db/octave, rather than re-enforcement in certain frequency bands only.

Shroud sound transmission information was obtained at locations I and II where microphones were located both inside and outside the shroud. The transmission data are plotted in Figure 21 along with estimated values from reference 4. In general, the values shown are in reasonable agreement.

The acoustic test levels have been further verified by subsequent acoustic measurements recorded during the OGO "C" launch (reference 5). OGO C was launched by a thrust-augmented Thor-Agena vehicle from the Western Test Range on October 14, 1965. These levels are plotted in Figure 22 along the test specification and actual test values for the same location. As indicated, they are all in excellent agreement in both overall level and spectral content.

VIBRATION RESPONSE

As previously stated, detailed power spectral density analyses of all vibration channels are presented in Appendix B. Naturally a comprehensive discussion pertaining to each data channel is prohibitive; however, in reviewing the vibration data, the following general observations are evident.

Boom-mounted experiments exhibited vibration levels on the order of 4-6 g-rms (over a bandwidth of 20 cps to 5 kc as are all vibration levels quoted in the following paragraphs) along the axis of the latching mechanism. As might be expected, the least response was noted along the longitudinal axis of the boom and ranged about 2-3 g-rms. Panel mounted experiments, such as those attached to the experiment doors, generally presented surprisingly low overall response levels of the order of 3 g-rms along the most responsive axes (normal to the plane of the panel). Internal truss-mounted experiments displayed the largest overall response levels. Even so, these were a modest 5-7 g-rms. The vibration response levels increased somewhat during the high-level run.

Vibration measurements recorded within the Agena section were an order of magnitude higher than those found to be in the spacecraft. At truss-mounted equipment locations inside the Agena section, overall vibration levels ranged from 9-16 g-rms during low-level runs and as high as 21 g-rms during the high-level run.

The difference in the magnitude of response between locations in the Agena and those in the spacecraft was probably due to more efficient transfer of the mechanical energy from vibrating exterior surfaces. A typical skin panel responded at 25 g-rms with most of the spectral content distributed in the vicinity of its estimated fundamental frequency (approximately 900 cps).

The energy from this source was present at the underside of the Agena ring (directly below an interstage fitting) where an overall response of 12 g-rms was noted. However, at the base of the interstage fittings (on the topside of the Agena ring) the energy was further attenuated to an overall level of about 3 g. The total reduction by a factor of 4 was apparently due to the filtering characteristics of the interstage structure.

It is also interesting to note that, although the acoustic input spectrum was continuous to beyond 10 kc, the vibration response at virtually all locations cuts off at 2500 cps or less.

A comparison of vibration and acoustic data from the low- and high-level runs indicated, in general, that the structure exhibited a linearity of response within this range.

The results of the solar-cell module acoustic exposure are presented in detail in reference 6. In general, damage to the modules was considered negligible with the exception of one module which exhibited two loose solder connections.

ACKNOWLEDGMENT

The author acknowledges the support and cooperation of the Langley Research Center and, in particular, the Aero-Thermal Facility Branch which helped to make this program possible.

REFERENCES

1. W. H. Mayes and P. M. Edge, Jr., "Application of a Blowdown Wind Tunnel for Large Scale Acoustic Environmental Testing," 61st Meeting of Acoustical Society of America.

2. S. A. Clevenson, D. A. Hilton, and W. T. Lauten, Jr., "Vibration and Noise Environmental Studies for Project Mercury," Proc. Inst. Environ. Sci., page 541 (1961).

3. W. H. Mayes, P. M. Edge, Jr., and J. S. O'Brien, Jr., "Near-Field and Far-Field Noise Measurements for a Blowdown Wind Tunnel Supersonic Exhaust Jet Having About 475,000 Pounds of Thrust," NASA TN D-517 (1961).

4. G. D. Hinshelwood, "Estimated Shock, Acceleration, and Vibration Environments for Atlas-Agena B and Thor-Agena B Spacecraft," GSFC Report, Agena-SAV-1 (rev. Aug. 1, 1961) (confidential).

5. Memorandum Report No. 661-13 from L. A. Williams, Structural Research and Technology Section to Structural Dynamics Branch Files dated July 7, 1966, Subject: Noise Level Measurements for the Improved Delta (3E), Atlas/Agena-B, and TAT/Agena Launch Vehicles (GSFC).

6. GSFC Memorandum from L. W. Slifer and N. V. Mejia to W. E. Scull dated April 23, 1965, Subject: OGO Acoustic Test, Solar Cell Modules.

ILLUSTRATIONS

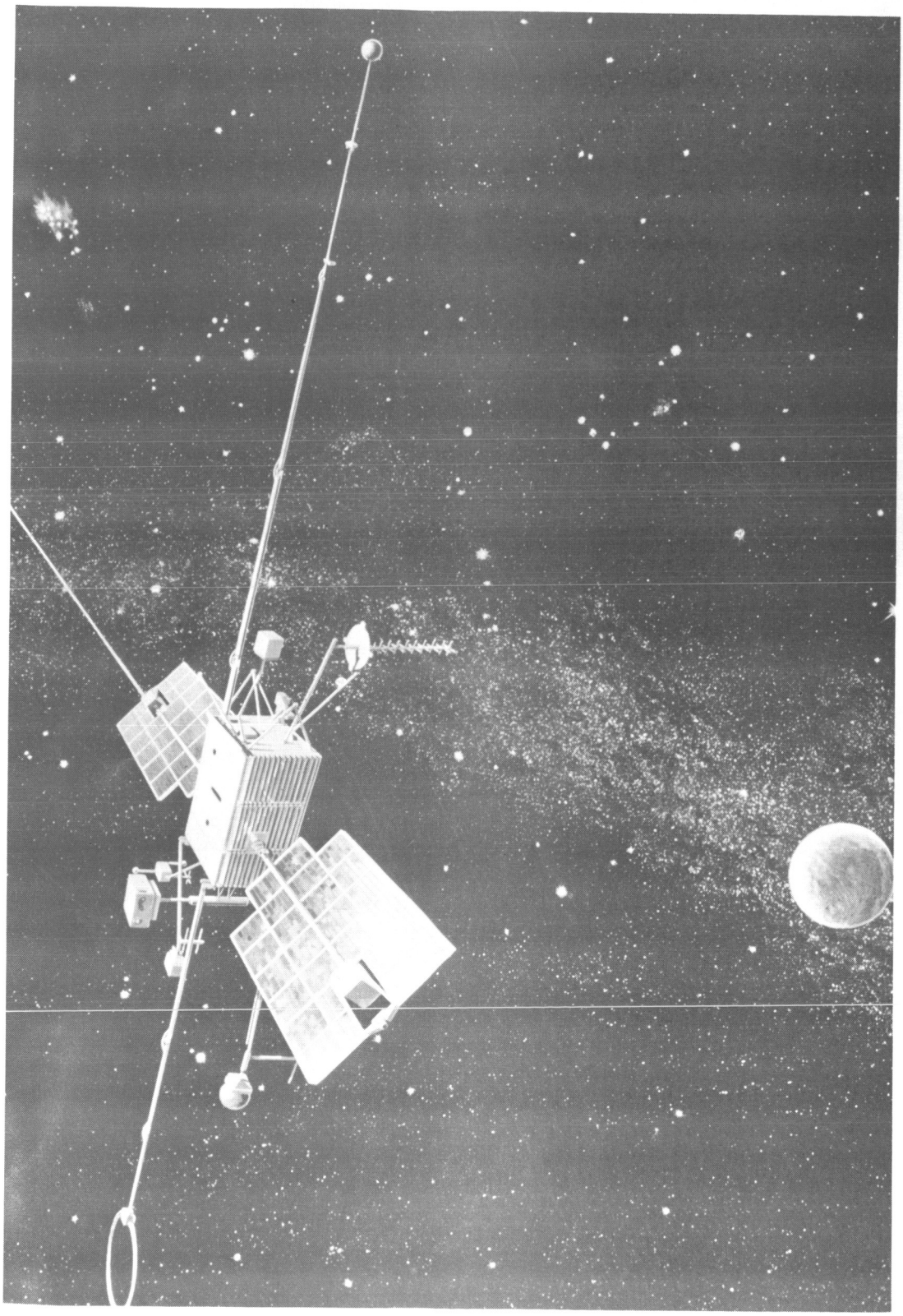

Figure 1. Artist's Conception of OGO in Orbit

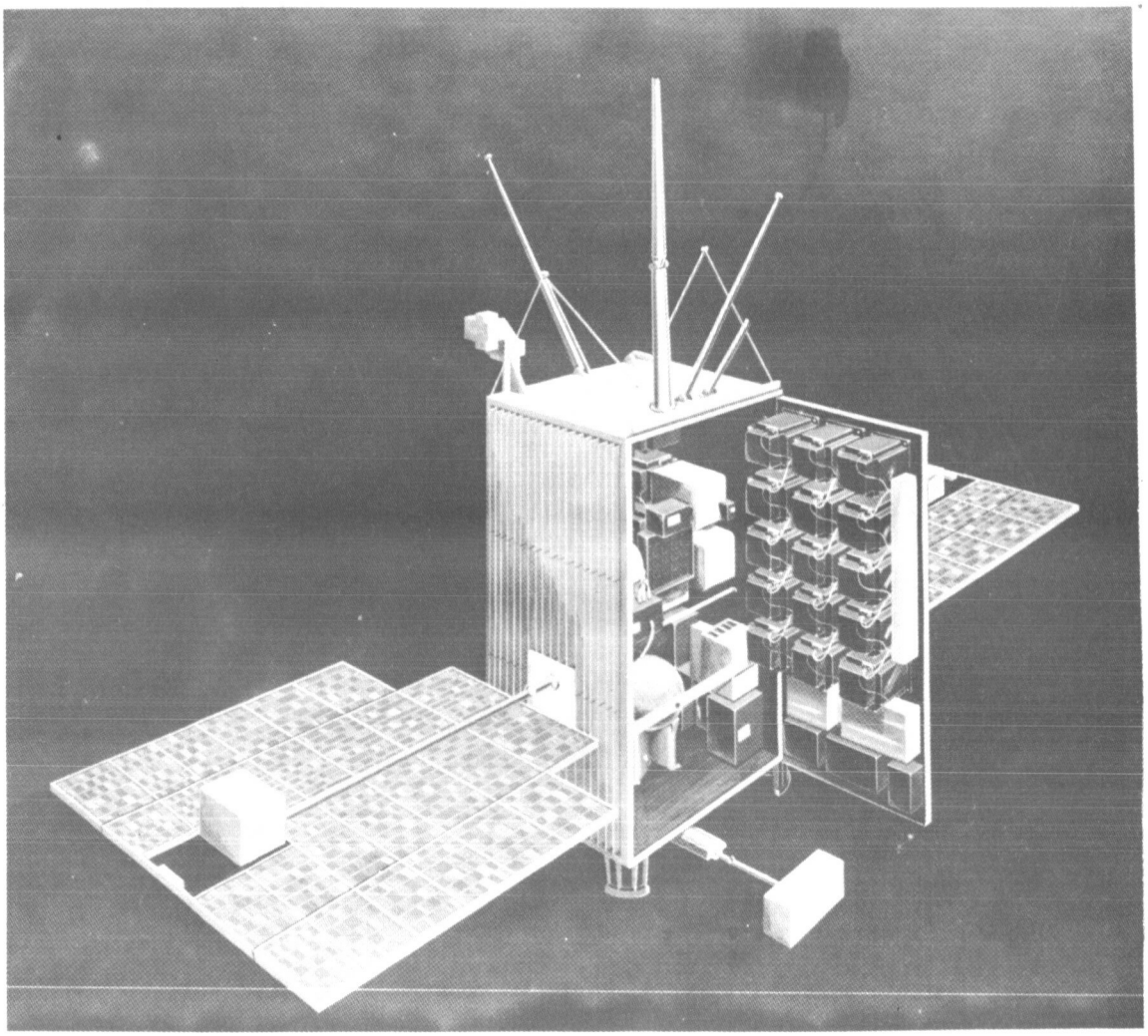

Figure 2. OGO With One Experiment Door Open

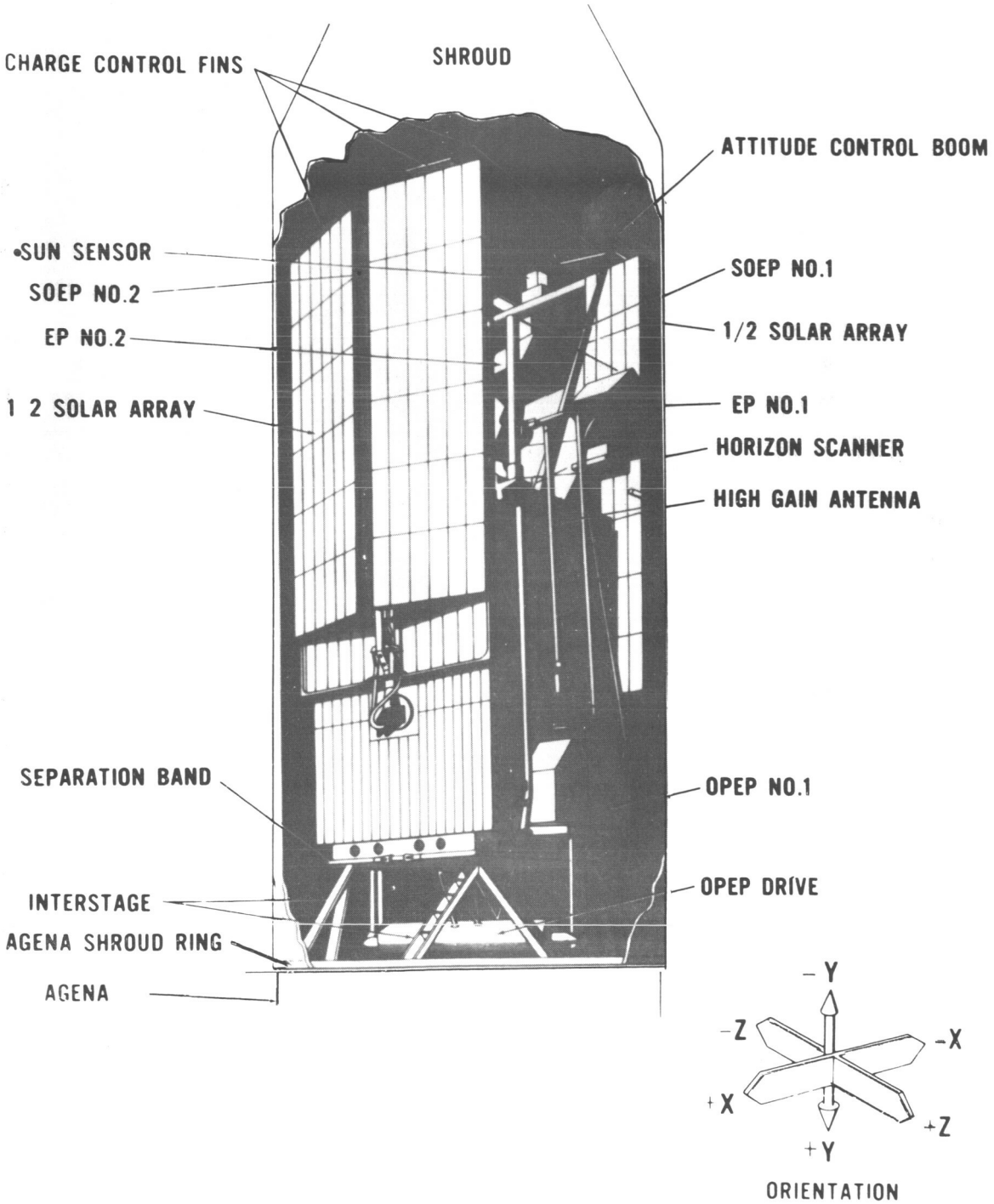

Figure 3. OGO In Launch (Folded) Configuration

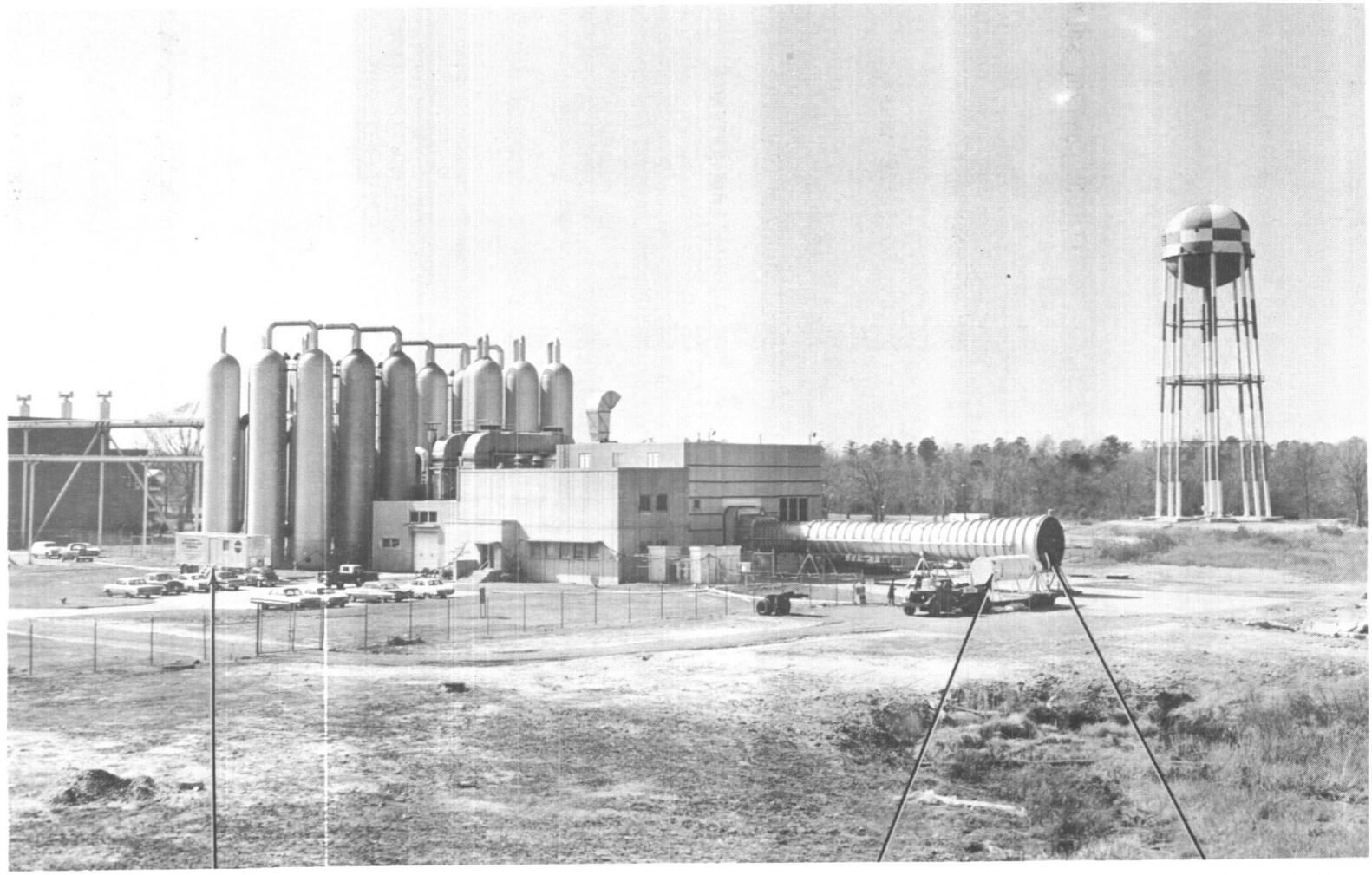

Figure 4. Test Set-up at the 9-Foot X 6-Foot Thermal Structures Tunnel

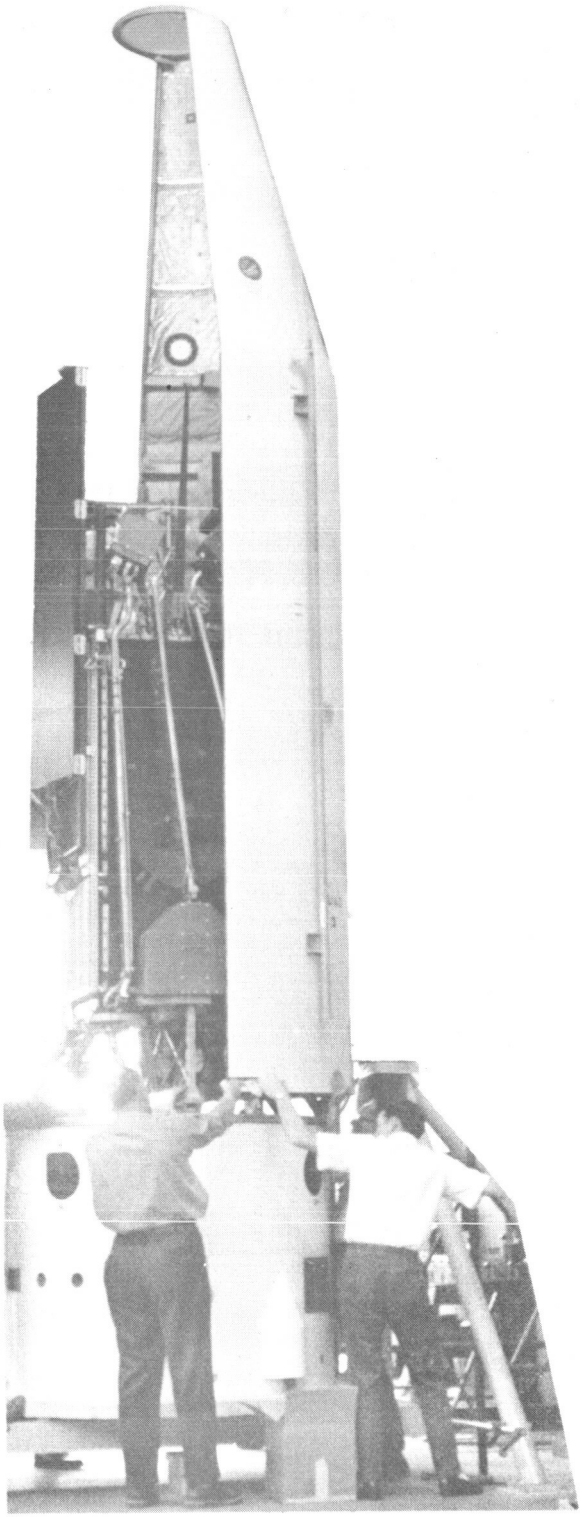

Figure 5. Test Specimen With One-Half of the Shroud Installed

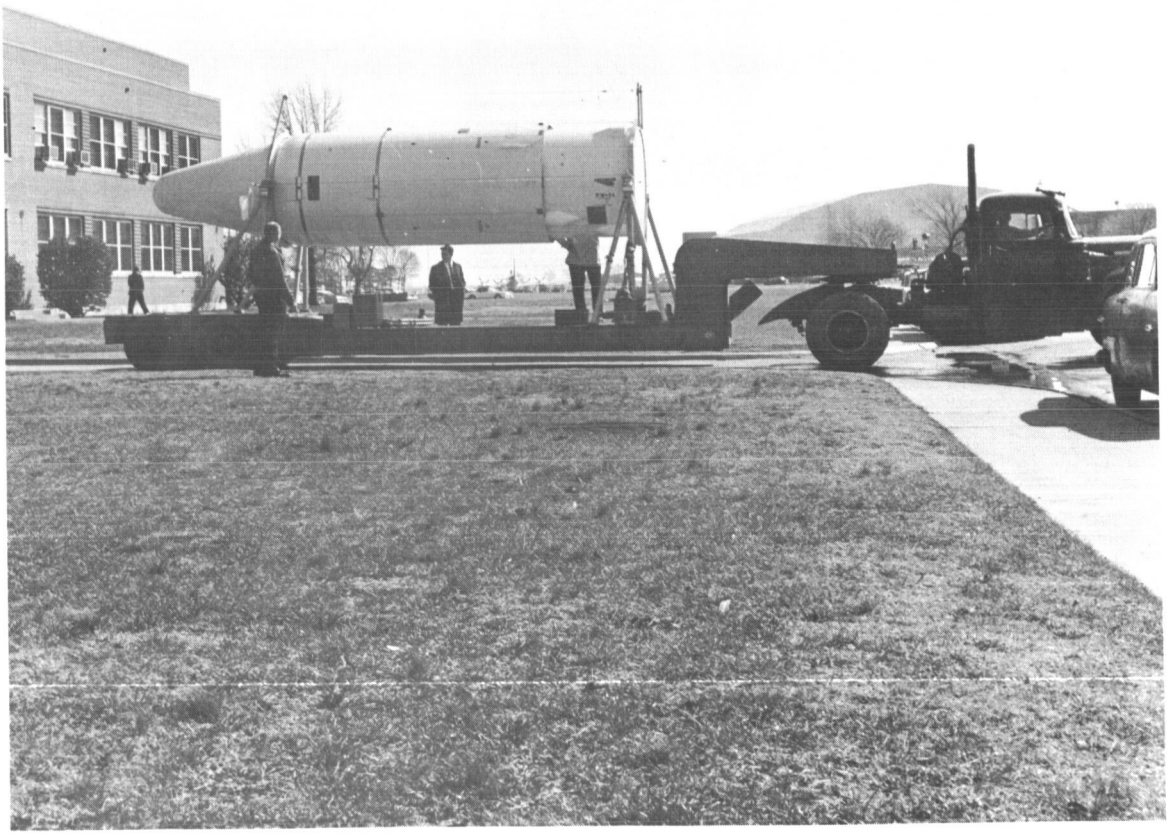

Figure 6. Trailer-Mounted Test Assembly

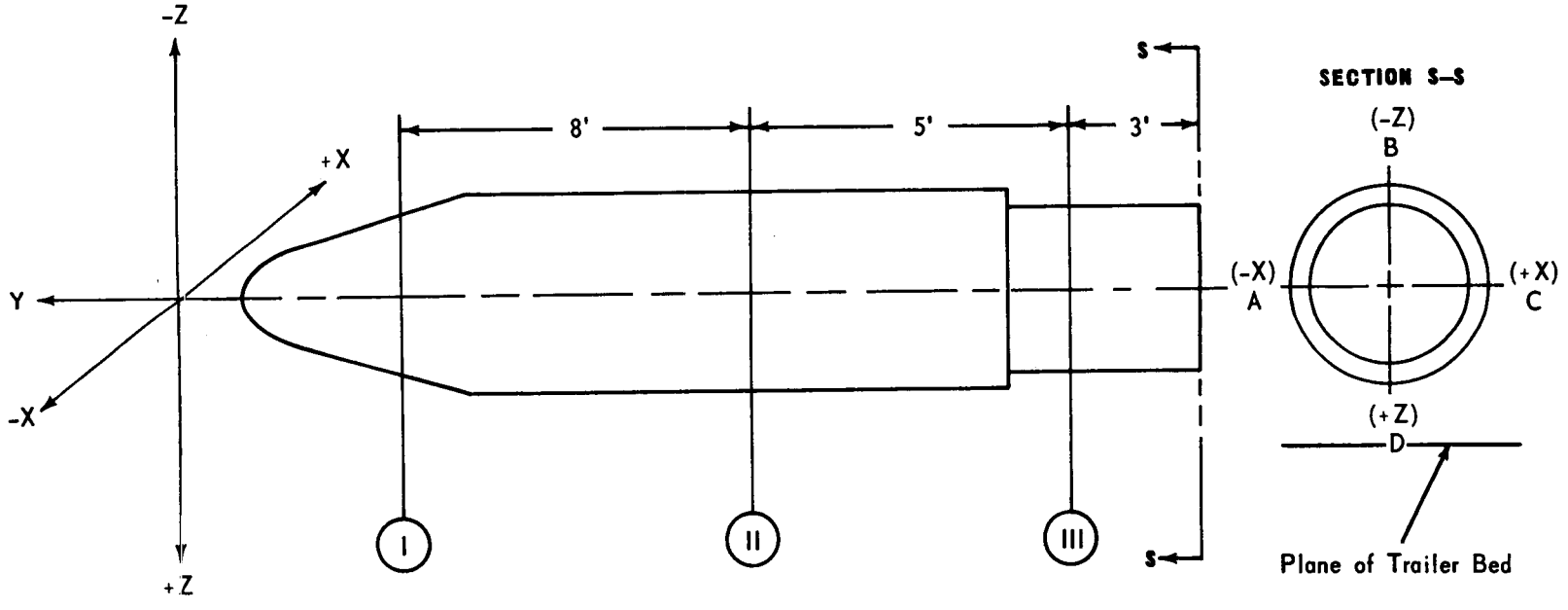

STL Axes

Figure 7. External Microphone Locations

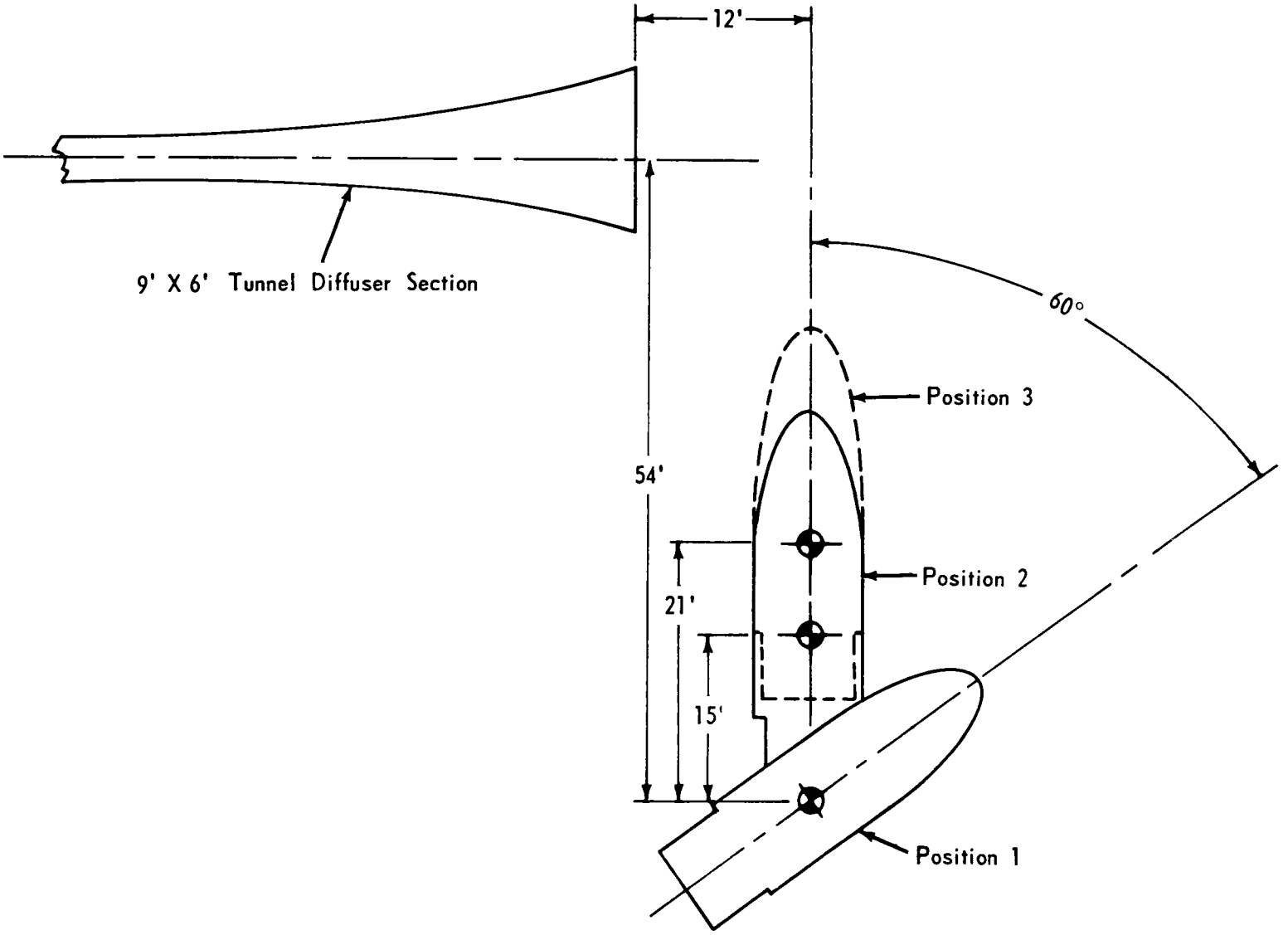

Figure 8. Test Specimen Position and Orientation

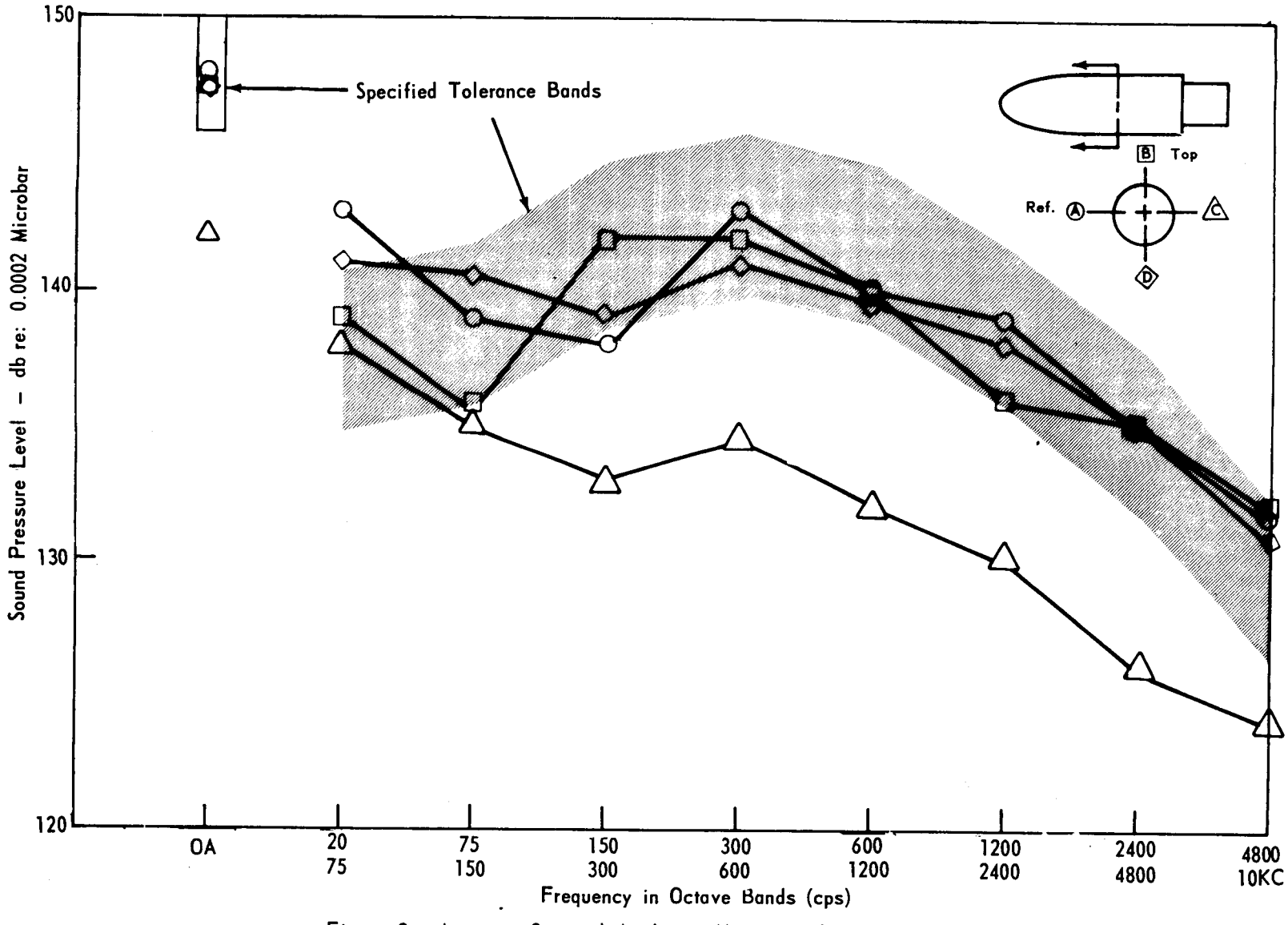

Figure 9. Acoustic Spectral Analysis, Misoriented at Position 1

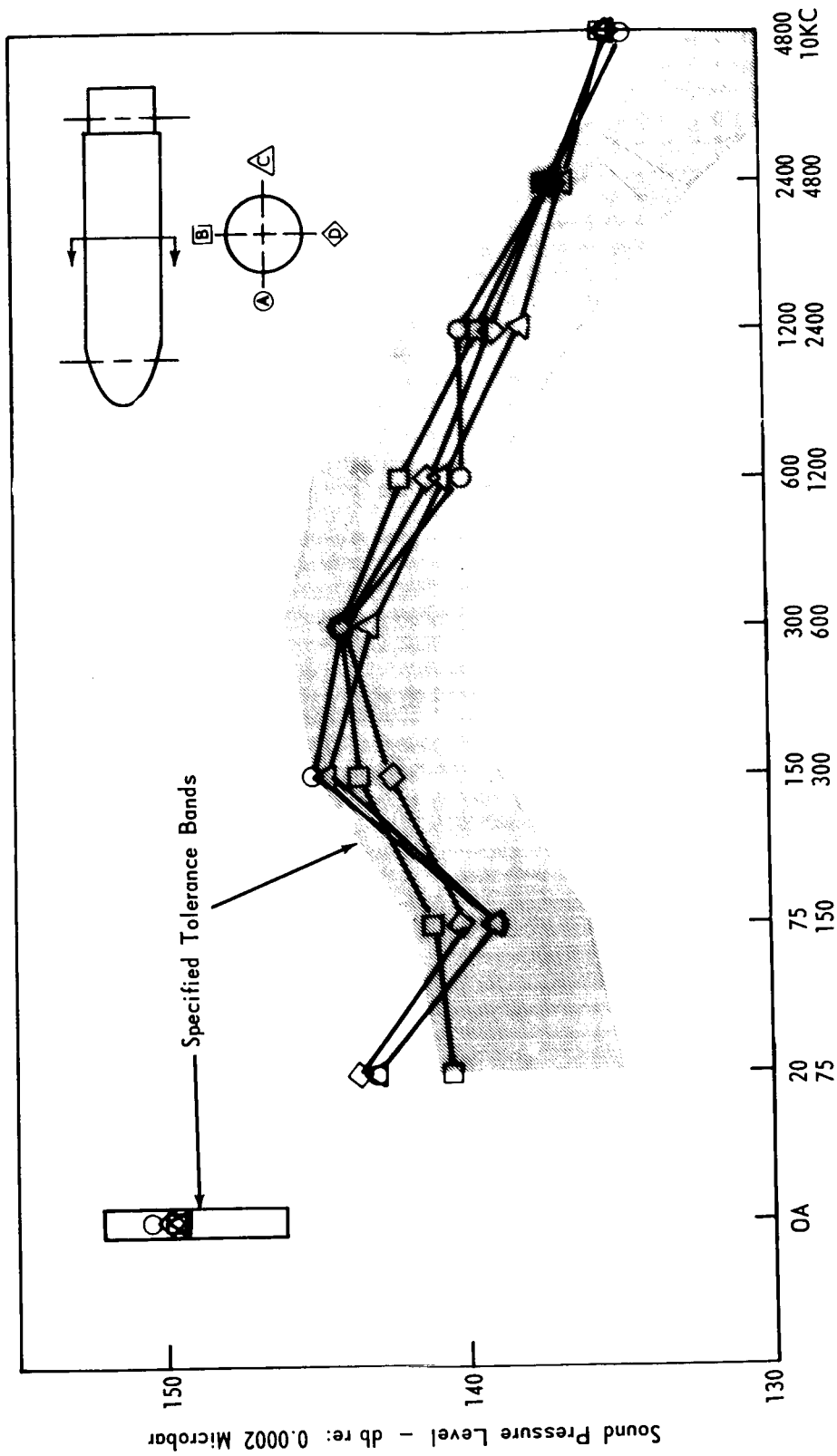

Figure 10. Acoustic Spectral Analysis, Correctly Oriented at Position 2

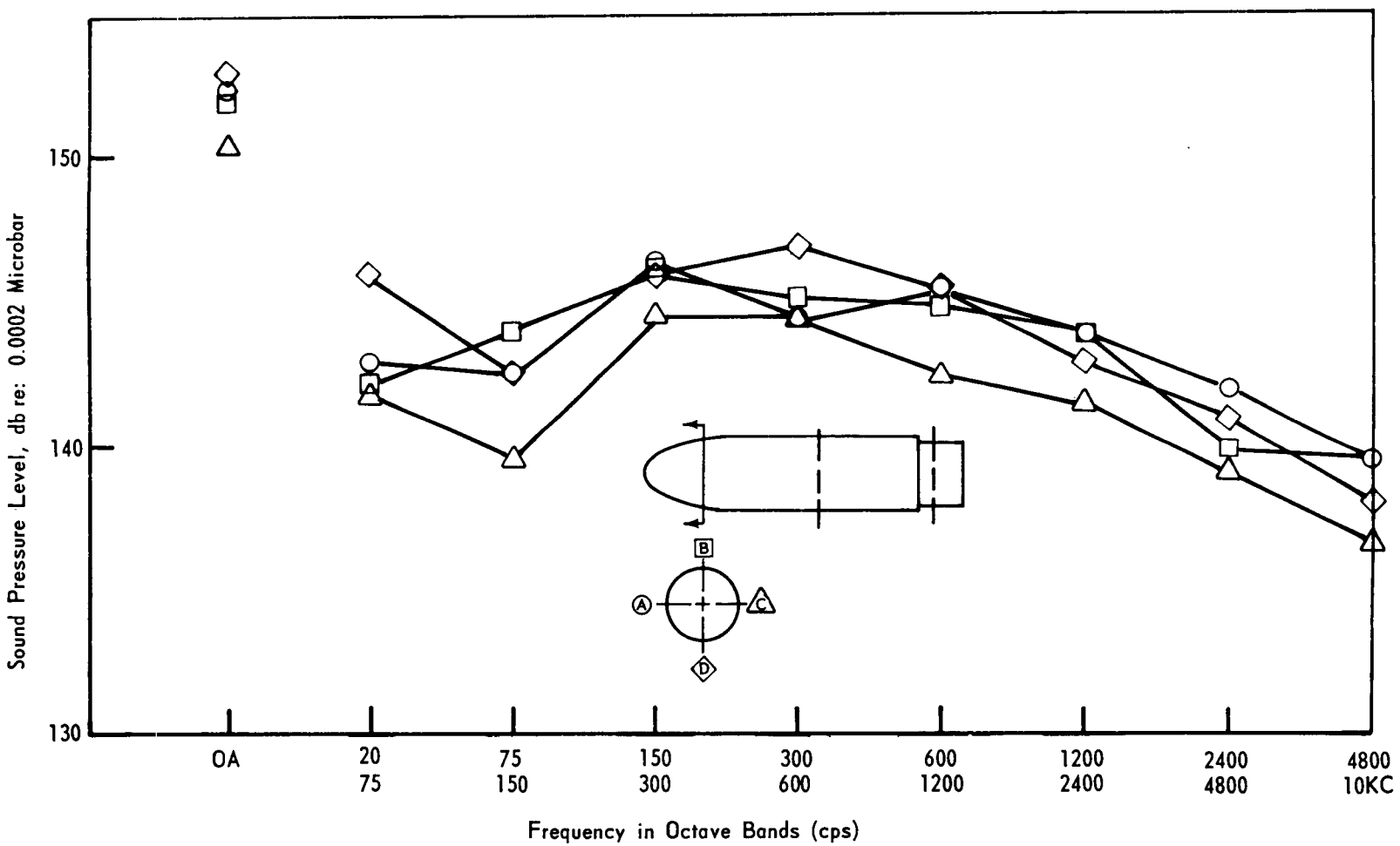

Figure 11. Acoustic Distribution Around Shroud (Fore), Position 2

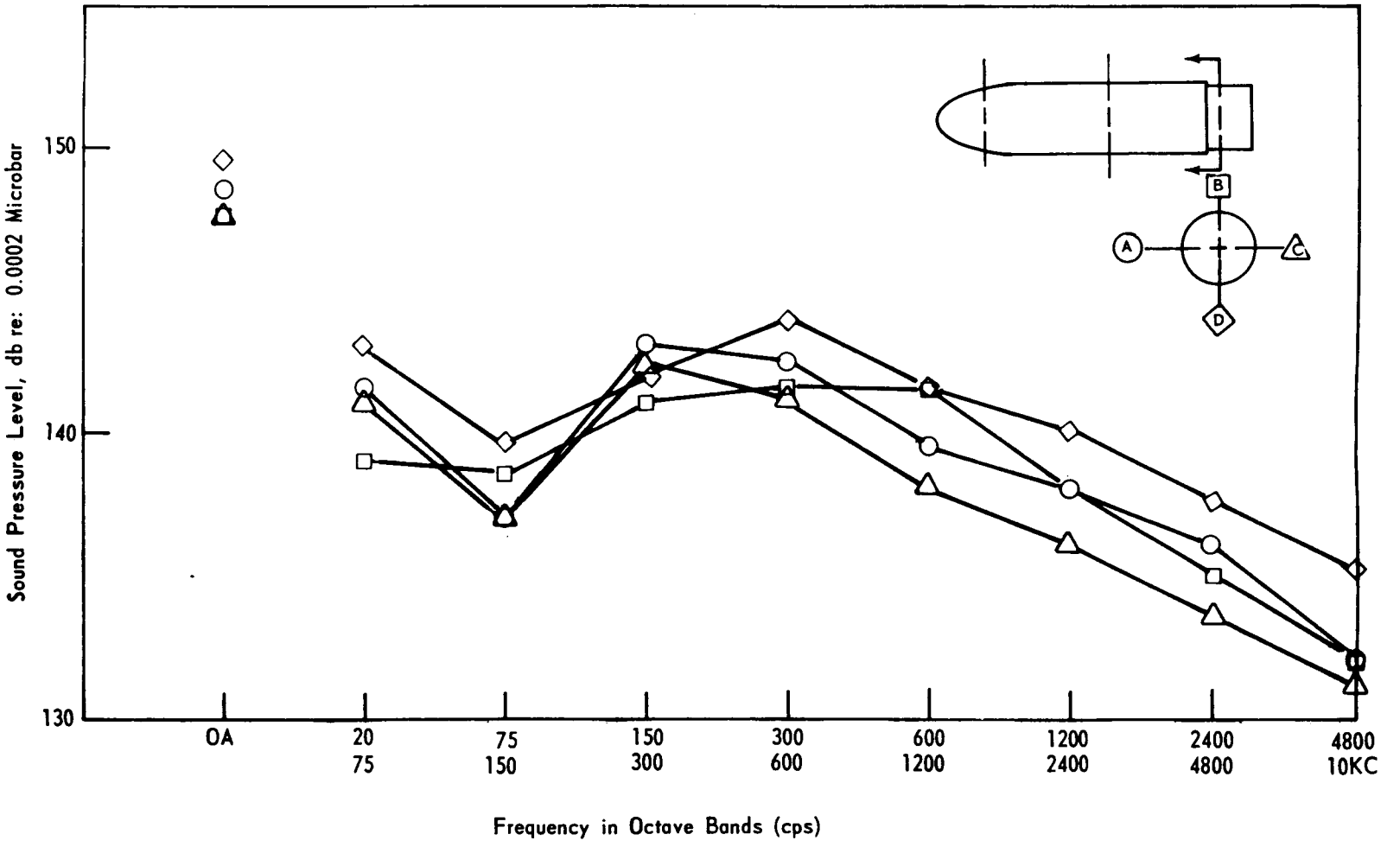

Figure 12. Acoustic Distribution Around Shroud (Aft), Position 2

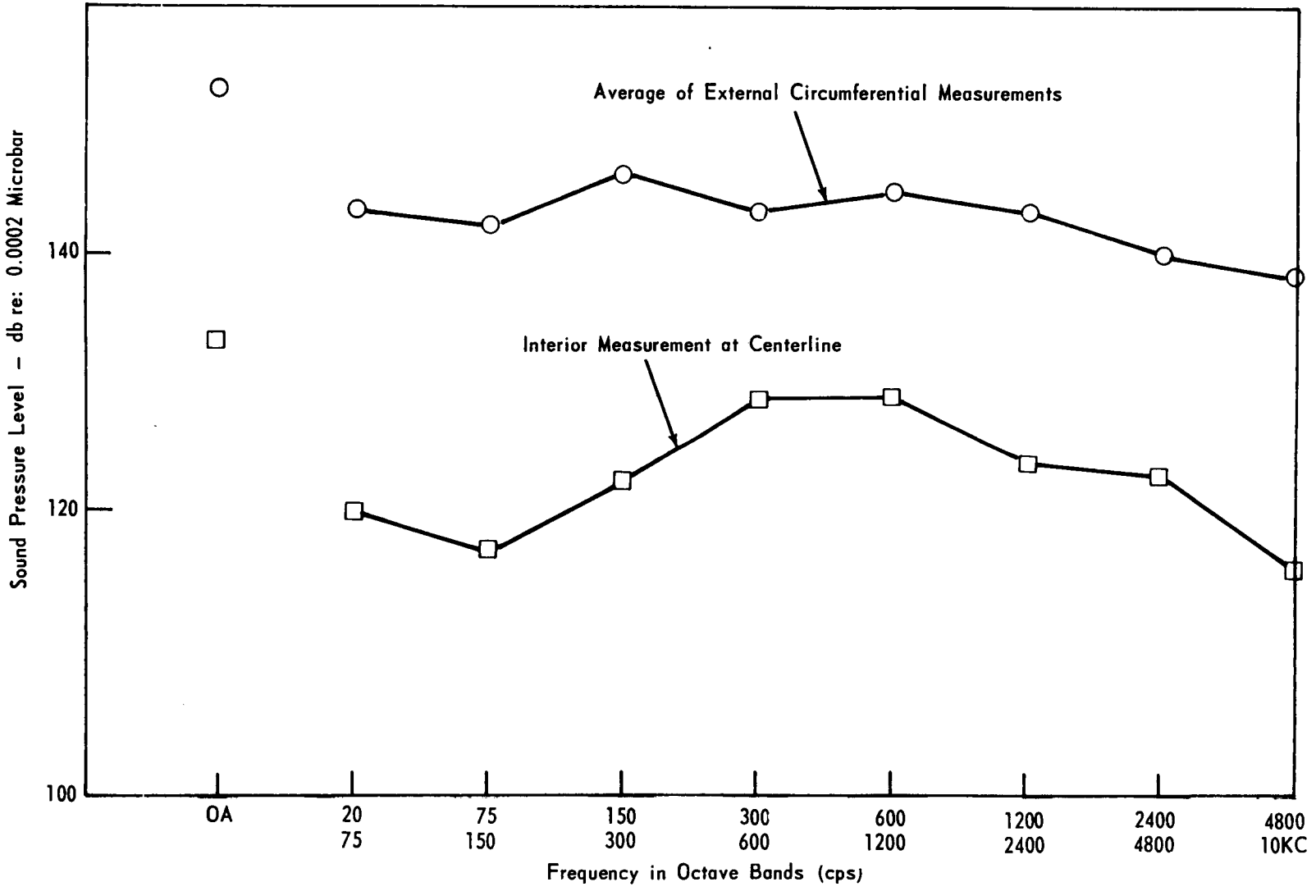

Figure 13. Acoustic Measurements at Location I, Position 2

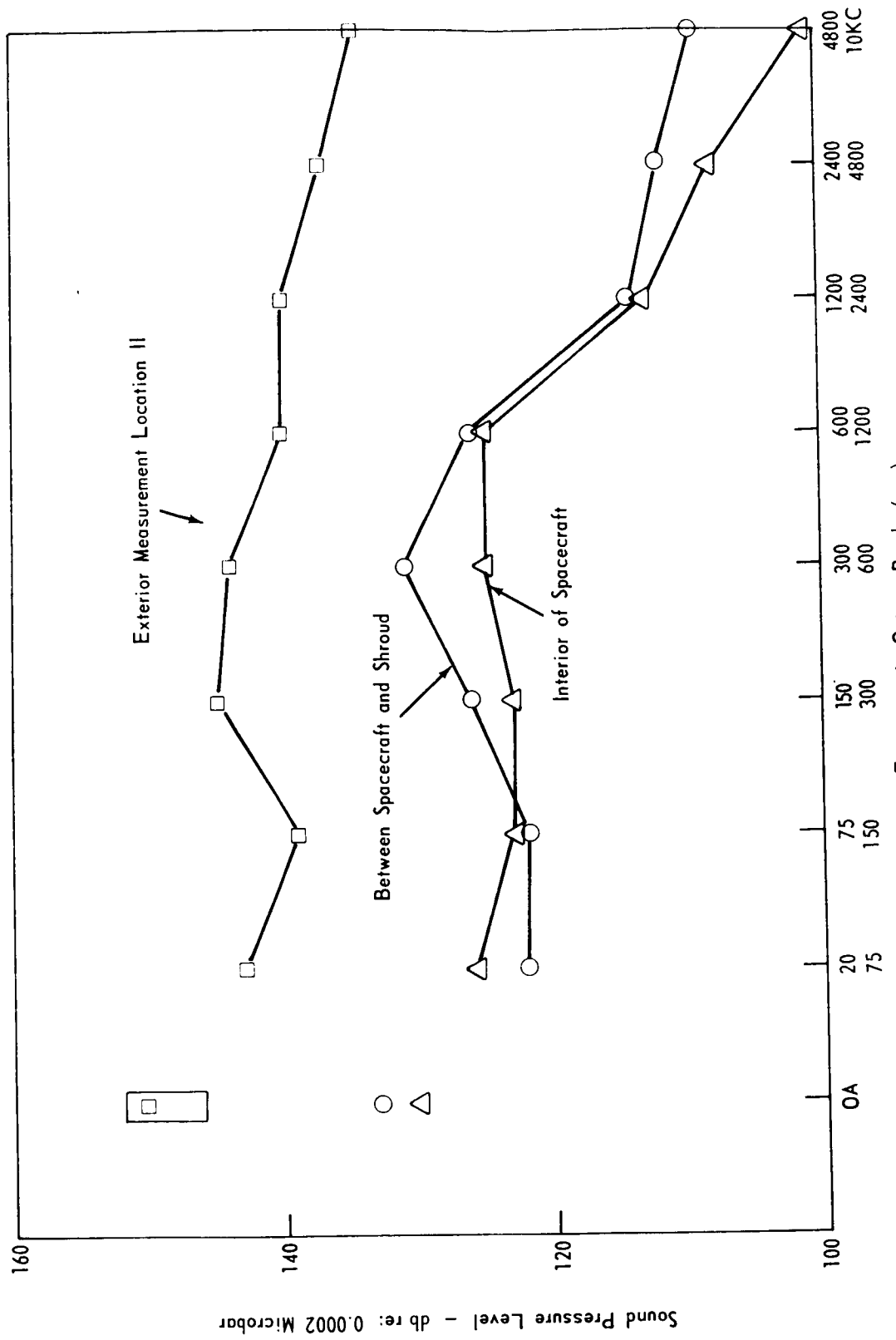

Figure 14. Acoustic Measurements at Location II, Position 2

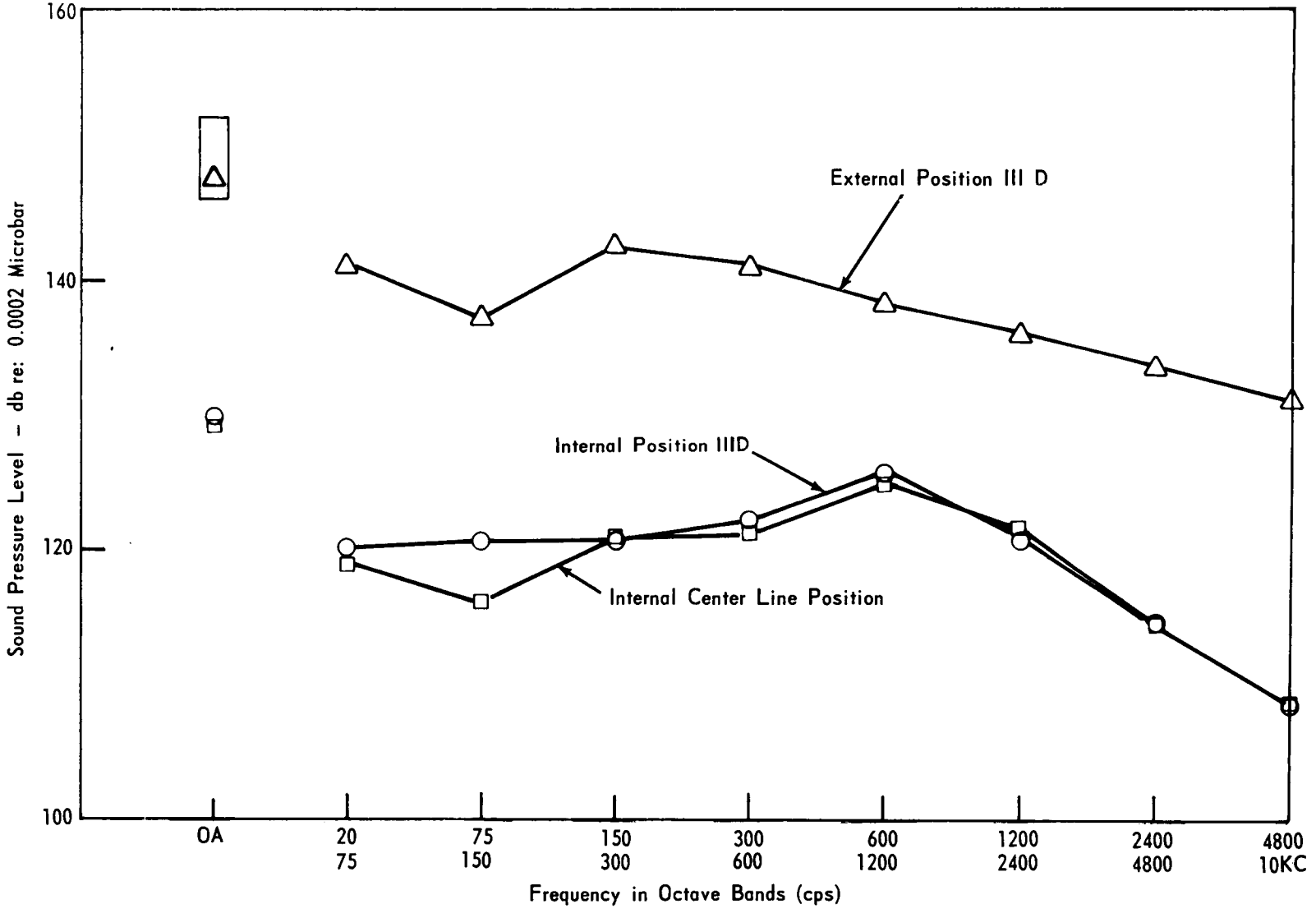

Figure 15. Acoustic Measurements at Location III (Agena Section), Position 2

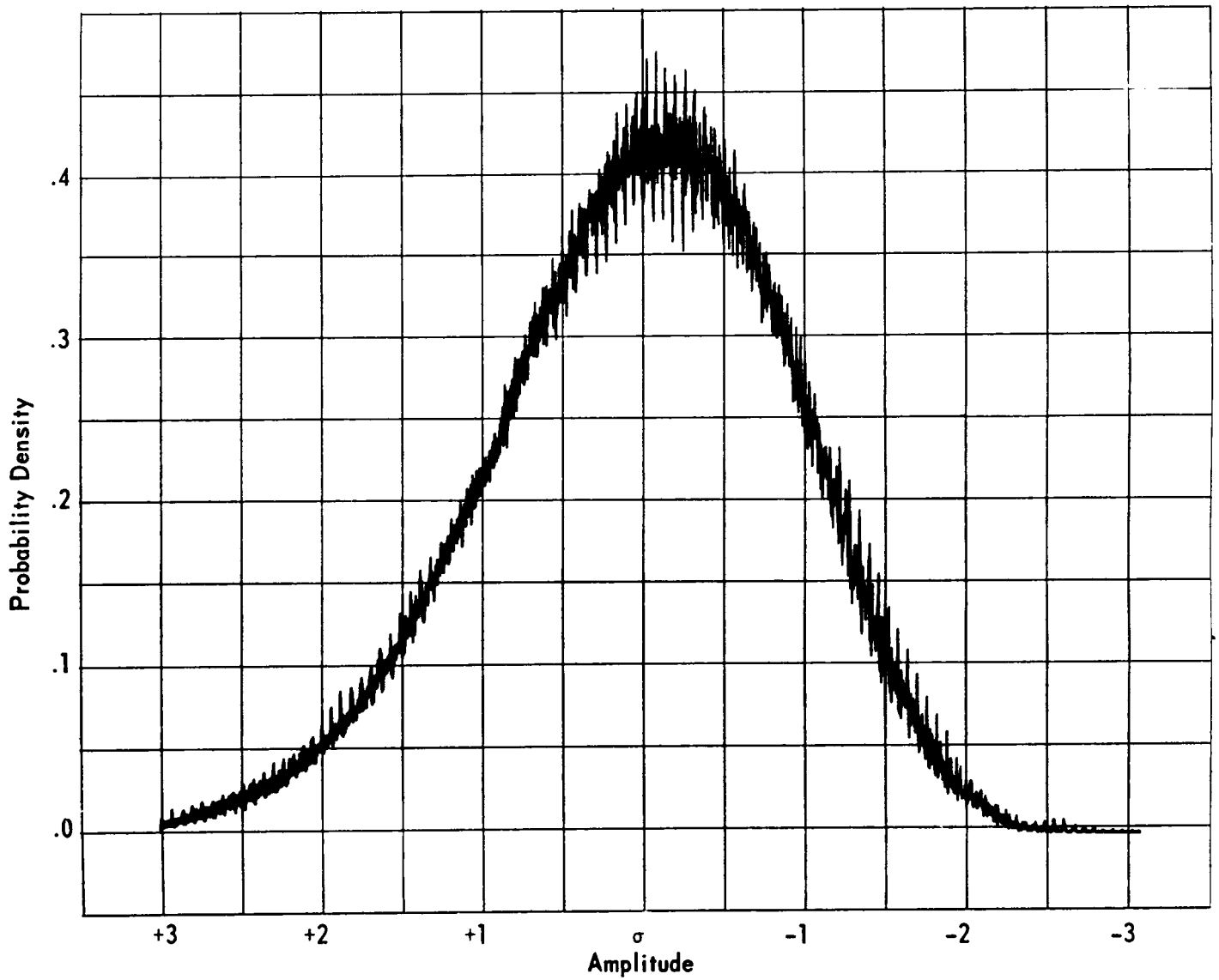

Figure 16. Probability Density Analysis – Acoustic Noise Exterior to Shroud

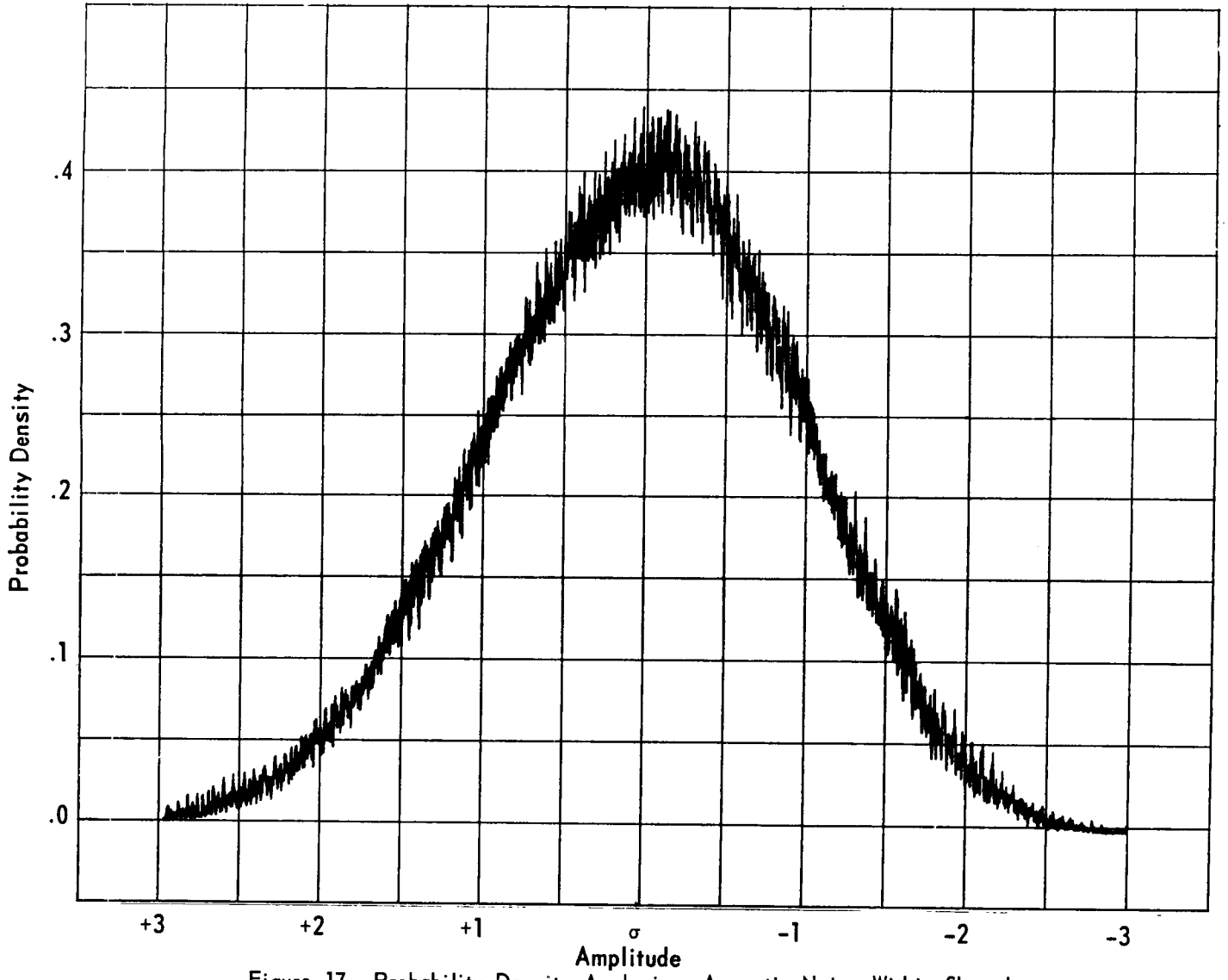

Figure 17. Probability Density Analysis – Acoustic Noise Within Shroud

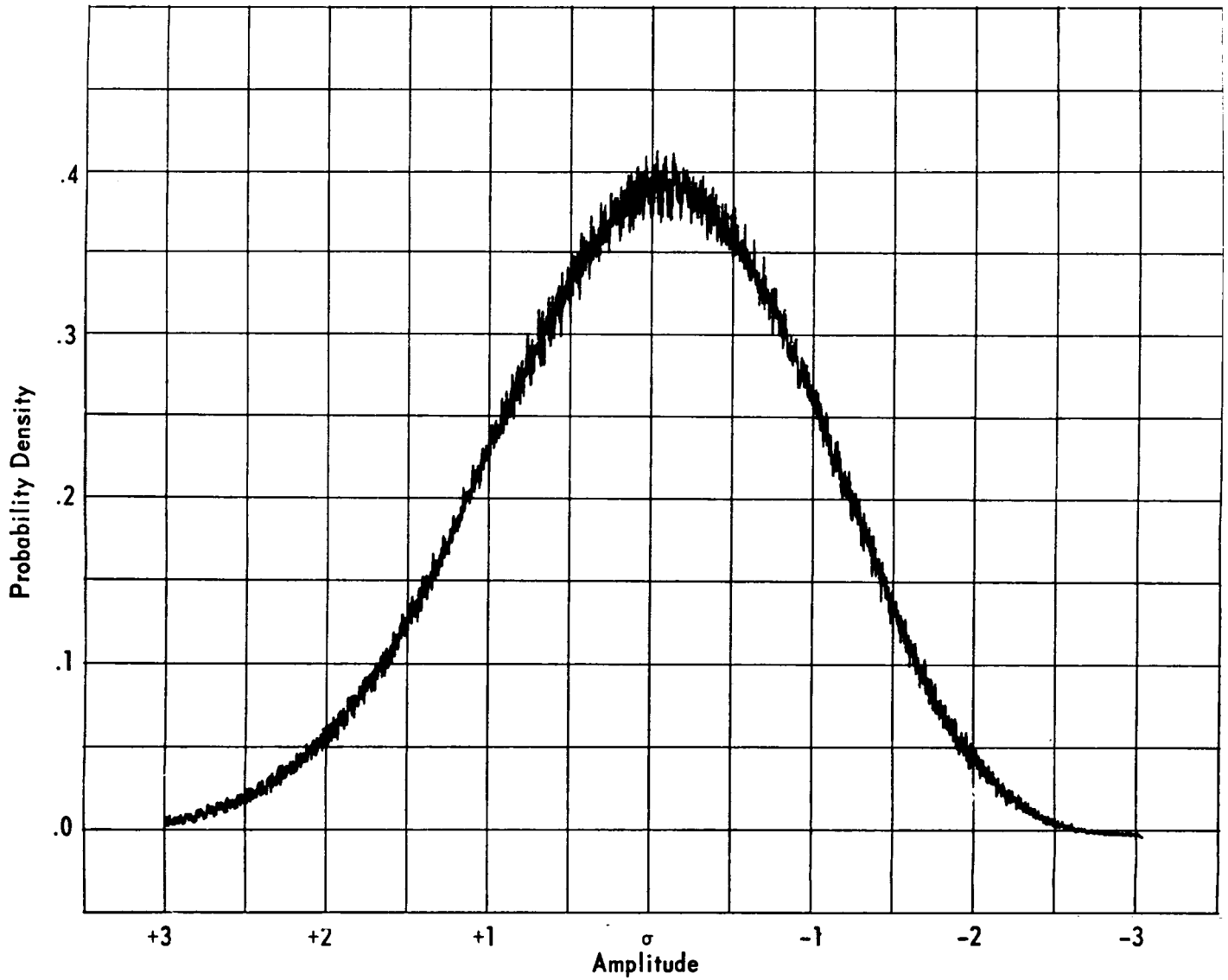

Figure 18. Probability Density Analysis – Vibration Response at Base of Interstage Fittings

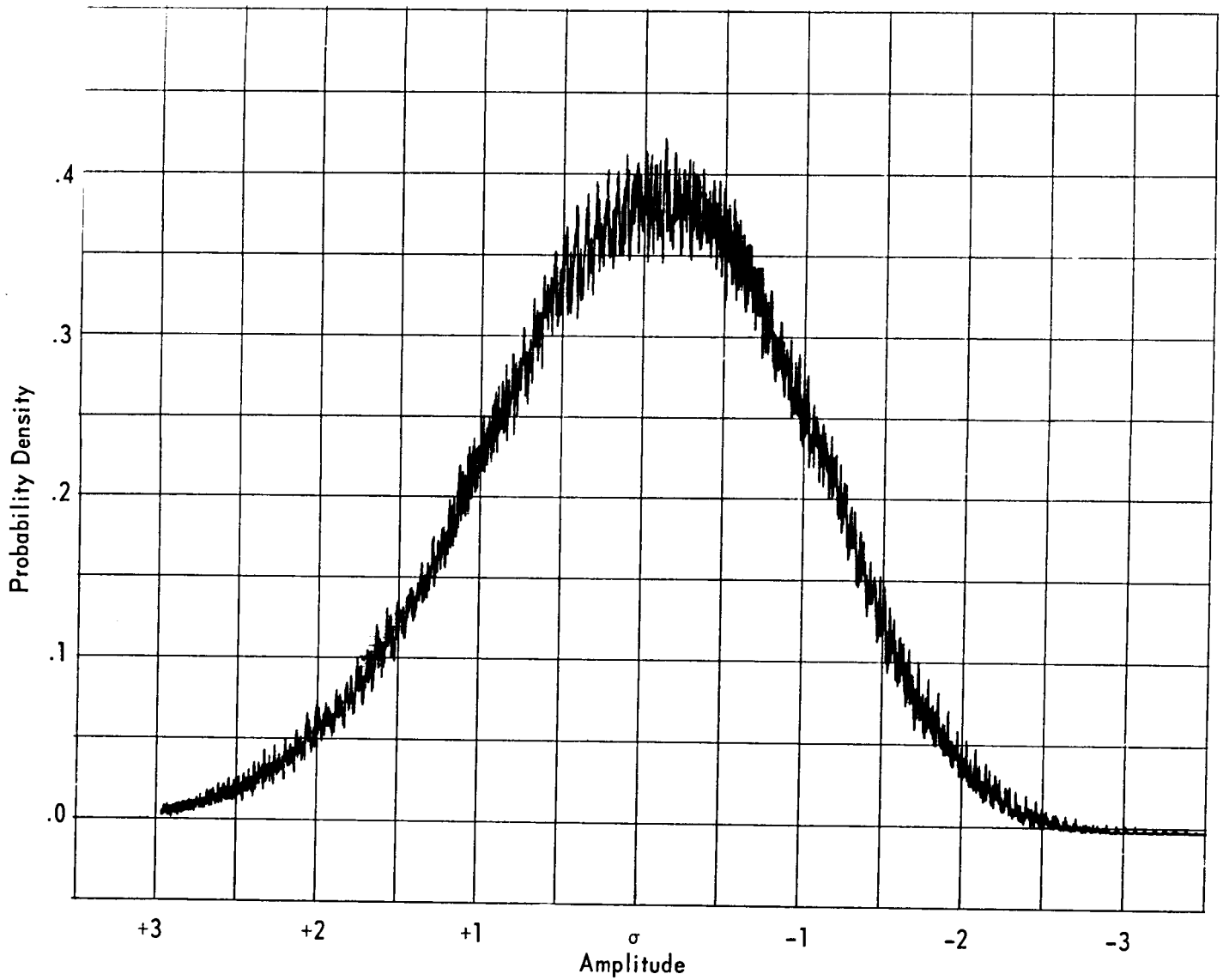

Figure 19. Probability Density Analysis – Vibration Response at Top of Spacecraft

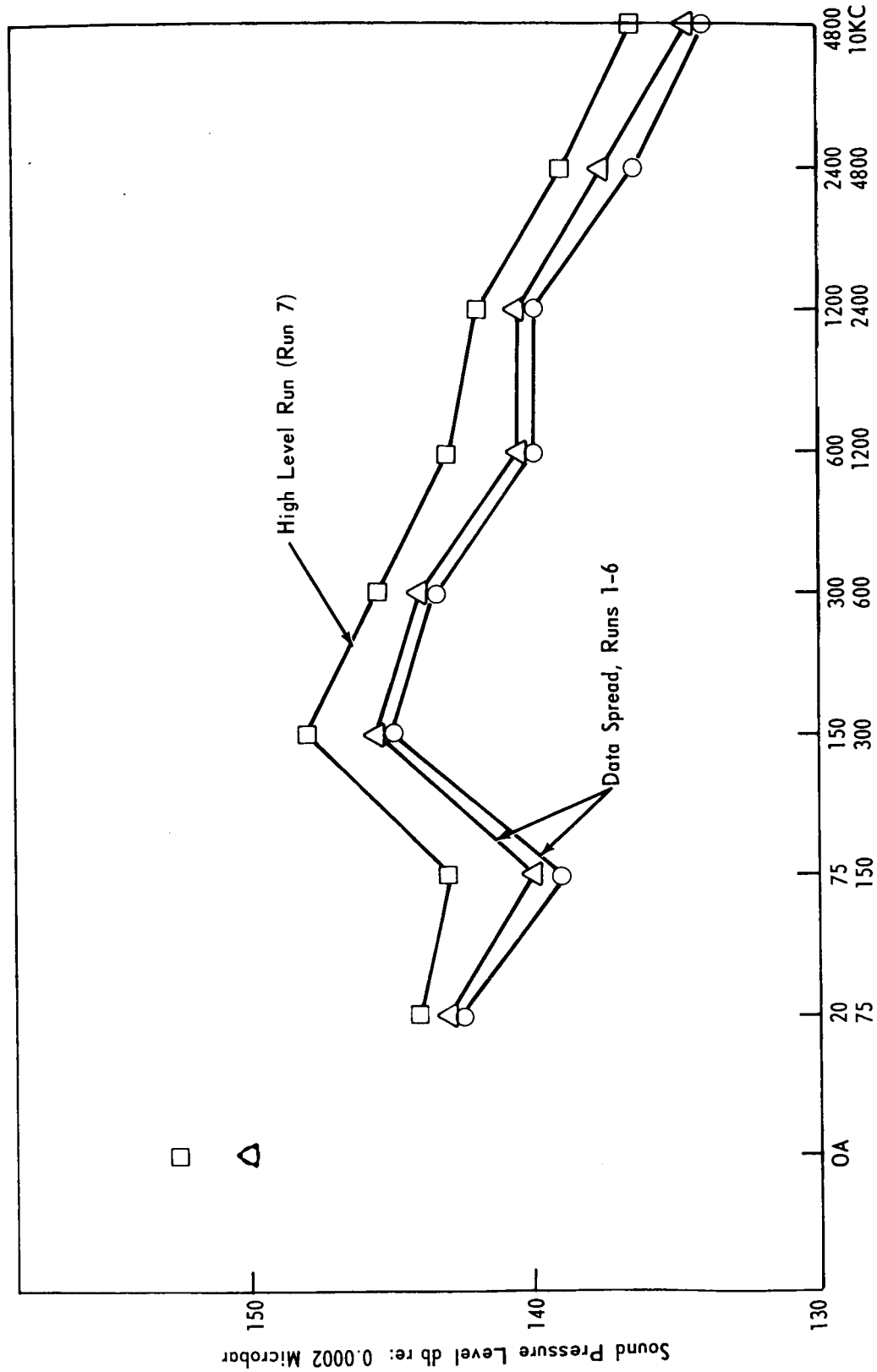

Figure 20. High-Level Run Spectrum and Data Spread at External Location II-A

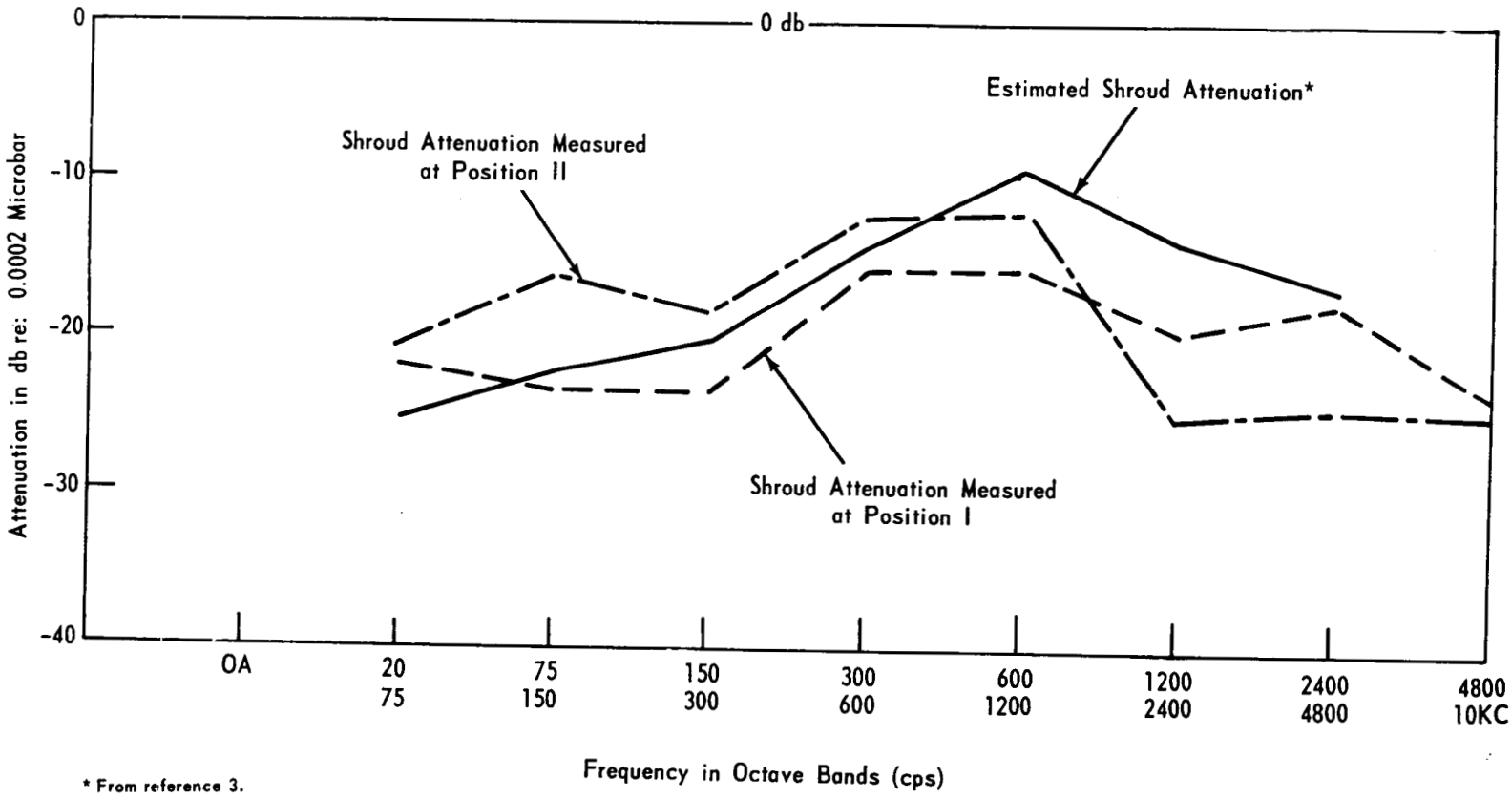

* From reference 3.

Figure 21. Typical Shroud Acoustic Transmission Characteristics

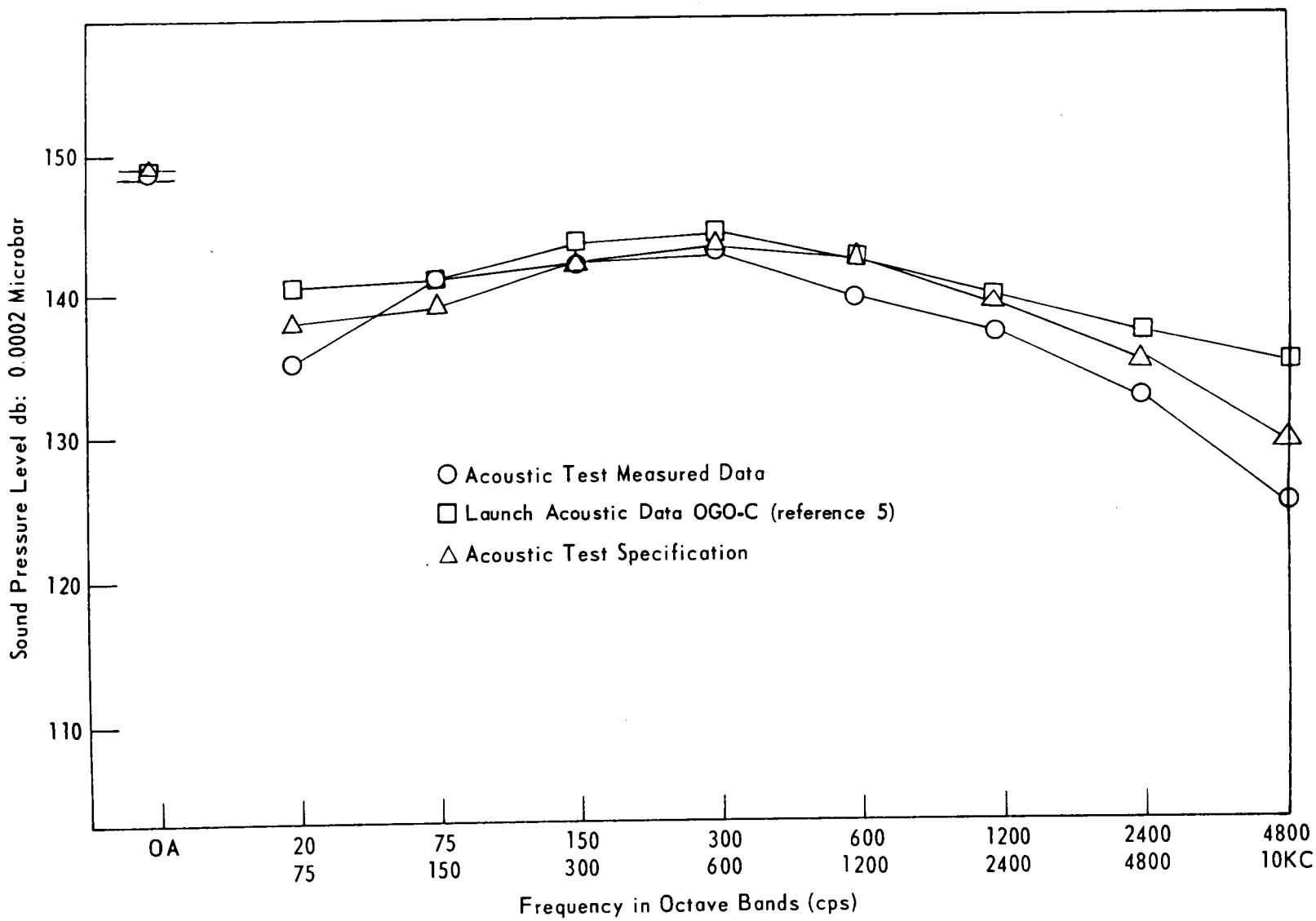

Figure 22. Comparison of Test Specification, Actual Test, and Measured Launch Acoustic Levels

TABLES

Table 1

OGO ACOUSTIC TEST SPECIFICATION LEVELS

Octave Band Frequency (cps)	Level (db)
20-75	138
75-150	139
150-300	142
300-600	143
600-1200	142
1200-2400	139
2400-4800	135
4800-10 kc	129
Overall level	149

The assigned tolerances were ± 3 db on both the overall and spectrum levels.

Table 2

PARTIAL LISTING OF ACCELEROMETER LOCATIONS

Test Plan Location	Description
C	-Z side of intercostal panel at the lower attachment point of the yaw reaction wheel assembly nearest center of spacecraft
D	Top of the pitch reaction wheel assembly at the attachment point adjoining the intercostal and nearest the center of the spacecraft
E	-X panel. Lower attachment point (nearest center of spacecraft) of battery unit No. 2
F	+X panel. Lower attachment point (nearest center of spacecraft) of battery unit No. 1
G	+X panel. Center attachment point along the lower edge of digital data-handling unit No. 1
H	+Z subsystem panel. Upper attachment point (nearest center of spacecraft) of tape recorder No. 1
I	-Z subsystem panel. At -X corner attachment point along upper edge for the command distribution unit
J	+Z experiment panel. Spacecraft station 337 near center of panel
K	+Z experiment panel. Spacecraft station 362 near center of panel
L	-Z experiment panel. Spacecraft station 364 near center of panel
M	-Z experiment panel. Spacecraft station 337 near center of panel

Table 3

OVERALL VIBRATION LEVELS AT REFERENCE LOCATION G RMS
(AGENA RING AT +27.5Z, -10.125X, STATION 418)

	SENSING ORIENTATION (RE:STL AXES)		
Run #	Y	X	Z
1B	2.65	3.35	4.50
2B	2.70	3.30	4.50
3B	2.80	3.33	4.75
4B	2.90	3.50	4.60
5B	2.75	3.35	4.85
6B	2.90	3.40	4.60
7 (high level)	3.60	5.70	4.39

NOTES:
1. Runs 1A through 5A were performed in the misoriented condition; thus the "B" series listed herein.
2. Overall vibration levels presented are in the 10-cps to 10-kc frequency band.

APPENDIX A

INSTRUMENTATION LOG

Table A-1

RUN #1-B

MEAS. NO.	RECORDER & TRACK NO.		TRANSDUCER LOCATION RE: TRW STATIONS		TRANSDUCER TYPE	SENSING DIRECTION RE: STL S/C AXIS	RMS VIBRATION LEVEL GRMS
	CP 100						10 cps - 10 kc**
1	1	AM	Voice Annotation & BCD Timing				
2	2	FM	Microphone Location II-A		Altec Mike 21BR-200	-Y	See Figure 9
3	3	FM	Microphone Location II-A (Internal)		B & K Mike 4134	-Y	See Figure 13
4	4	FM	Microphone Location I-C (Internal)		B & K Mike 4134	-Y	See Figure 12
5	5	FM	Base Interstage Fitting RV 1	+ 27 1/2 Z	Endevco Model #2221	Y	2.65
6	6	FM	Base Interstage Fitting RV 2	- 10 1/8 X	Endevco Model #2221	X	3.35
7	7	FM	Base Interstage Fitting RV 3	Sta. 418	Endevco Model #2221	Z	4.5
8	8	FM	Microphone Location I-A		Altec Mike 21BR-200	-Y	See Figure 10
9	9	FM	Top of S/C +Z Side - Y+X Corner		Endevco Model #2221	+Y	2.34
10	10	FM	Top of S/C +Z Side - Y+X Corner		Endevco Model #2221	+X	1.6
11	11	FM	Top of S/C +Z Side - Y+X Corner		Endevco Model #2221	+Z	3.4
12	12	FM	Horizon Scanner		Endevco Model #2228	+Y	3.18
13	13	FM	Horizon Scanner		Endevco Model #2228	+X	3.11
14	14	FM	Horizon Scanner		Endevco Model #2228	+Z	3.55
	FR 100 C						
15	1	FM	Base of EP-1 Box		Endevco Model #2228	+Y	2.25
16	2	FM	Base of EP-1 Box		Endevco Model #2228	+X	4.0
17	3	FM	Base of EP-1 Box		Endevco Model #2228	+Z	3.25
18	4	FM	Microphone Location I-D		Altec Mike 21BR-200	-Y	See Figure 10
19	5	AM	Base of EP-2 Box		Endevco Model #2228	+Y	2.65
20	5	AM	Base of EP-2 Box		Endevco Model #2228	+X	5.7
21	5	AM	Base of EP-2 Box		Endevco Model #2228	+Z	4.3
22	5	AM	Deleted from Test		---	---	---
23	5	AM	Deleted from Test		---	---	---
24	6	FM	Base of EP-5 Box		Endevco Model #2228	+Y	5.6
25	7	FM	Base of EP-5 Box		Endevco Model #2228	+X	6.0
26	8	FM	Base of EP-5 Box		Endevco Model #2228	+Z	3.35
27	9	FM	Base of EP-3 Box		Endevco Model #2228	Y	4.5
28	10	FM	Base of EP-3 Box		Endevco Model #2228	X	4.0
29	11	FM	Base of EP-3 Box		Endevco Model #2228	Z	3.8
30	12	FM	Microphone Location III-C		Altec Mike 21BR-200	-Y	See Figure 11
31	13	FM	Outer Skin Agena Section	Sta. 427	Endevco Model #2221	Z	25.0
32	14	AM	Voice & BCD Timing				

**Frequency Response of Track 5AM is 10 cps to 5 kc

Table A-2

RUN #2-B

MEAS. NO.	RECORDER & TRACK NO.		TRANSDUCER LOCATION RE: TRW STATIONS	TRANSDUCER TYPE	SENSING DIRECTION RE: STL S/C AXIS	RMS VIBRATION LEVEL GRMS
	CP 100					10 cps - 10 kc**
1	1	AM	Voice Annotation & BCD Timing			
2	2	FM	Microphone Location II-A	Altec Mike 21BR-200	-Y	See Figure 9
3	3	FM	Microphone Location II-A (Internal)	B&K Mike Model #4134	-Y	See Figure 13
4	4	FM	Microphone Location II-B (Internal)	B&K Mike Model #4134	-Y	—
5	5	FM	Base Interstage Fitting RV 1 + 27 1/2 Z	Endevco Model #2221C	X	2.7
6	6	FM	Base Interstage Fitting RV 2 - 10 1/8 X	Endevco Model #2221C	Y	3.3
7	7	FM	Base Interstage Fitting RV 3 Sta. 418	Endevco Model #2221C	Z	4.5
8	8	FM	Microphone Location III (Agena Internal)	Altec Mike 21BR-150	-Y	See Figure 14
9	9	FM	Base of EP-4 Box	Endevco Model #2228	Y	2.2
10	10	FM	Base of EP-4 Box	Endevco Model #2228	X	3.65
11	11	FM	Base of EP-4 Box	Endevco Model #2228	Z	9.5
12	12	FM	Top of Folded EP-6 Boom	Endevco Model #2221C	Y	1.0
13	13	FM	Top of Folded EP-6 Boom	Endevco Model #2221C	X	1.15
14	14	FM	Top of Folded EP-6 Boom	Endevco Model #2221C	Z	1.4
	FR 1300					
15	1	FM	1/3 Way Up -Z Gas Boom	Endevco Model #2221C	Y	3.0
16	2	FM	1/3 Way Up -Z Gas Boom	Endevco Model #2221C	X	2.85
17	3	FM	1/3 Way Up -Z Gas Boom	Endevco Model #2221C	Z	3.75
18	4	FM	Microphone Location I-C	Altec Mike 21BR-200	Y	See Figure 10
19	5	AM	Agena Section +28Z, +7X, Sta. 419.5	Endevco Model #2221C	Radial	8.0
20	5	AM	Agena Section +12Z, +9X, Sta. 419.5	Endevco Model #2221C	Radial	10.3
21	5	AM	Deleted - Noisy Channel	—	—	—
22	5	AM	Faulty Channel	Endevco Model #2221C	Y	2.2
23	5	AM	Deleted - Noisy Channel	—	—	—
24	6	FM	Base of 50 EP-1 Box	Endevco Model #2228	Y	5.3
25	7	FM	Base of 50 EP-1 Box	Endevco Model #2228	X	Faulty Cable
26	8	FM	Base of 50 EP-1 Box	Endevco Model #2228	Z	3.65
27	9	FM	Top Hinge on Main 50 EP-1 Panel	Endevco Model #2221C	Y	1.6
28	10	FM	Top Hinge on Main 50 EP-1 Panel	Endevco Model #2221C	X	1.65
29	11	FM	Top Hinge on Main 50 EP-1 Panel	Endevco Model #2221C	Z	1.75
30	12	FM	Microphone Location II Inside S/C Box	Altec Mike 21BR-150	-Y	See Figure 13
31	13	FM	Microphone Location III-D (Agena Internal)	Altec Mike 21BR-150	Radial	See Figure 14
32	14	AM	Voice & BCD Timing			

**Frequency Response of Track #5 AM is 10 cps to 5 kc

Table A-3

RUN #3-B

MEAS. NO.	RECORDER & TRACK NO.	TRANSDUCER LOCATION RE: TRW STATIONS	TRANSDUCER TYPE	SENSING DIRECTION RE: STL S/C AXIS	RMS VIBRATION LEVEL GRMS
	CP 100				10 cps - 10 kc**
1	1 AM	Voice Annotation & BCD Timing			
2	2 FM	Microphone Location II-A	Altec Mike 21BR-200	-Y	See Figure 9
3	3 FM	Microphone Location II-A (Internal)	B & K Mike 4134	-Y	See Figure 13
4	4 FM	Microphone Location III-B (Agena Internal)	B & K Mike 4134	-X	Faulty Mike
5	5 FM	Base of Interstage Fitting RV 1 + 27 1/2 Z	Endevco Model #2221C	Y	2.8
6	6 FM	Base of Interstage Fitting RV 2 - 10 1/8 X	Endevco Model #2221C	X	3.33
7	7 FM	Base of Interstage Fitting RV 3 Sta. 418	Endevco Model #2221C	Z	4.75
8	8 FM	Microphone Location I-B	Altec Mike 21BR-200	-Y	See Figure 10
9	9 FM	Solar Panel, 1/2 Way Between Supports on SPAR	Endevco Model #2221	X	2.2
10	10 FM	Solar Panel, 1/2 Way Between Supports on SPAR	Endevco Model #2221	Z	0.95
11	11 FM	Inside Edge of Solar Panel (SOEP-1)	Endevco Model #2221	X	3.0
12	12 FM	Deployment Hinge on Solar Panel (SOEP-1)	Endevco Model #2223	Y	0.82
13	13 FM	Deployment Hinge on Solar Panel (SOEP-1)	Endevco Model #2223	X	1.4
14	14 FM	Deployment Hinge on Solar Panel (SOEP-1)	Endevco Model #2223	Z	1.07
	FR 1300				
15	1 FM	Deployment Hinge OPEP-1	Endevco Model #2221	Y	1.8
16	2 FM	Deployment Hinge OPEP-1	Endevco Model #2221	X	2.25
17	3 FM	Deployment Hinge OPEP-1	Endevco Model #2221	Z	1.45
18	4 FM	Microphone Location III-B	Altec Mike 21BR-200	-Y	See Figure 11
19	5 AM	Agena IRP Mounting -2Z -12X Sta. 437	Endevco Model #2221	Radial	9
20	5 AM	Agena IRP Mounting -2Z -28X Sta. 437	Endevco Model #2221	Radial	16
21	5 AM	137 KC Channel Deleted - Noisy	—	—	—
22	5 AM	Faulty Channel	—	—	—
23	5 AM	212.5 KC Channel Deleted - Noisy	—	—	—
24	6 FM	Base of OPEP-1 Box	Endevco Model #2221	Y	1.4
25	7 FM	Base of OPEP-1 Box	Endevco Model #2221	X	2.2
26	8 FM	Base of OPEP-1 Box	Endevco Model #2221	Z	2.0
27	9 FM	-Z Experiment Panel Location L*	Endevco Model #2223	Y	2.5
28	10 FM	-Z Experiment Panel Location L*	Endevco Model #2223	X	2.5
29	11 FM	-Z Experiment Panel Location L*	Endevco Model #2223	Z	3.0
30	12 FM	Microphone Location II-B	Altec Mike 21BR-200	-Y	See Figure 9
31	13 FM	Base of S/C Box, -X +Z Corner	Endevco Model #2221	Y	1.85
32	14 AM	Voice Annotation & BCD Timing			

*For definition of accelerometer location see Table 2

**Frequency Response of Track #5AM is 10 cps to 5 kc

Table A-4

RUN #4-B

MEAS. NO.	RECORDER & TRACK NO.		TRANSDUCER LOCATION RE: TRW STATIONS	TRANSDUCER TYPE	SENSING DIRECTION RE: STL S/C AXIS	RMS VIBRATION LEVEL GRMS
	CP 100					10 cps - 10 kc**
1	1	AM	Voice Annotation & BCD Timing			
2	2	FM	Microphone Location II-A	Altec Mike 21BR-200	-Y	See Figure 9
3	3	FM	Microphone Location II-A (Internal)	B & K Mike 4134	-Y	See Figure 13
4	4	FM	External Skin of AFMB Sta. 418 & -6.5X	Endevco Model #2221C	Radial	Faulty Cable
5	5	FM	Base of Interstage Fitting RV 1 + 27 1/2 Z	Endevco Model #2221C	Y	2.9
6	6	FM	Base of Interstage Fitting RV 2 - 10 1/8 X	Endevco Model #2221C	X	3.5
7	7	FM	Base of Interstage Fitting RV 3 Sta. 418	Endevco Model #2221C	Z	4.6
8	8	FM	Microphone Location II-D	Altec Mike 21BR-200	-Y	See Figure 9
9	9	FM	-Z Experiment Panel Location M*	Endevco Model #2223	Y	2.05
10	10	FM	-Z Experiment Panel Location M*	Endevco Model #2223	X	3.2
11	11	FM	-Z Experiment Panel Location M*	Endevco Model #2223	Z	2.35
12	12	FM	+Z Experiment Panel Location J*	Endevco Model #2223	Y	2.3
13	13	FM	+Z Experiment Panel Location J*	Endevco Model #2223	X	2.1
14	14	FM	+Z Experiment Panel Location J*	Endevco Model #2223	Z	3.45
	FR 1300					
15	1	FM	+Z Experiment Panel Location K*	Endevco Model #2223	Y	1.9
16	2	FM	+Z Experiment Panel Location K*	Endevco Model #2223	X	1.8
17	3	FM	+Z Experiment Panel Location K*	Endevco Model #2223	Z	2.1
18	4	FM	Microphone Location III-A	Altec Mike 21BR-200	-X	See Figure 11
19	5	AM	Mixer Box Mounting +13.2Z - 7.2X Sta. 421	Endevco Model #2221	Radial	11.3
20	5	AM	On Mixer Box +15.2Z - 7.2X Sta. 421	Endevco Model #2221	Radial	5.0
21	5	AM	Deleted - Noisy Channel	—	—	—
22	5	AM	Faulty Channel	—	—	—
23	5	AM	Deleted	—	—	—
24	6	FM	Test Plan Location E*	Endevco Model #2228	Y	4.7
25	7	FM	Test Plan Location E*	Endevco Model #2228	X	5.4
26	8	FM	Test Plan Location E*	Endevco Model #2228	Z	2.1
27	9	FM	Deleted	—	—	—
28	10	FM	Deleted	—	—	—
29	11	FM	Deleted	—	—	—
30	12	FM	Microphone Location II-C	Altec Mike 21BR-200	-Y	See Figure 9
31	13	FM	Deleted	—	—	—
32	14	AM	Voice Annotation & BCD Timing			

*For definition of accelerometer location, see Table 2

**Frequency Response of Track #5AM is 10 cps to 5 kc

Table A-5

RUN #5-B

MEAS. NO.	RECORDER & TRACK NO.	TRANSDUCER LOCATION RE: TRW STATIONS	TRANSDUCER TYPE	SENSING DIRECTION RE: STL S/C AXIS	RMS VIBRATION LEVEL GRMS
	CP 100				10 cps - 10 kc***
1	1 AM	Voice Annotation & BCD Timing			
2	2 FM	Microphone Location II-A	Altec Mike 21BR-200	-Y	See Figure 9
3	3 FM	Microphone Location II-A (Internal)	B&K Mike	-Y	See Figure 13
4	4 FM	Agena Ring Beneath Interstage Fitting	Endevco Model #2221	Y	3.65
5	5 FM	Base of Interstage Fitting RV 1 + 27 1/2 Z	Endevco Model #2221C	Y	2.75
6	6 FM	Base of Interstage Fitting RV 2 - 10 1/8 X	Endevco Model #2221C	X	3.35
7	7 FM	Base of Interstage Fitting RV 3 Sta. 418	Endevco Model #2221C	Z	4.85
8	8 FM	Microphone Location IV-Interstage (Internal)	Altec Mike 21BR-150	X	See Figure 14
9	9 FM	-Z Side Intercoastal Panel Location C*	Endevco Model #2228B	Y	2.75
10	10 FM	-Z Side Intercoastal Panel Location C*	Endevco Model #2228B	X	10.5
11	11 FM	-Z Side Intercoastal Panel Location C*	Endevco Model #2228B	Z	2.65
12	12 FM	Base of S/C -X +Z Interstage Fitting	Endevco Model #2221	Y	Faulty Cable
13	13 FM	Base of S/C -X +Z Interstage Fitting	Endevco Model #2221	X	1.5
14	14 FM	Base of S/C -X +Z Interstage Fitting	Endevco Model #2221	Z	2.7
	FR 1300				
15	1 FM	Base Interstage Fitting + 27 1/2 Z	Endevco Model #2221	Y	Faulty Cable
16	2 FM	Base Interstage Fitting + 9 1/2 X	Endevco Model #2221	X	3.56
17	3 FM	Base Interstage Fitting Sta. 418	Endevco Model #2221	Z	4.8
18	4 FM	Microphone III-A	Altec Mike 21BR-200	-X	See Figure 11
19	5 AM	STL Test Plan Location D*	Endevco Model #2228	Y	
20	5 AM	STL Test Plan Location D*	Endevco Model #2228	X	5.4
21	5 AM	Deleted - Noisy Channel	—	—	—
22	5 AM	Faulty Channel	—	—	—
23	5 AM	Deleted - Noisy Channel	—	—	—
24	6 FM	Test Plan Location G*	Endevco Model #2223	Y	5
25	7 FM	Test Plan Location G*	Endevco Model #2223	X	3.9
26	8 FM	Test Plan Location G*	Endevco Model #2223	Z	Faulty Cable
27	9 FM	+Z Subsystem Panel Location H*	Endevco Model #2228	Y	Faulty Cable
28	10 FM	+Z Subsystem Panel Location H*	Endevco Model #2228	X	Faulty Cable
29	11 FM	+Z Subsystem Panel Location H*	Endevco Model #2228	Z	Faulty Cable
30	12 FM	Microphone Location III-D	Altec Mike 21BR-200	-Y	See Figure 11
31	13 FM	Microphone Location III-C	Altec Mike 21BR-200	-X	See Figure 11
32	14 AM	Voice Annotation & BCD Timing			

*For definition of accelerometer location see Table 2

***Frequency Response of Track #5 is 10 cps to 5 kc

Table A-6

RUN #6-B

MEAS. NO.	RECORDER & TRACK NO.		TRANSDUCER LOCATION RE: TRW STATIONS		TRANSDUCER TYPE	SENSING DIRECTION RE: STL S/C AXIS	RMS VIBRATION LEVEL GRMS
	CP 100						10 cps - 10 kc**
1	1	AM	Voice Annotation & BCD Timing				
2	2	FM	Microphone Location II-A		Altec Mike 21BR-200	-Y	See Figure 9
3	3	FM	Microphone Location II-A (Internal)		B&K Mike 4134	-Y	See Figure 13
4	4	FM	Microphone Location I-C (Internal)		B&K Mike 4134	-Y	See Figure 12
5	5	FM	Base of Interstage Fitting	+ 27 1/2 Z	Endevco Model #2221	Y	2.9
6	6	FM	Base of Interstage Fitting	- 10 1/8 X	Endevco Model #2221	X	3.4
7	7	FM	Base of Interstage Fitting	Sta. 418	Endevco Model #2221	Z	4.6
8	8	FM	Microphone Location I-A		Altec Mike 21BR-200	-Y	See Figure 10
9	9	FM	-Z Subsystem Panel Location I*		Endevco Model #2228	Y	2.65
10	10	FM	-Z Subsystem Panel Location I*		Endevco Model #2228	X	3.05
11	11	FM	-Z Subsystem Panel Location I*		Endevco Model #2228	Z	13.0
12	12	FM	Base of EP-6 Box		Endevco Model #2221	Y	Faulty Cable
13	13	FM	Base of EP-6 Box		Endevco Model #2221	X	2.25
14	14	FM	Base of EP-6 Box		Endevco Model #2221	Z	2.05
	FR 100 C						
15	1	FM	Base of S/C Box +X +Z Interstage Fitting		Endevco Model #2221	Y	2.2
16	2	FM	Base of S/C Box -X +Z Interstage Fitting		Endevco Model #2221	X	2.2
17	3	FM	Base of S/C Box +X +Z Interstage Fitting		Endevco Model #2221	Z	1.6
18	4	FM	Center Test Article 5 Ft. Below RA 1 ONMIC. Std. (Ext.)		Altec Mike 21BR-200	-Y	
19	5	AM	Base of Interstage Fitting	+ 10 1/8 Z, + 27 1/2 X	Endevco Model #2221	Y	3.2
20	5	AM	Base of Interstage Fitting	Sta. 418	Endevco Model #2221	X	5.3
21	5	AM	Deleted - Noisy Channel		—	—	—
22	5	AM	Faulty Channel		—	—	—
23	5	AM	Deleted - Noisy Channel		—	—	—
24	6	FM	Base of Interstage Fitting	+ 10 1/8 Z	Endevco Model #2221		
25	7	FM	Base of Interstage Fitting	- 27 1/2 X	Endevco Model #2221	X	4.45
26	8	FM	Base of Interstage Fitting	Sta. 418	Endevco Model #2223	Z	3.16
27	9	FM	Top of Pressure Vessel		Endevco Model #2223	Y	Faulty Cable
28	10	FM	Top of Pressure Vessel		Endevco Model #2223	X	Faulty Cable
29	11	FM	Top of Pressure Vessel		Endevco Model #2223	Z	Faulty Cable
30	12	FM	Microphone Location III (Agena Internal)		Altec Mike 21BR-150	Y	See Figure 14
31	13	FM	Center, (-Z Upper Experiment Panel)		Endevco Model #2221	Z	10.7
32	14	AM	Voice Annotation & BCD Timing		Endevco Model #2221	Z	

*For definition of accelerometer location, see Table 2

**Frequency Response of Track #5AM is 10 cps to 10 kc

Table A-7

RUN #7 (HIGH LEVEL RUN)

MEAS. NO.	RECORDER & TRACK NO.	TRANSDUCER LOCATION RE: TRW STATIONS	TRANSDUCER TYPE	SENSING DIRECTION RE: STL S/C AXIS	RMS VIBRATION LEVEL GRMS
	CP 100				10 cps - 10 kc**
1	1 AM	Voice Annotation & BCD Timing			
2	2 FM	Microphone Location II-A	Altec Mike 21BR-200	-Y	See Figure 19
3	3 FM	Microphone Location II-A (Internal)	B&K Mike 4134	-Y	See Figure 19
4	4 FM	Microphone Location II ℄ Inside S/C Box	B&K Mike 4134	-Y	See Figure 19
5	5 FM	Base of S/C Box -X-Z Interstage Fitting + 10 1/8 Z	Endevco Model #2221	Y	3.6
6	6 FM	Base of S/C Box -X-Z Interstage Fitting - 27 1/2 X	Endevco Model #2221	X	5.7
7	7 FM	Base of S/C Box -X-Z Interstage Fitting Sta. 418	Endevco Model #2221	Z	4.39
8	8 FM	Microphone Location III-A	Altec Mike 21BR-200	-Y	See Figure 19
9	9 FM	Base of Interstage Fitting + 10 1/8 Z	Endevco Model #2221	Y	4.4
10	10 FM	Base of Interstage Fitting + 27 1/2 X	Endevco Model #2221	X	7.07
11	11 FM	Base of Interstage Fitting Sta. 418	Endevco Model #2221	Z	5.1
12	12 FM	STL Test Plan Location D*	Endevco Model #2228	Z	2.95
13	13 FM	STL Test Plan Location G*	Endevco Model #2223	X	4.9
14	14 FM	Deployment Hinge OPEP-1	Endevco Model #2221	X	3.95
	FR 1300				
15	1 FM	-Z Experiment Panel Location M*	Endevco Model #2223	Y	3.0
16	2 FM	-Z Experiment Panel Location M*	Endevco Model #2223	X	2.3
17	3 FM	-Z Experiment Panel Location M*	Endevco Model #2223	Z	3.35
18	4 FM	Microphone Location II-A	Altec Mike 21BR-200	-Y	See Figure 19
19	5 AM	Solar Panel Halfway Between Supports on SPAR	Endevco Model #2221	X	2.8
20	5 AM	Agena IRP Mounting -2Z, -28X Sta. 437	Endevco Model #2221	Radial	21
21	5 AM	Deleted - Noisy	---	---	---
22	5 AM	Faulty Channel	---	---	---
23	5 AM	Deleted - Noisy	---	---	---
24	6 FM	+Z Experiment Panel Location J*	Endevco Model #2223	Y	3.25
25	7 FM	+Z Experiment Panel Location J*	Endevco Model #2223	X	3.16
26	8 FM	+Z Experiment Panel Location J*	Endevco Model #2223	Z	4.2
27	9 FM	Center, -Z Upper Experiment Panel	Endevco Model #2221	Z	4.25
28	10 FM	External Skin Agena Section Sta. 427	Endevco Model #2221	Radial	10.0
29	11 FM	Base of EP-4 Box	Endevco Model #2228	Z	5.0
30	12 FM	Microphone Location II- ℄ (Internal)	Altec Mike 21BR-150	-Y	See Figure 19
31	13 FM	Base of SOEP-1 Box	Endevco Model #2228	Y	4.0
32	14 AM	Voice Annotation & BCD Timing			

*For definition of accelerometer location, see Table 2

**Frequency Response of Track #5AM is 10 cps to 5 kc

APPENDIX B

VIBRATION RESPONSE DATA

APPENDIX B (continued)

VIBRATION RESPONSE DATA

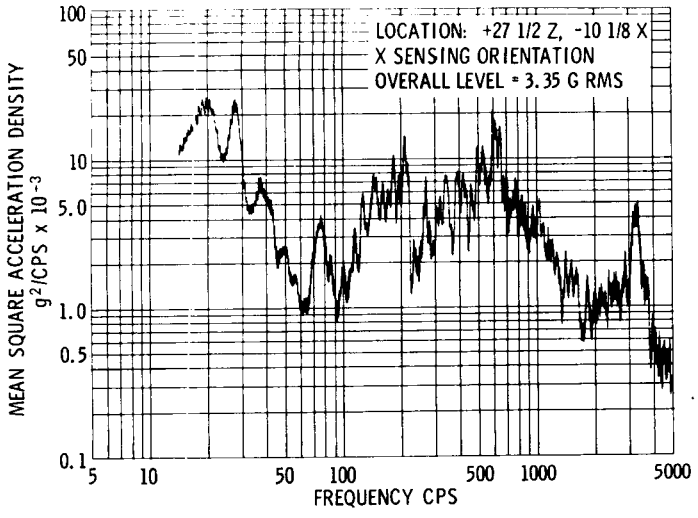

B-1-a

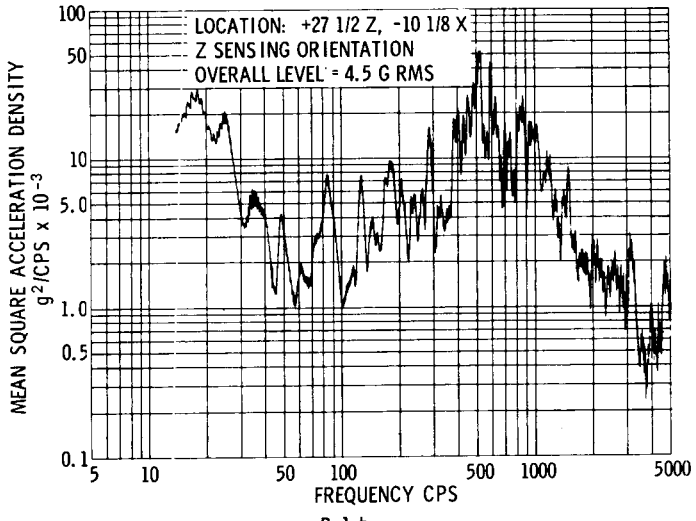

B-1-b

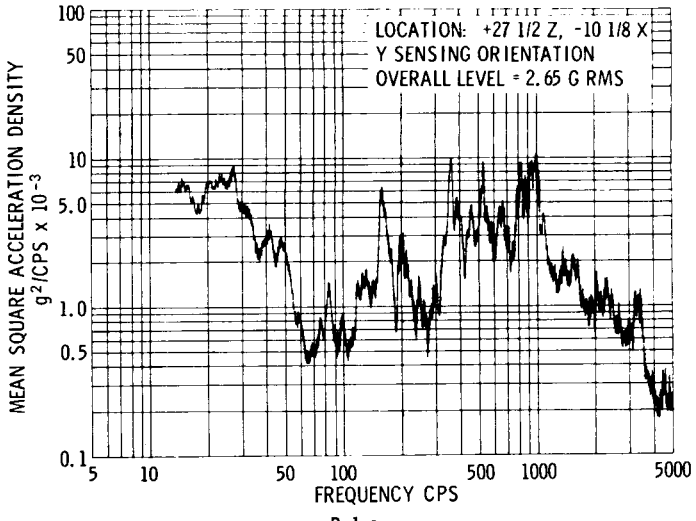

B-1-c

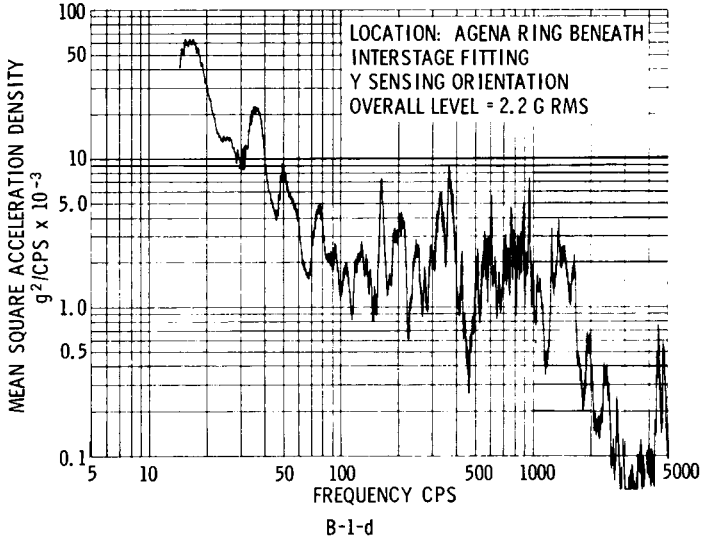

B-1-d

Figure B-1. Base of Interstage Fitting, Station 418

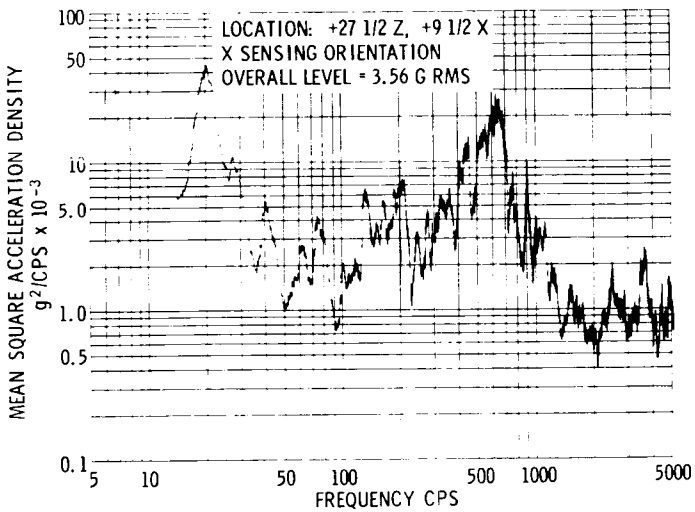

B-2-a

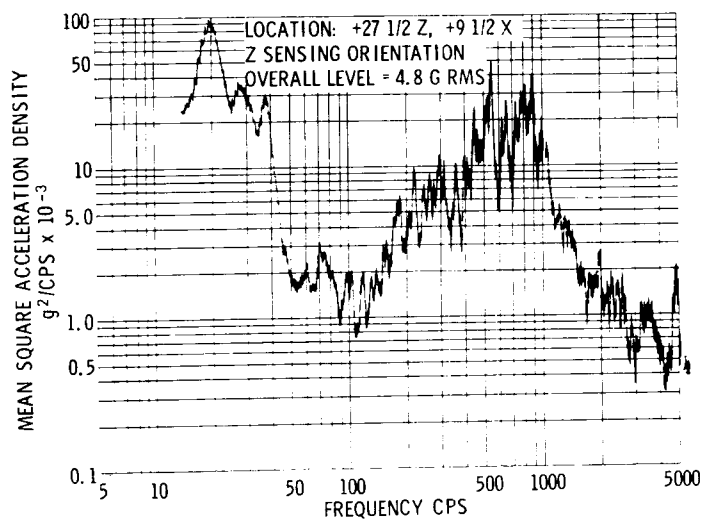

B-2-b

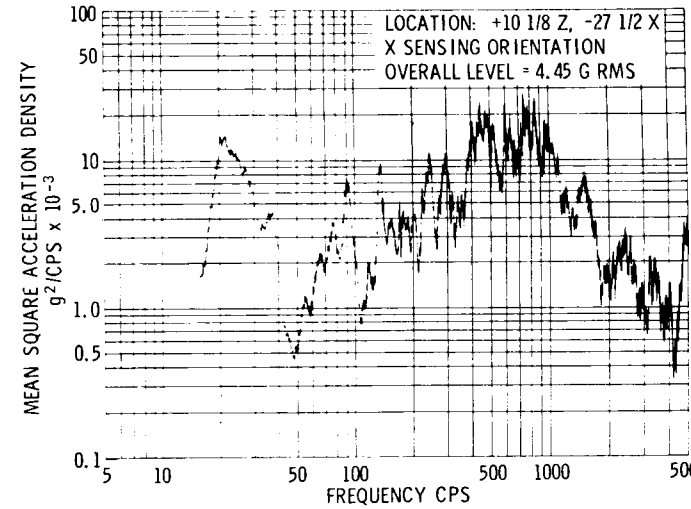

B-2-c

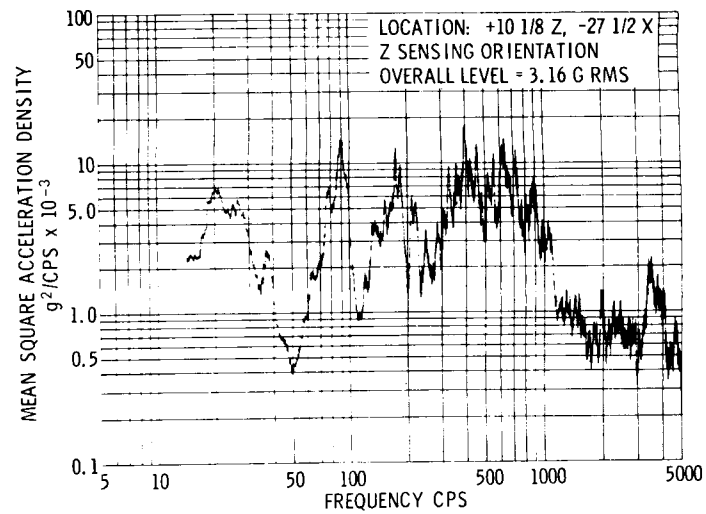

B-2-d

Figure B-2. Base of Interstage Fitting, Station 418

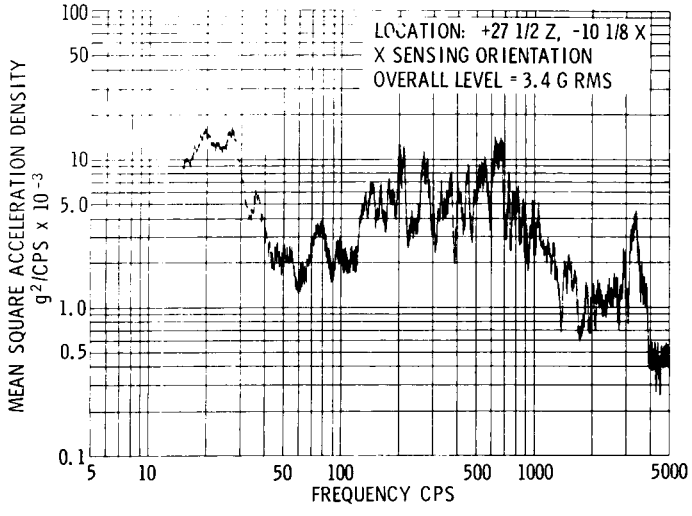

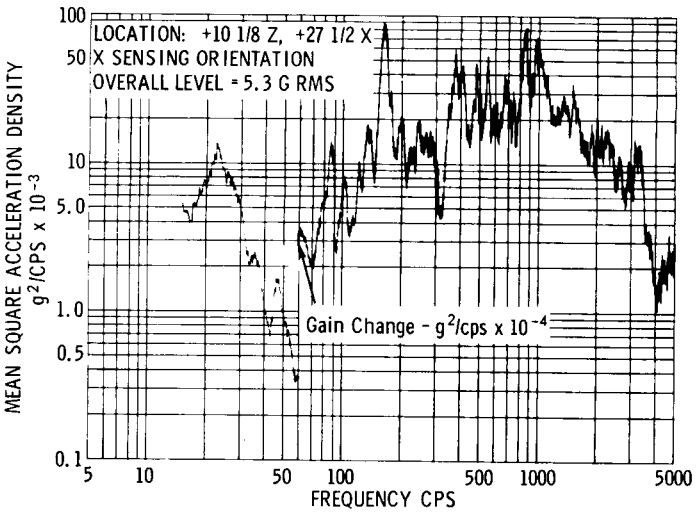

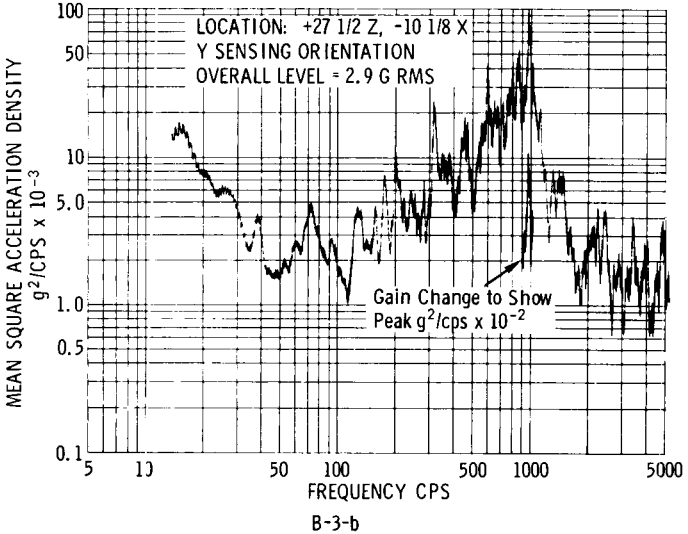

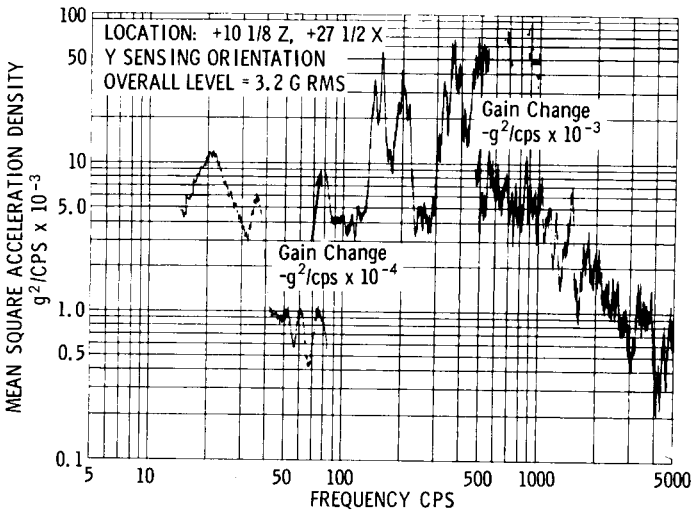

Figure B-3. Base of Interstage Fitting, Station 418

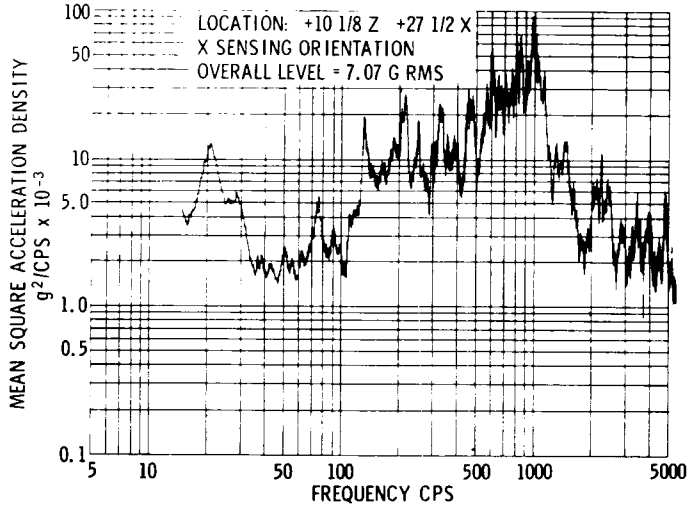

B-4-a

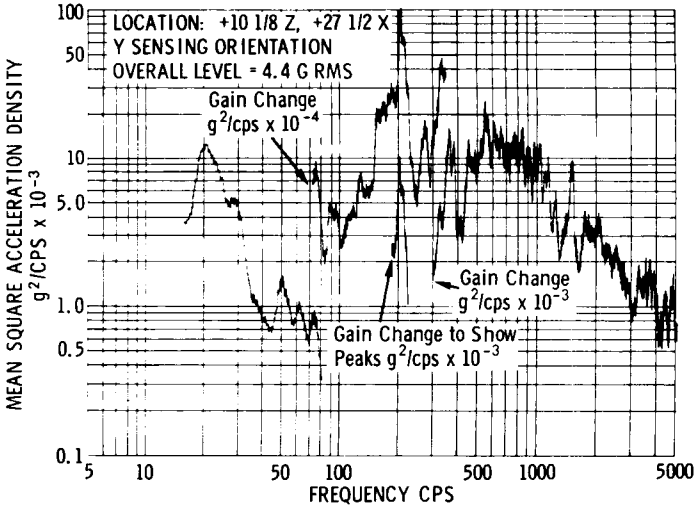

B-4-b

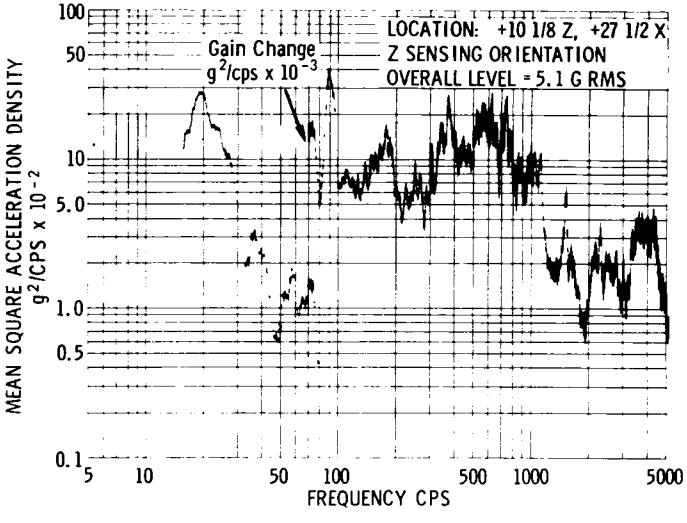

B-4-c

Figure B-4. Base of Interstage Fitting, Station 418 (High-Level Run)

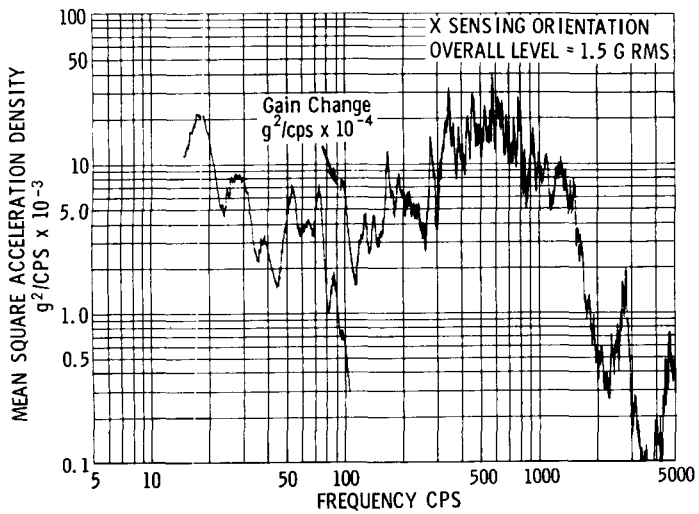

B-5-a

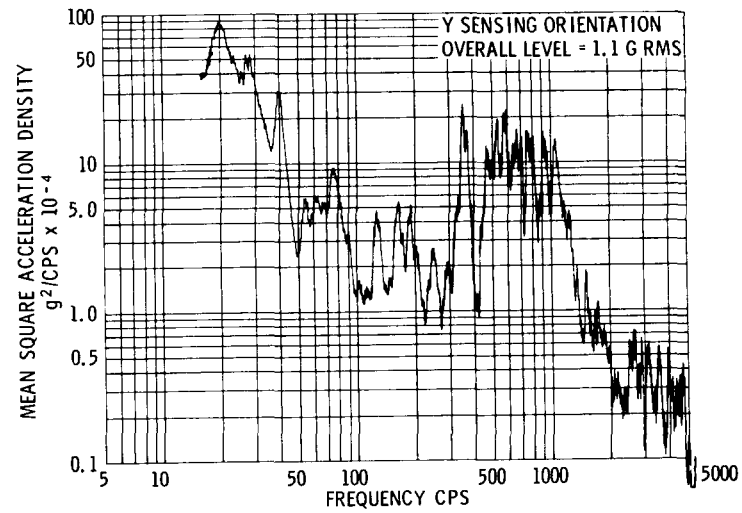

B-5-b

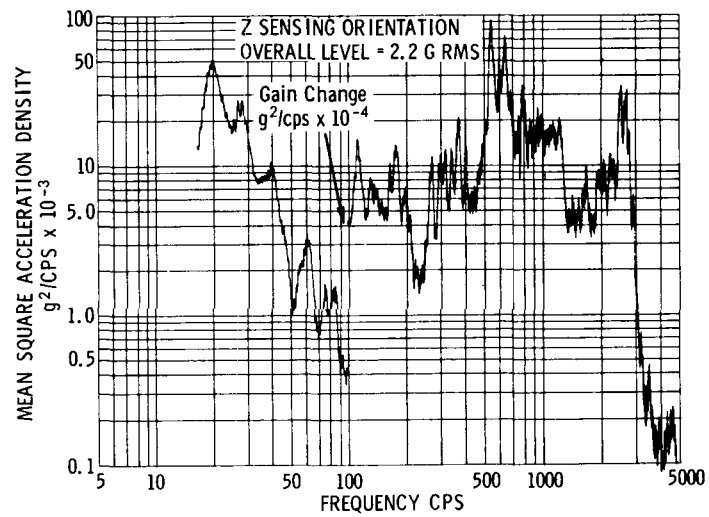

B-5-c

Figure B-5. Base of Spacecraft Box, –X–Z Corner

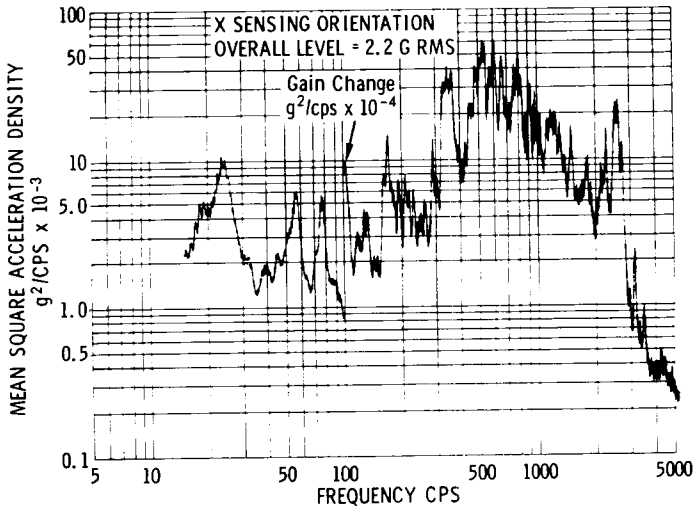

B-6-a

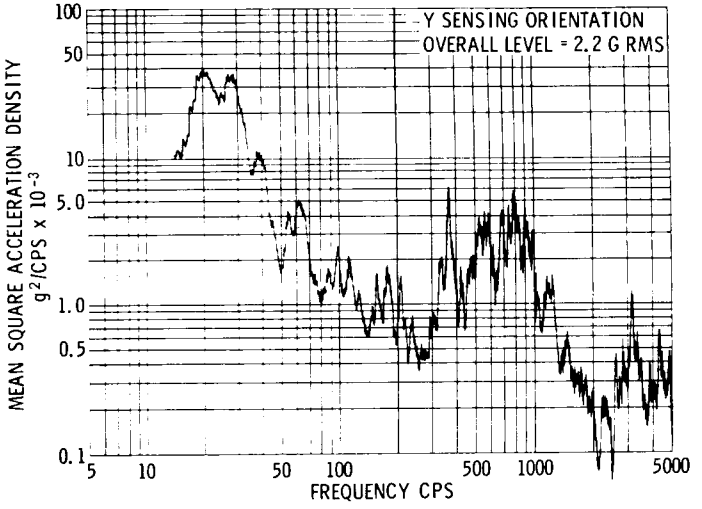

B-6-b

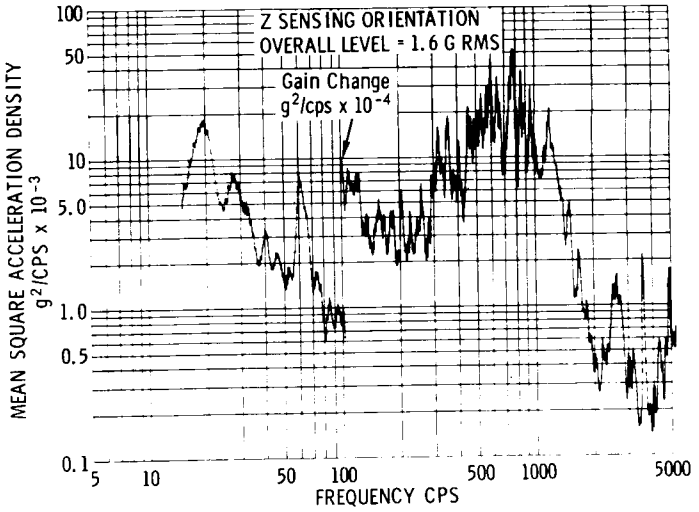

B-6-c

Figure B-6. Base of Spacecraft Box, +X +Z Corner

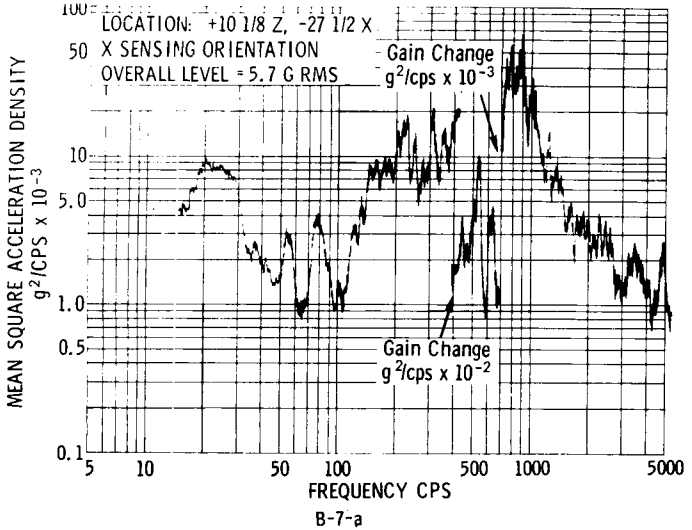

B-7-a

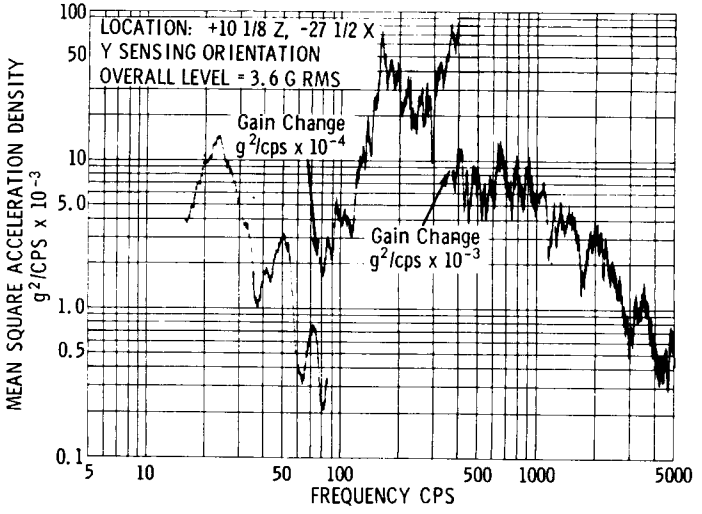

B-7-b

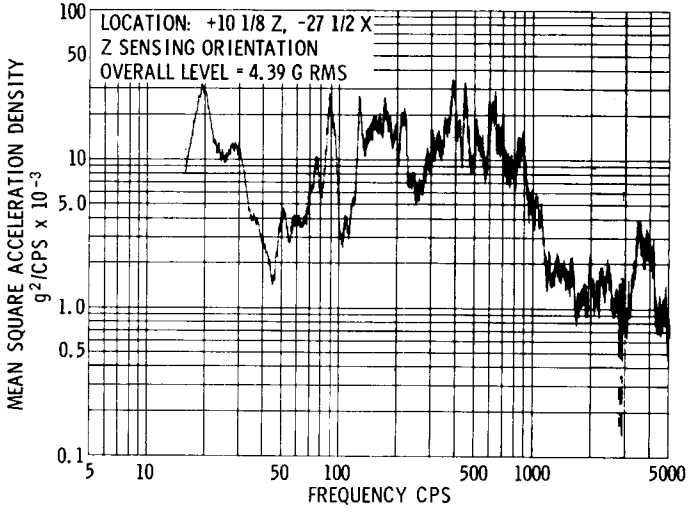

B-7-c

Figure B-7. Base of Spacecraft Box, –X–Z Corner, Station 418 (High-Level Run)

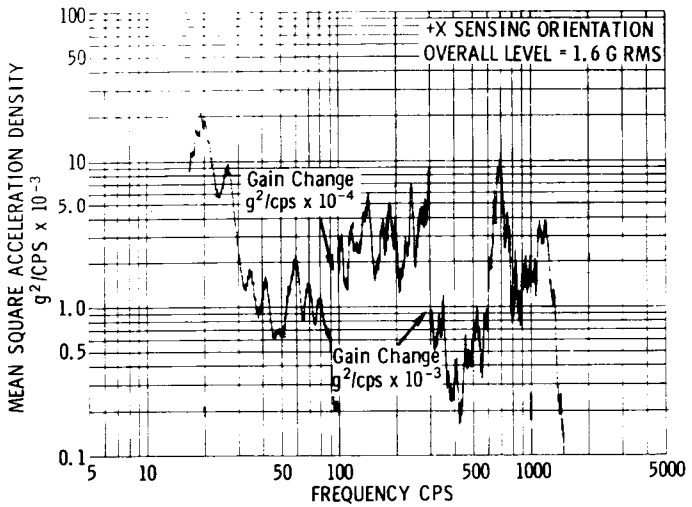

B-8-a

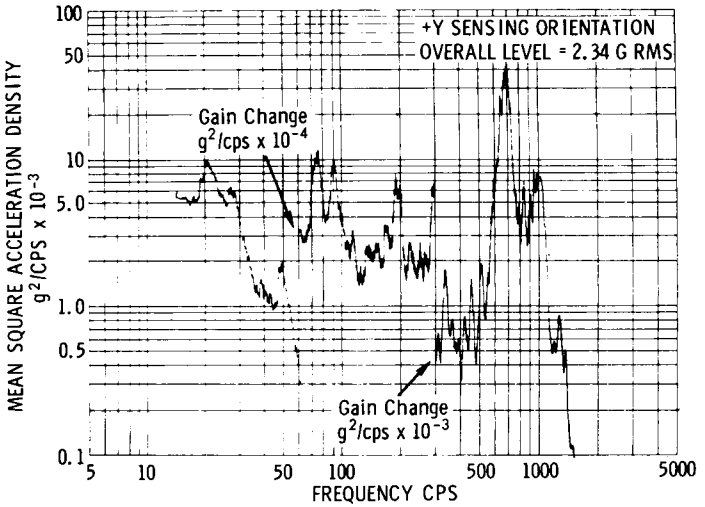

B-8-b

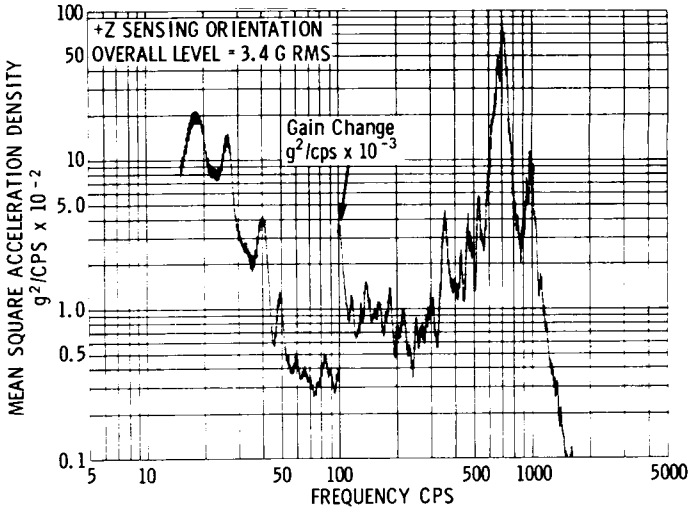

B-8-c

Figure B-8. Top of Spacecraft, +Z Side, −Y+X Corner

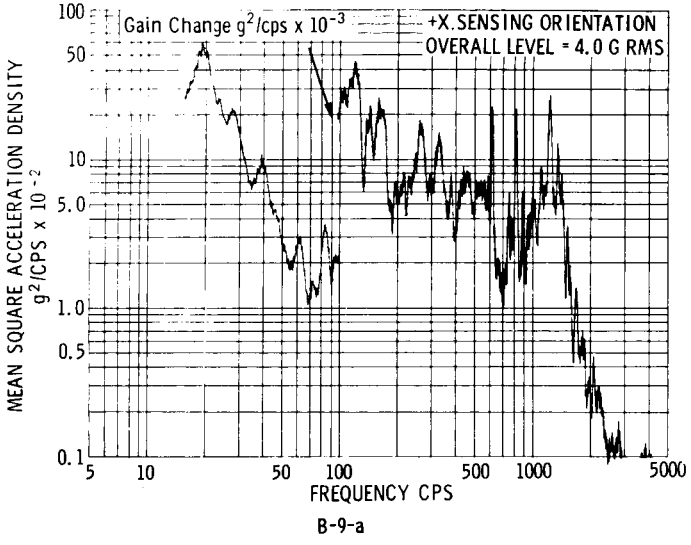

B-9-a

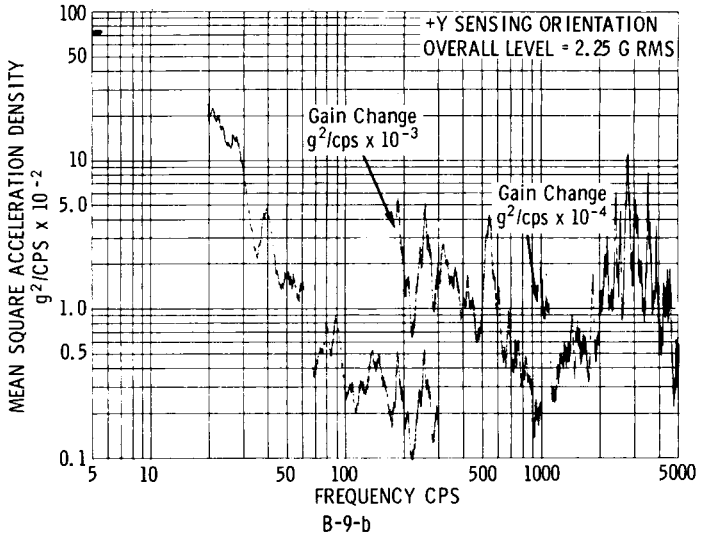

B-9-b

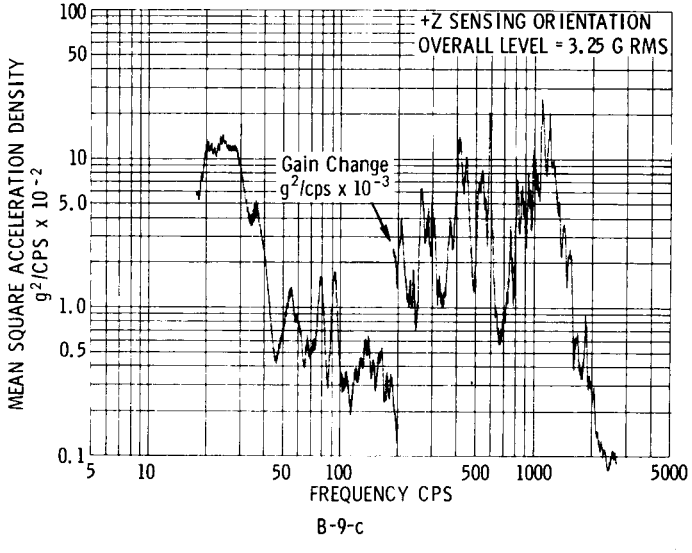

B-9-c

Figure B-9. Base of EP-1 Box

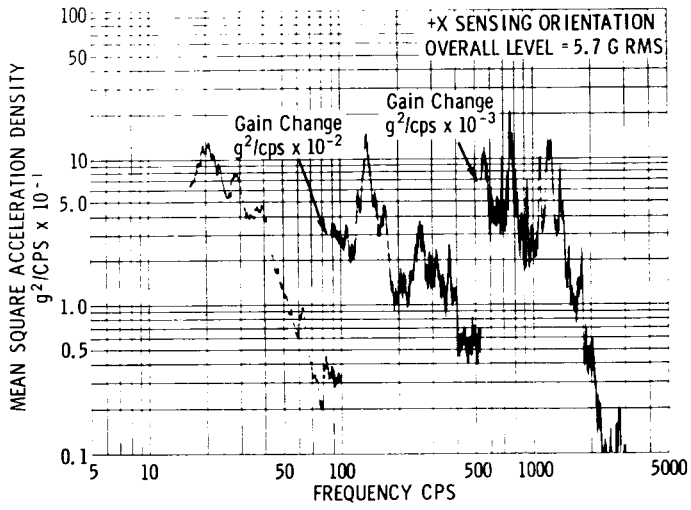

B-10-a

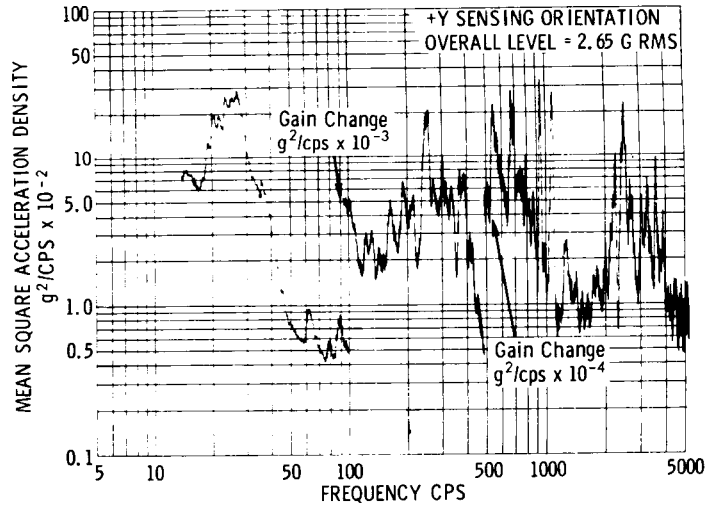

B-10-b

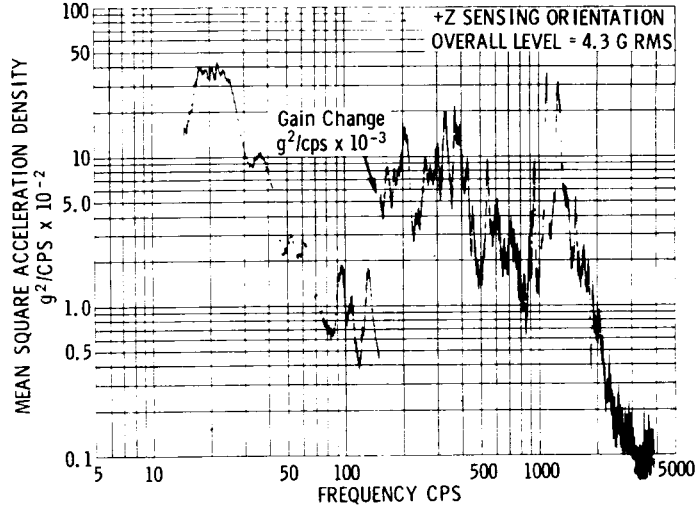

B-10-c

Figure B-10 Base of EP-2 Box

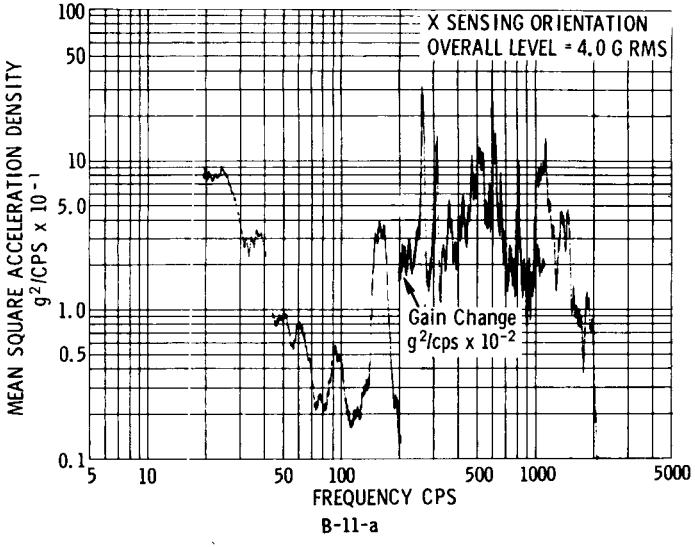

B-11-a

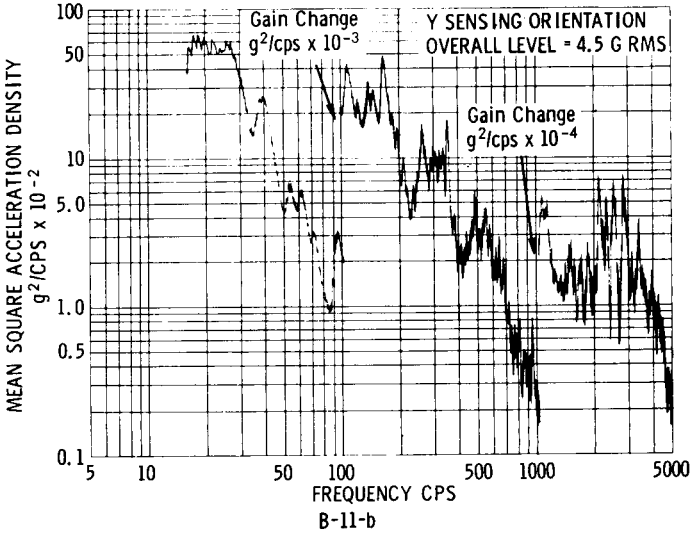

B-11-b

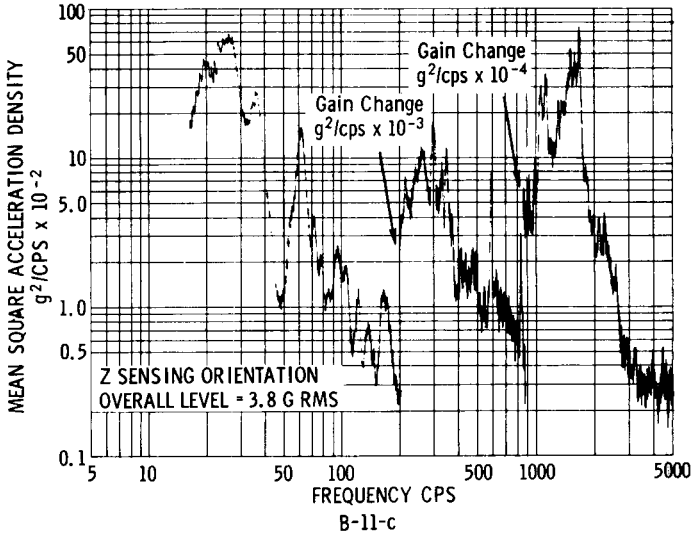

B-11-c

Figure B-11 Base of EP-3 Box

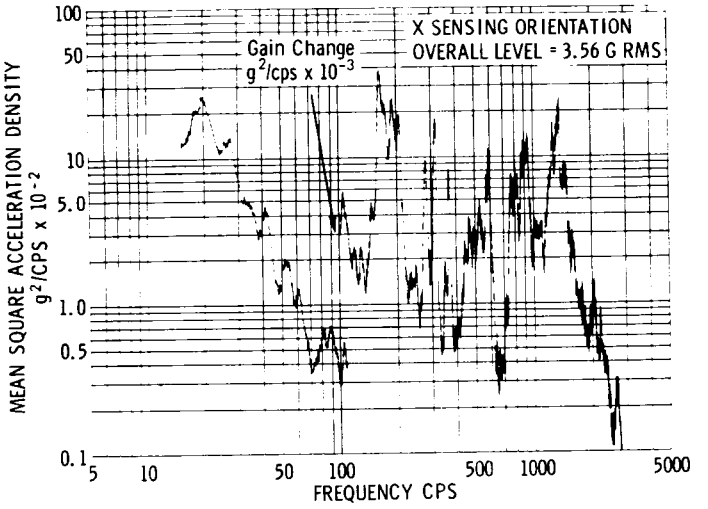

B-12-a

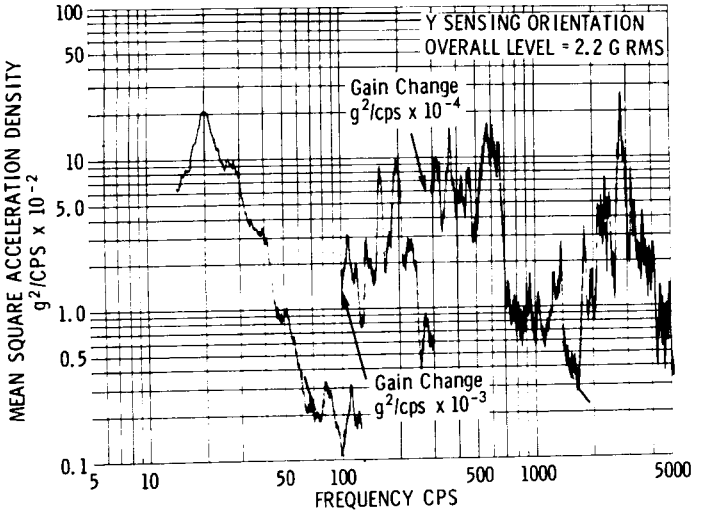

B-12-b

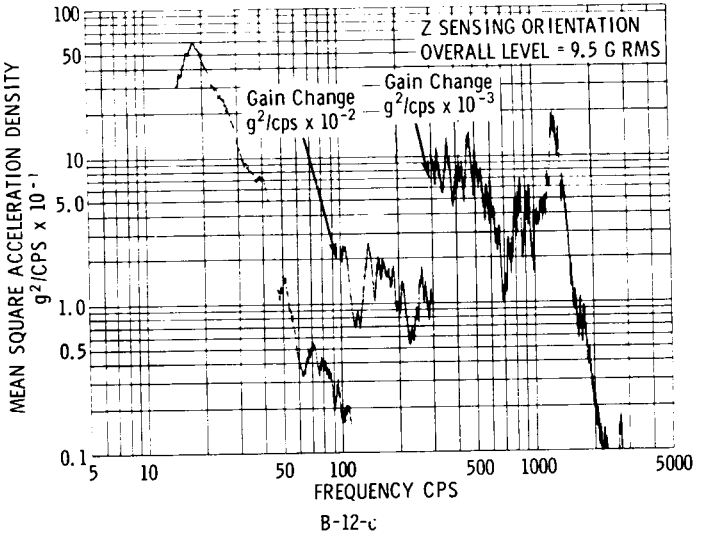

B-12-c

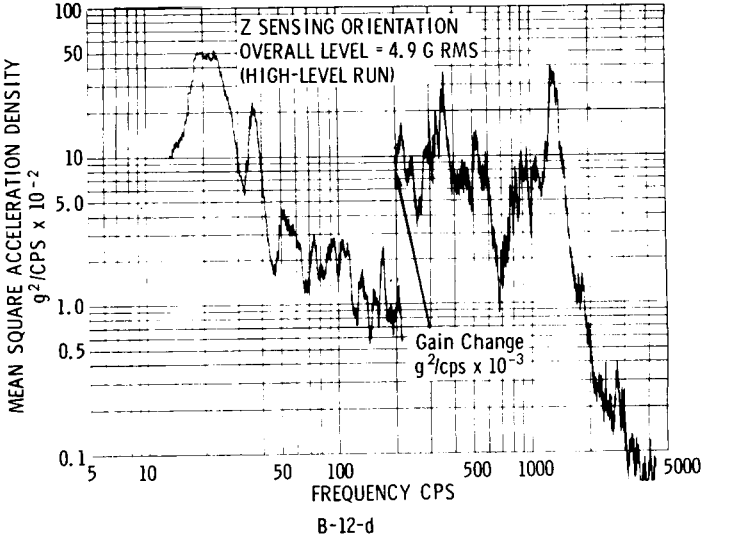

B-12-d

Figure B-12. Base of EP-4 Box

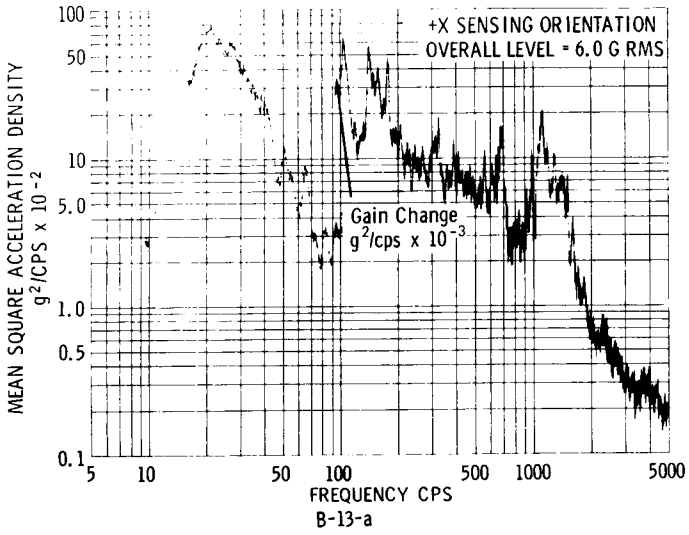

B-13-a

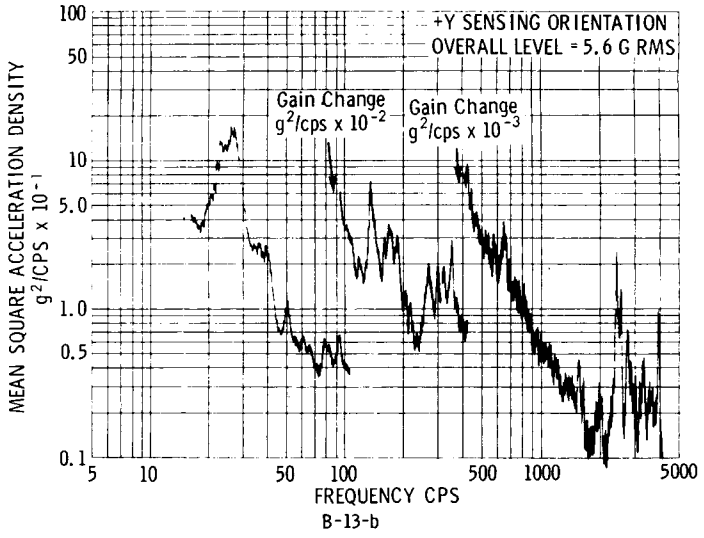

B-13-b

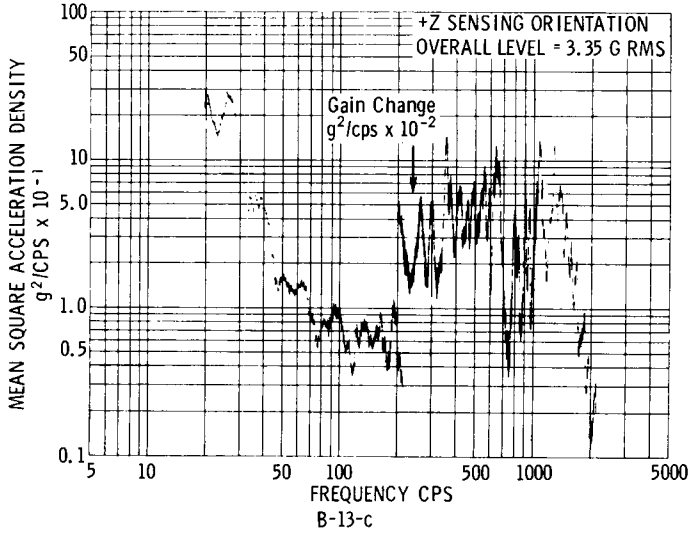

B-13-c

Figure B-13. Base of EP-5 Box

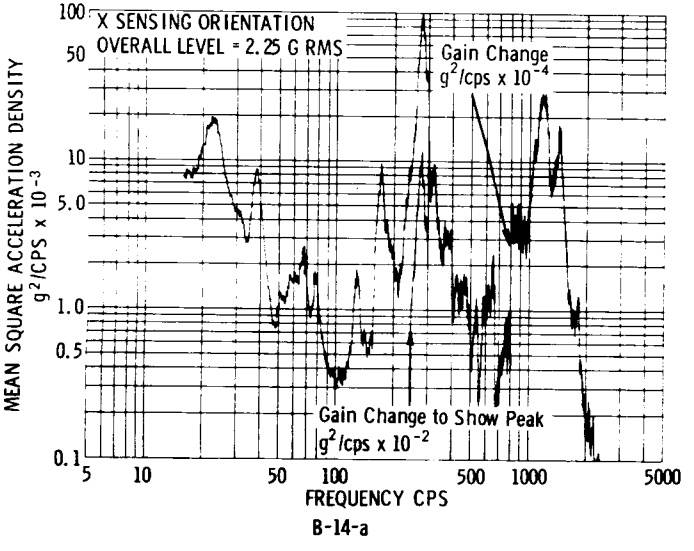

B-14-a

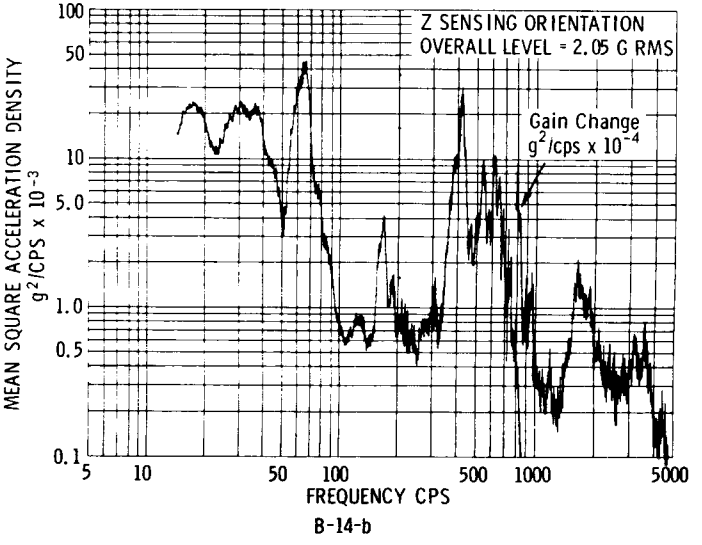

B-14-b

Figure B-14. Base of EP-6 Box

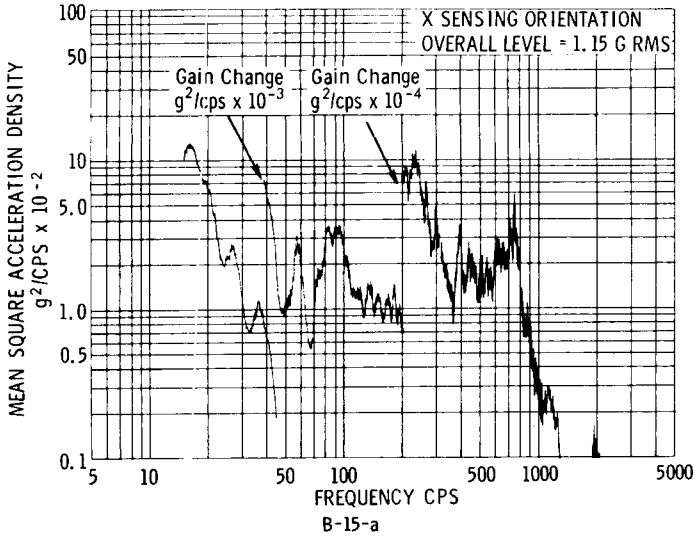

B-15-a

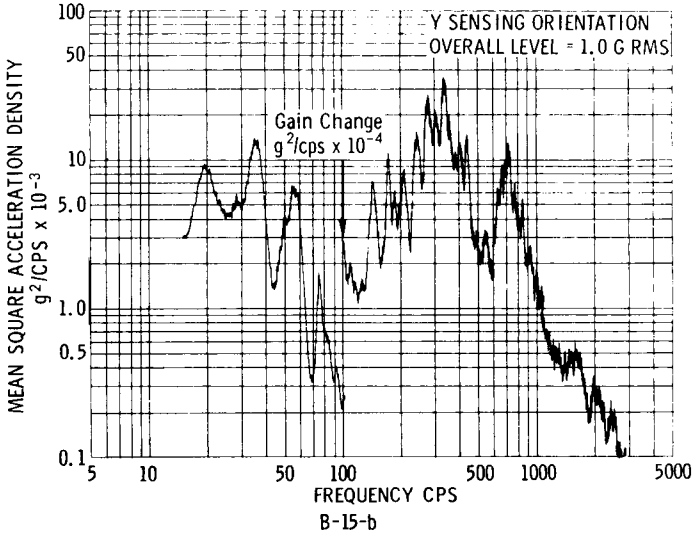

B-15-b

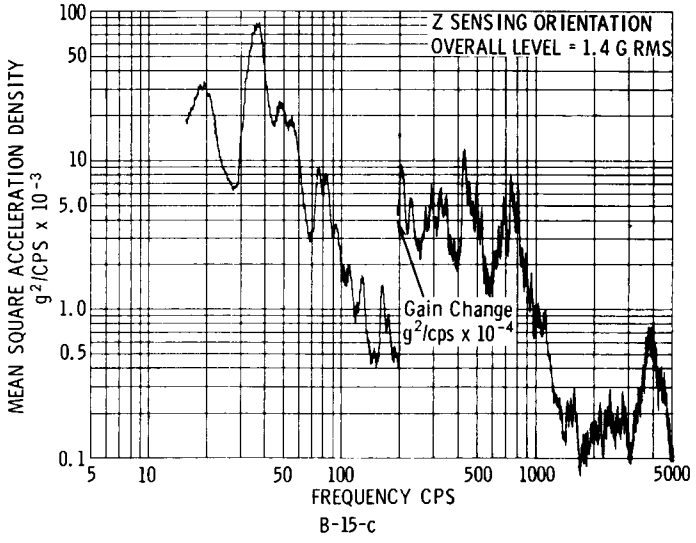

B-15-c

Figure B-15. Top of Folded EP-6 Boom

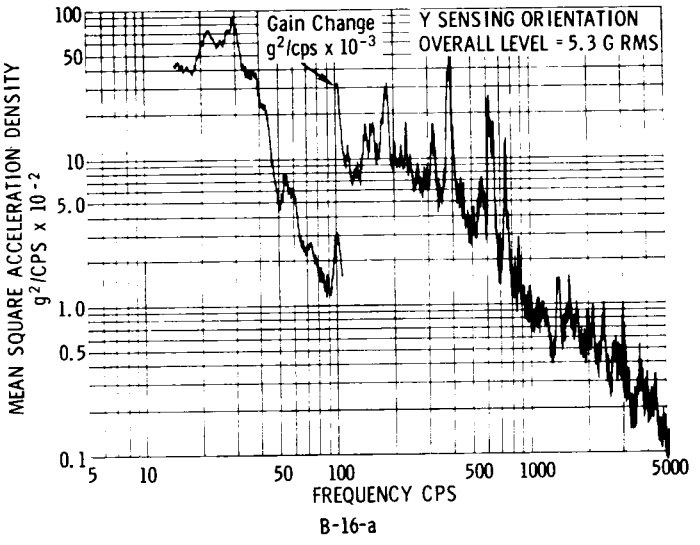

B-16-a

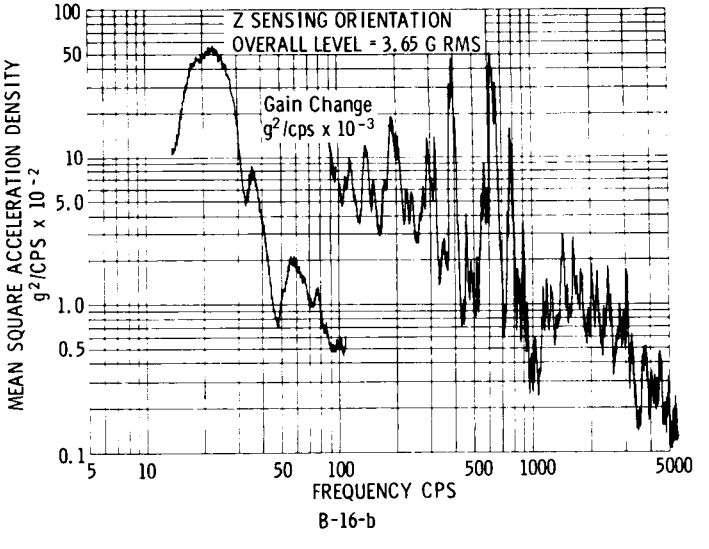

B-16-b

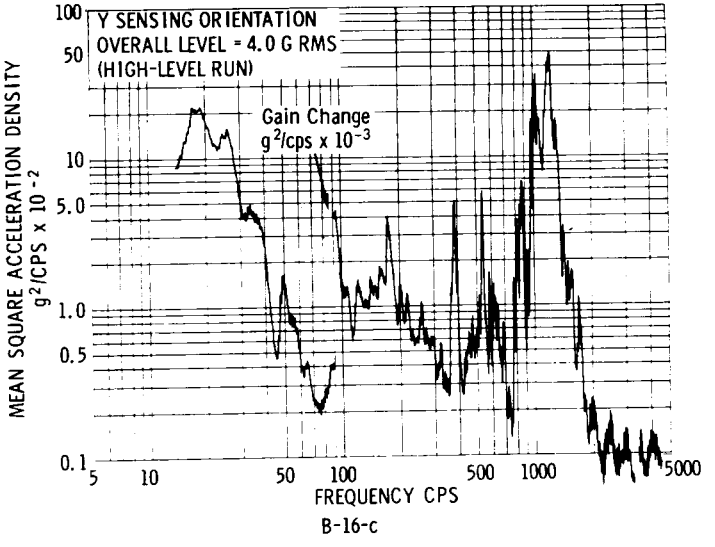

B-16-c

Figure B-16. Base of SOEP-1 Box

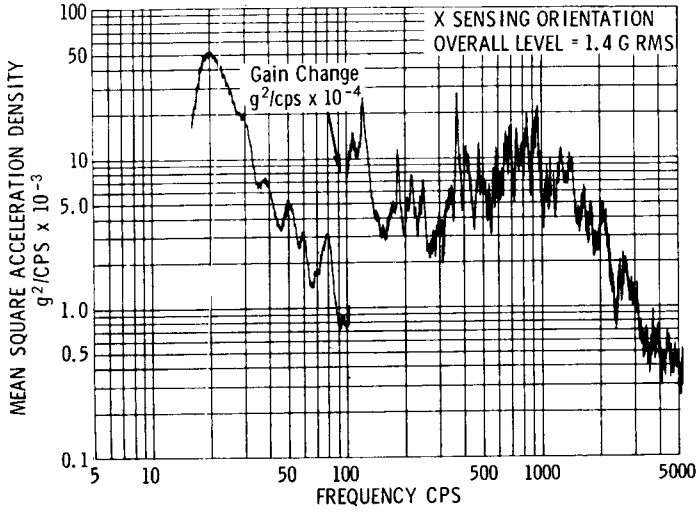

B-17-a

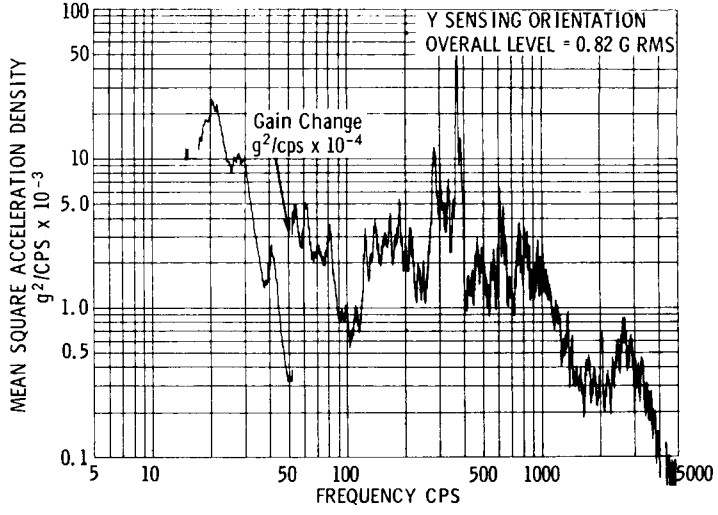

B-17-b

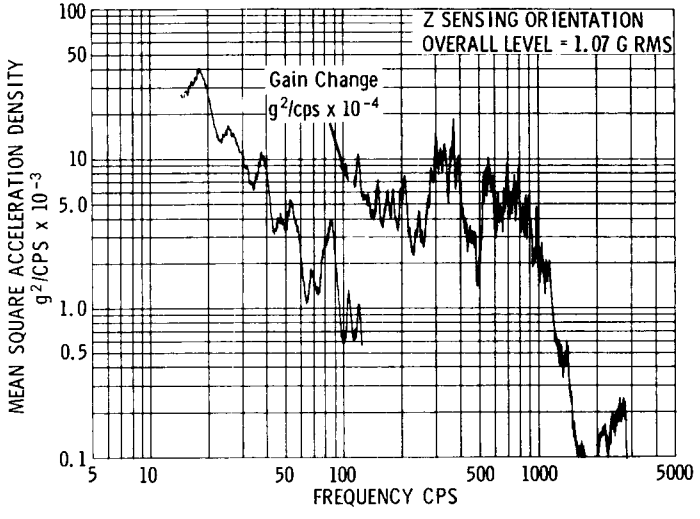

B-17-c

Figure B-17. Deployment Hinge on Solar Panel (SOEP-1)

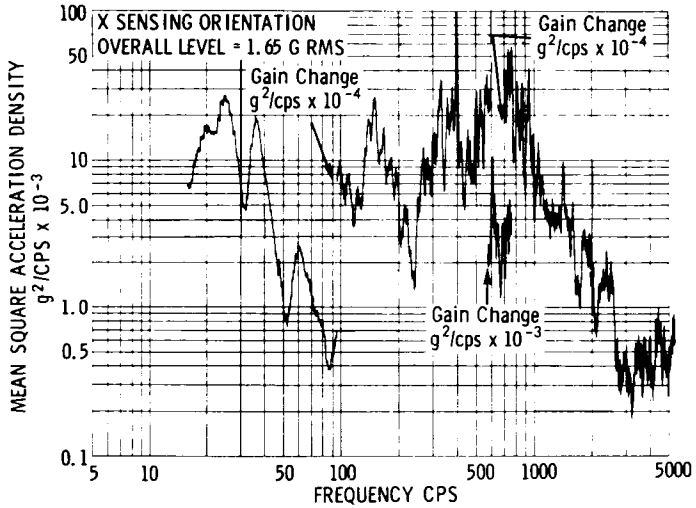

B-18-a

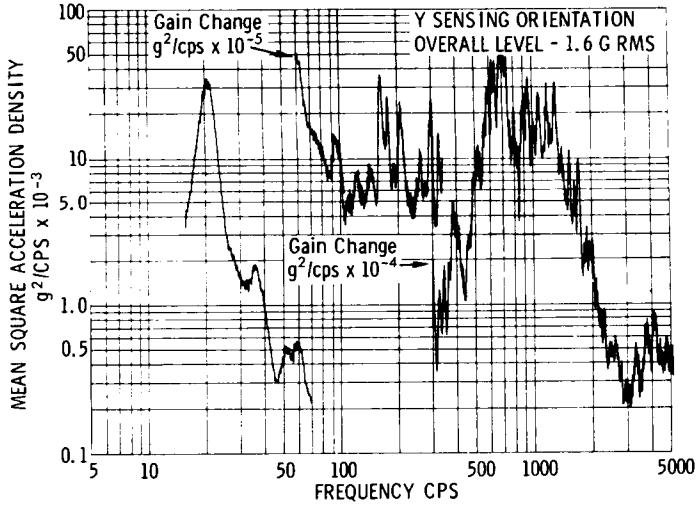

B-18-b

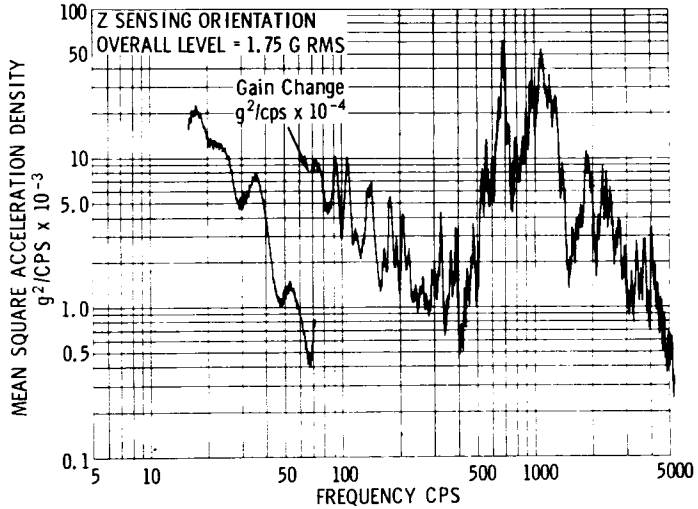

B-18-c

Figure B-18. Top Hinge on Main SOEP-1 Panel

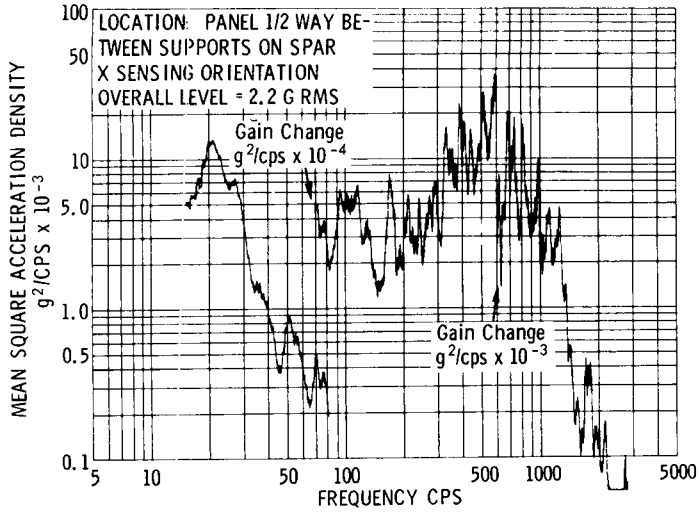

B-19-a

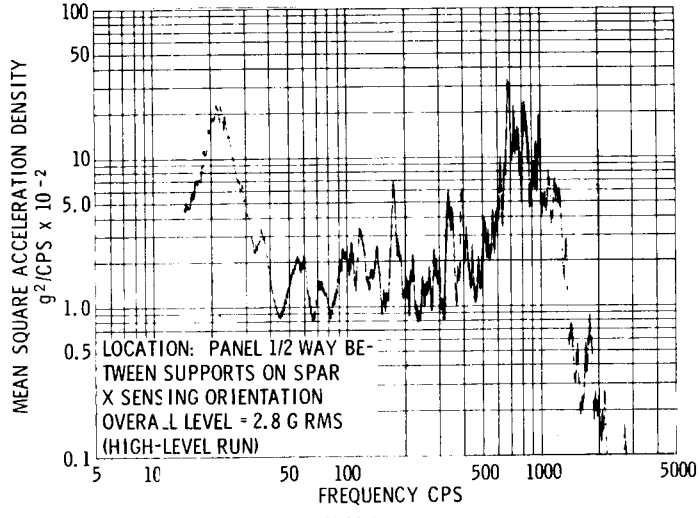

B-19-b

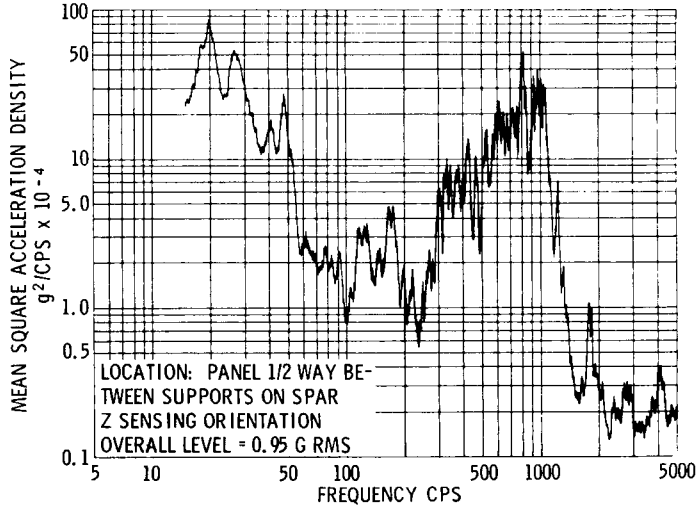

B-19-c

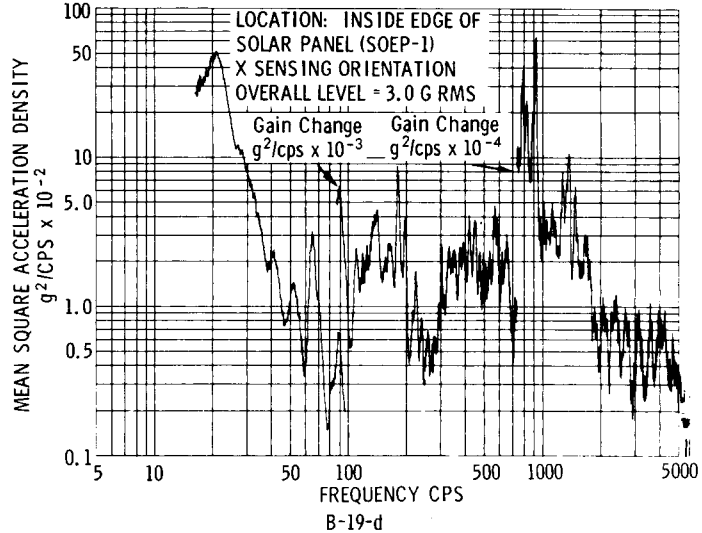

B-19-d

Figure B-19. Solar Panel (SOEP-1)

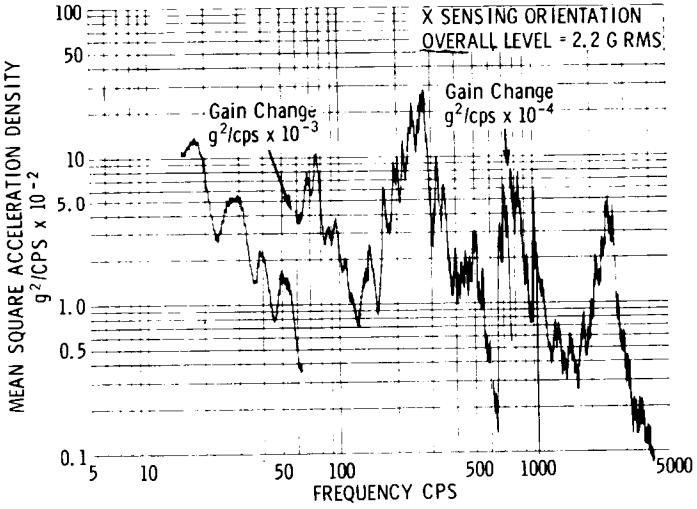

B-20-a

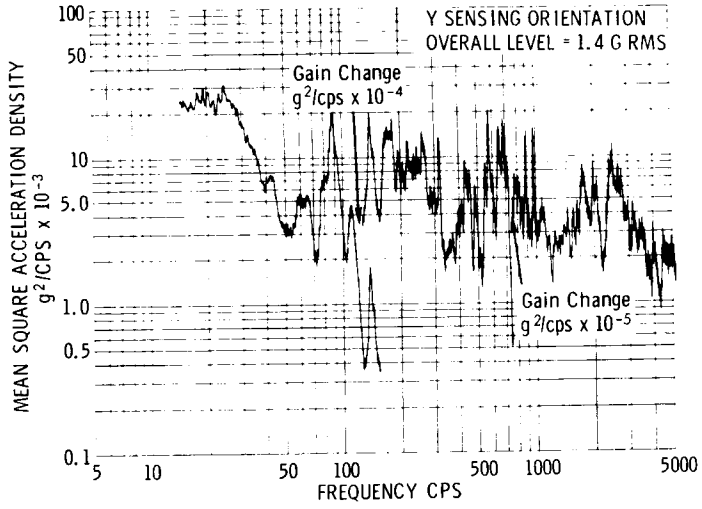

B-20-b

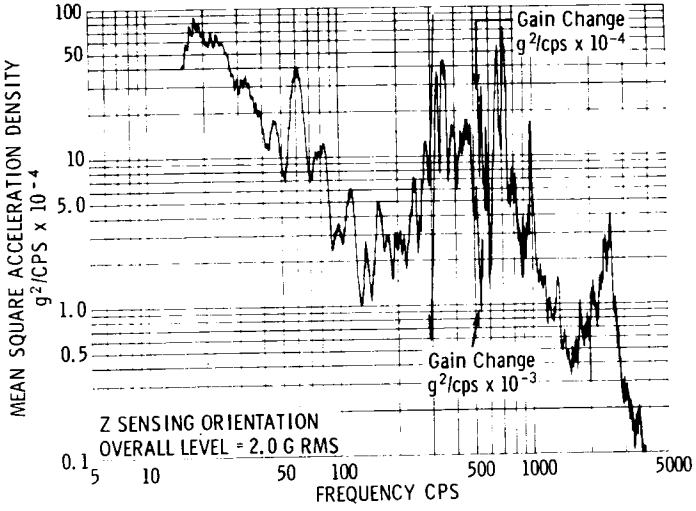

B-20-c

Figure 20. Base of Opep-1 Box

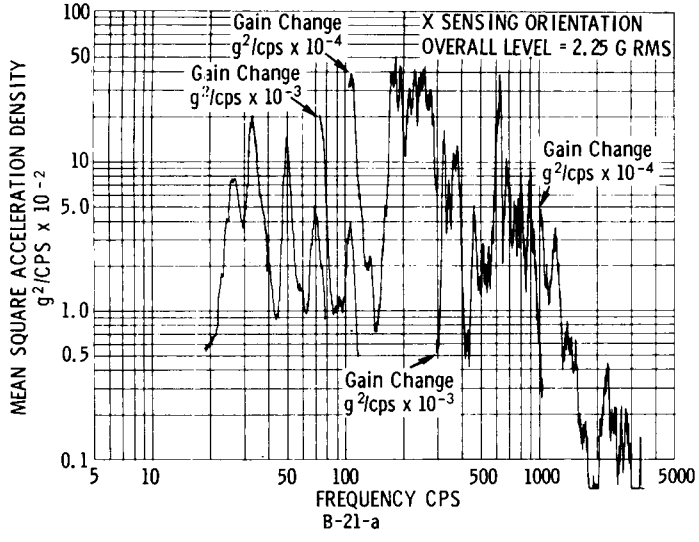

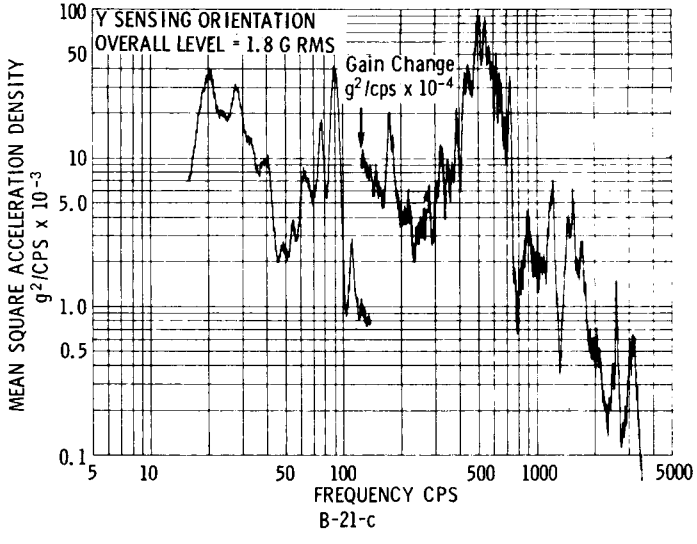

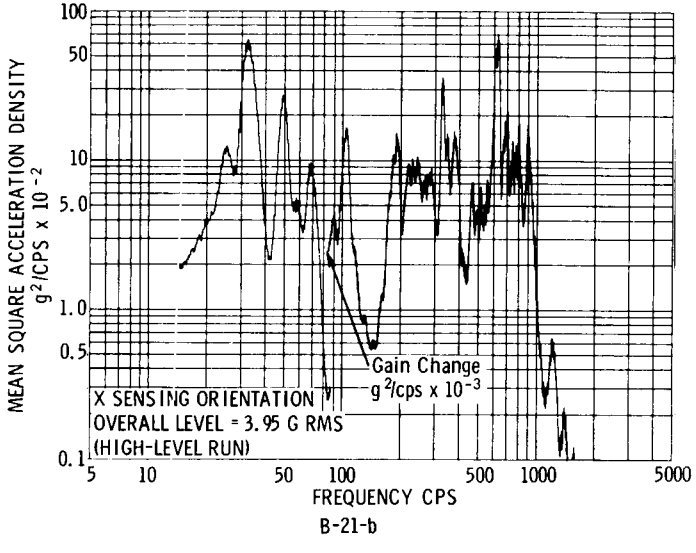

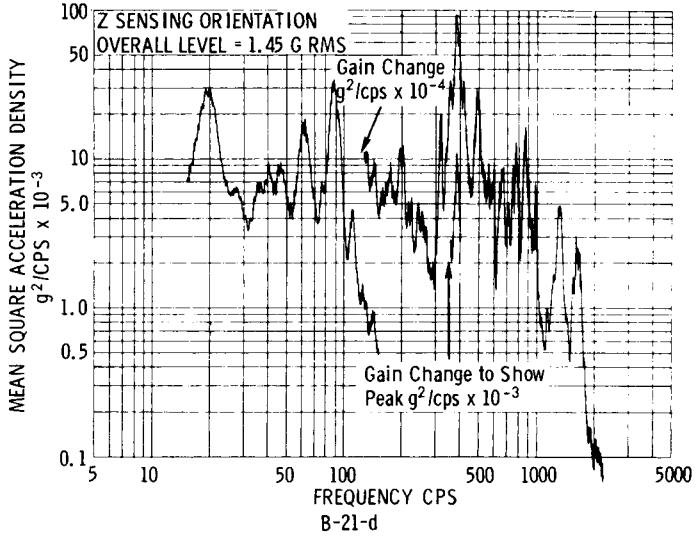

Figure B-21. Deployment Hinge OPEP-1

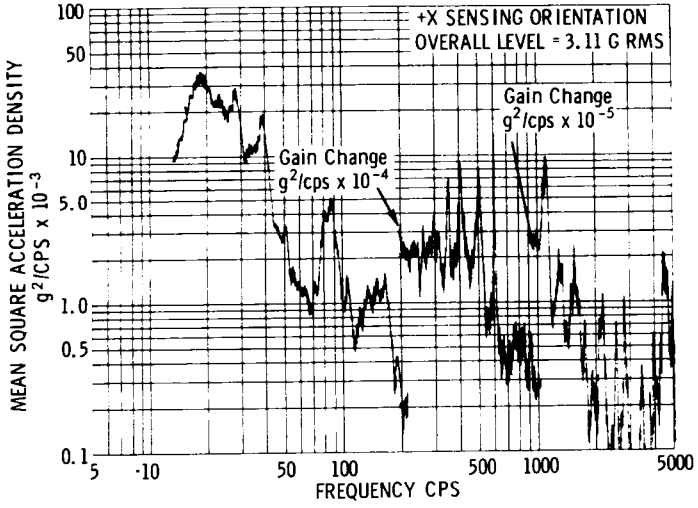

B-22-a

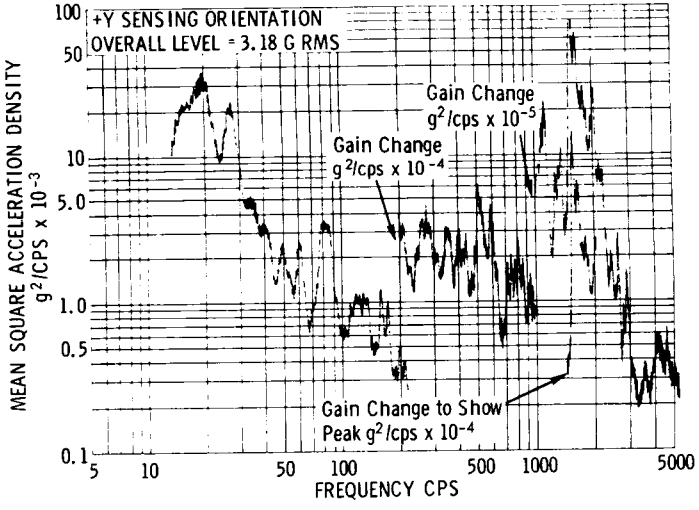

B-22-b

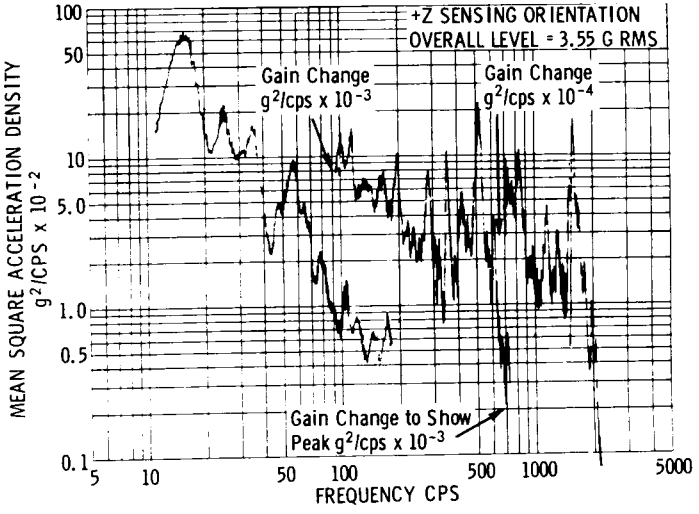

B-22-c

Figure B-22. Horizon Scanner

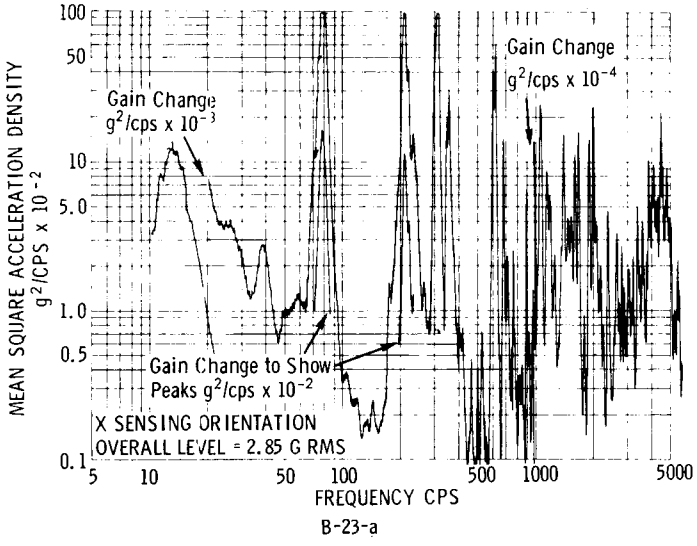

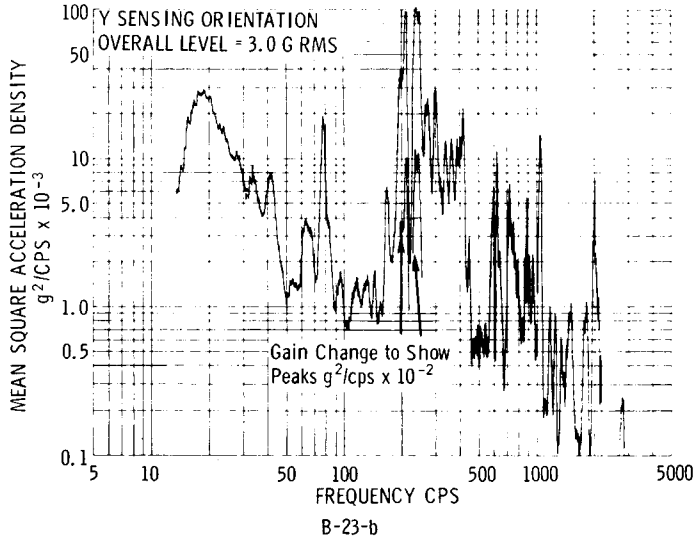

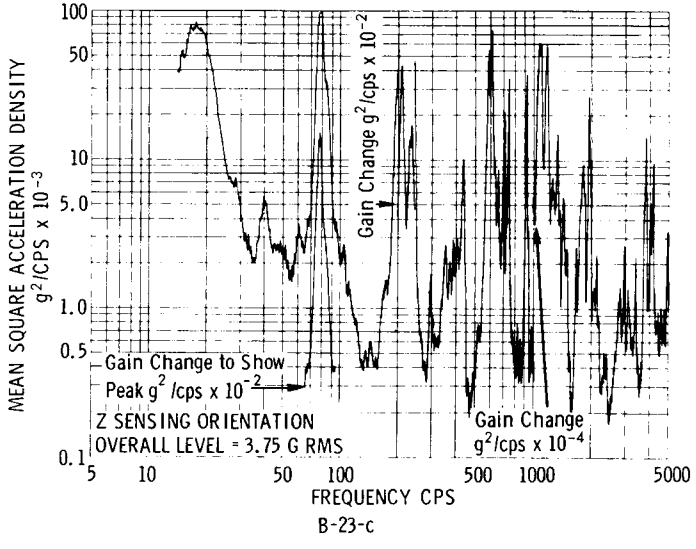

Figure B-23. One-Third Way Up –Z Gas Boom

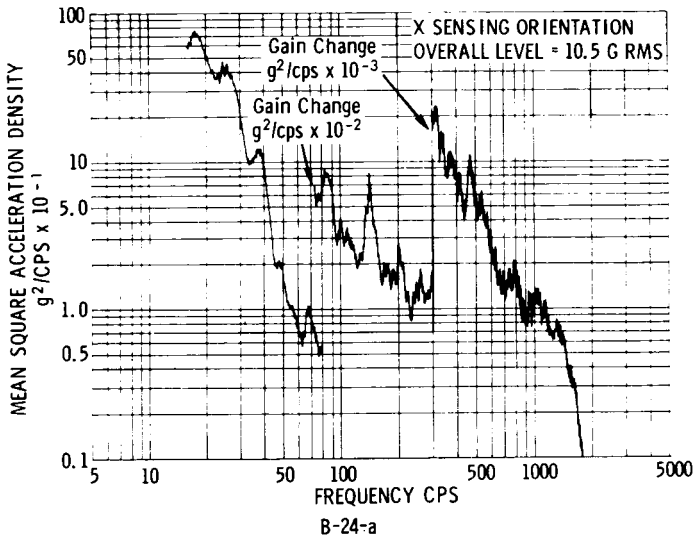

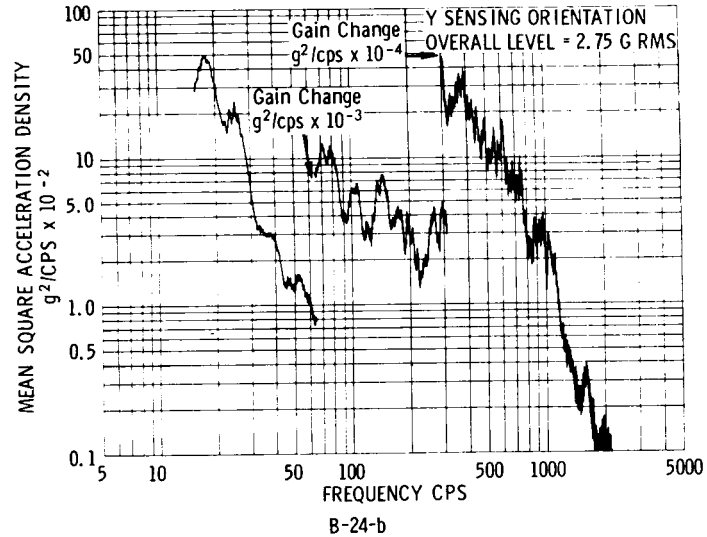

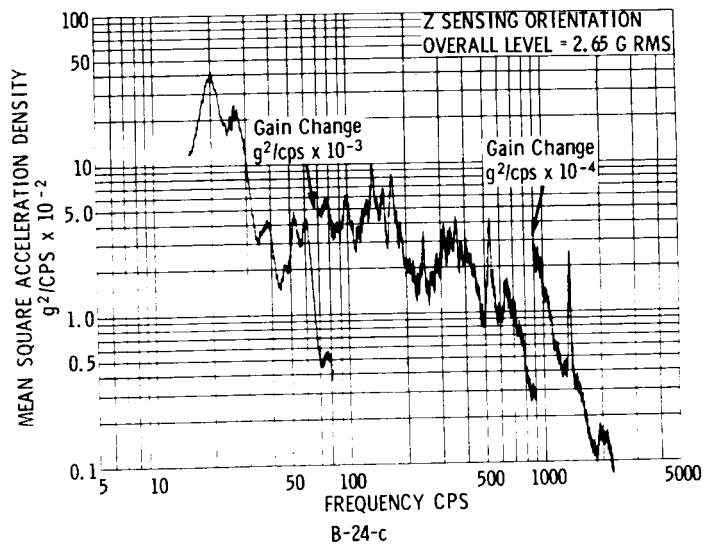

Figure B-24. –Z Side Intercoastal Panel, Location C

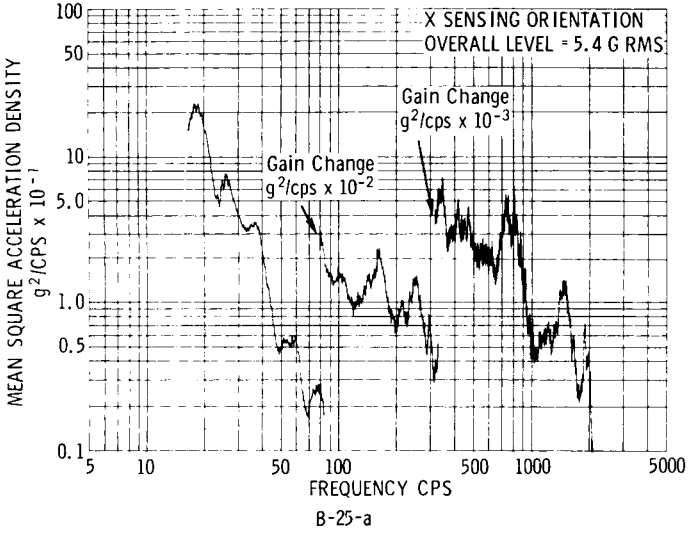

B-25-a

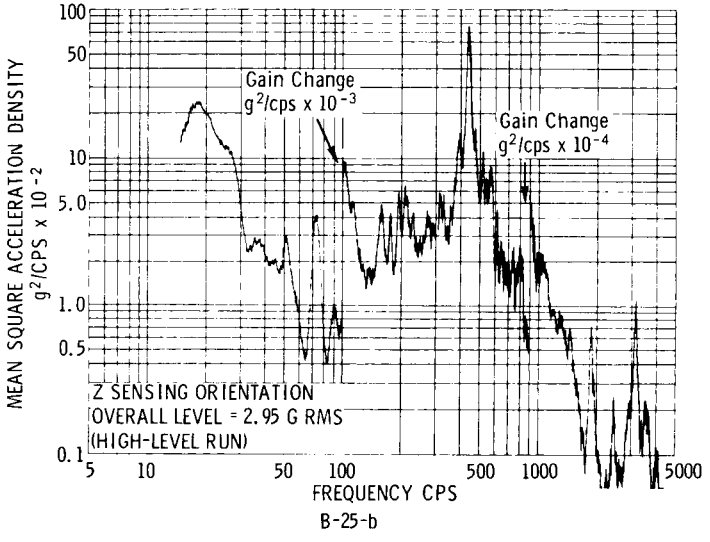

B-25-b

Figure B-25. STL Test Plan, Location D

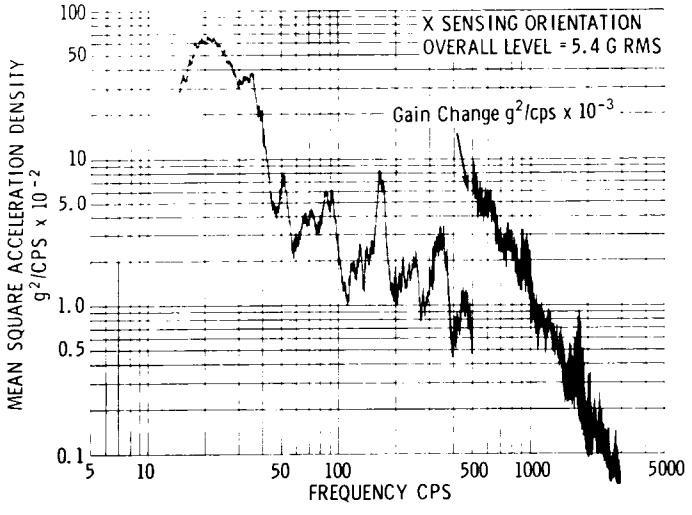

B-26-a

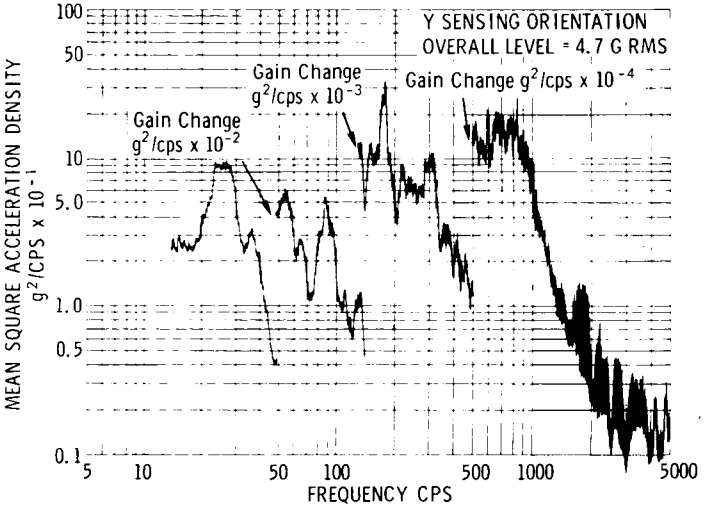

B-26-b

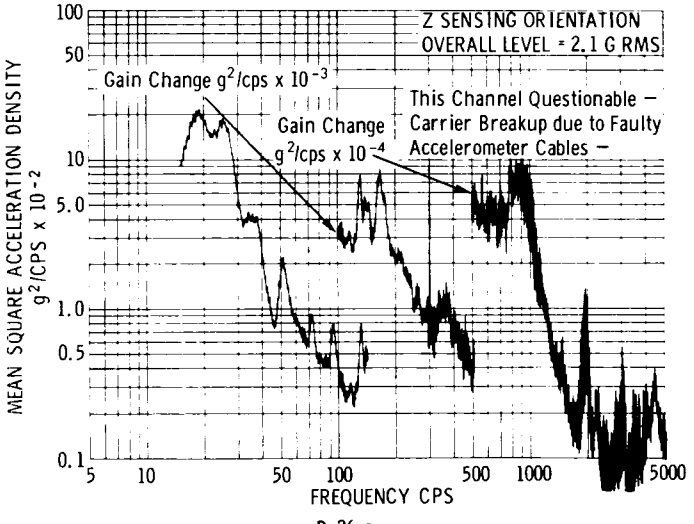

B-26-c

Figure B-26. Test Plan, Location E

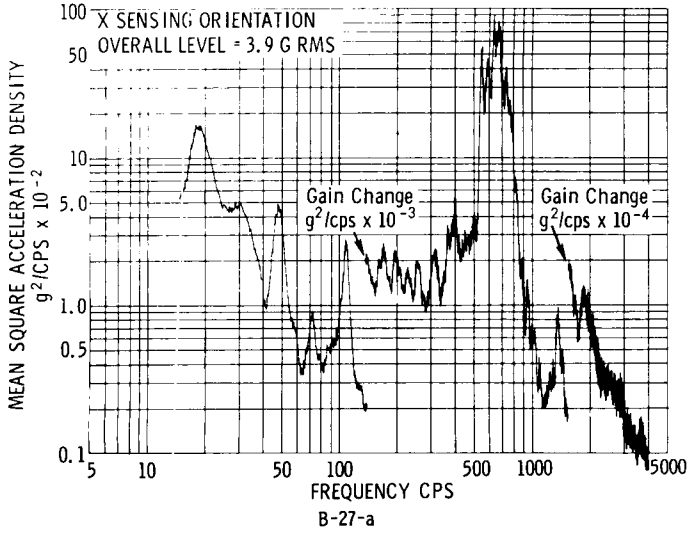

B-27-a

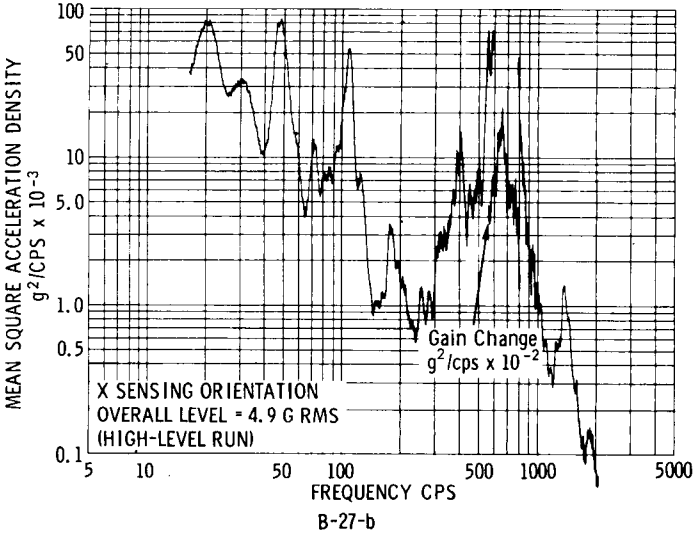

B-27-b

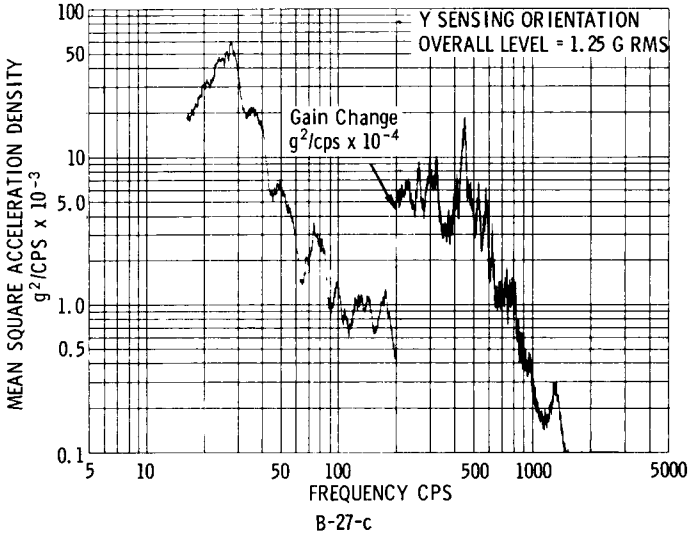

B-27-c

Figure B-27. STL Test Plan, Location G

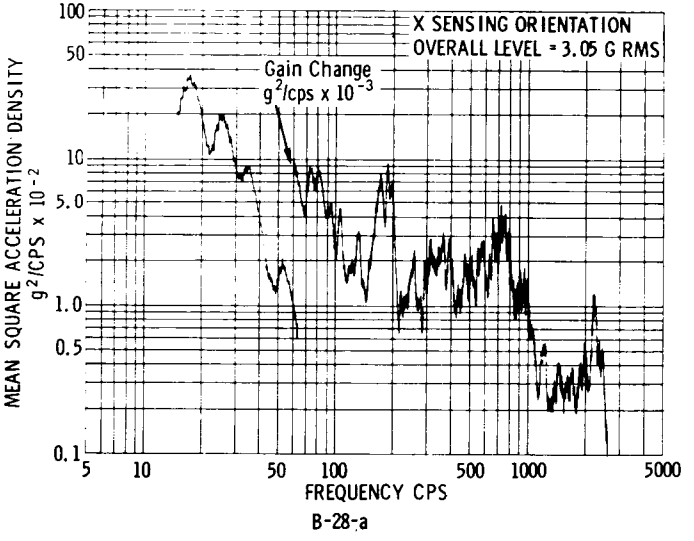

B-28-a

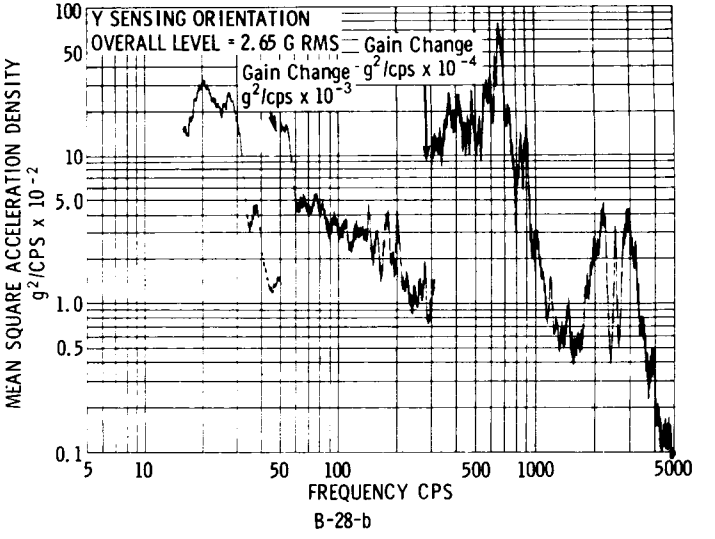

B-28-b

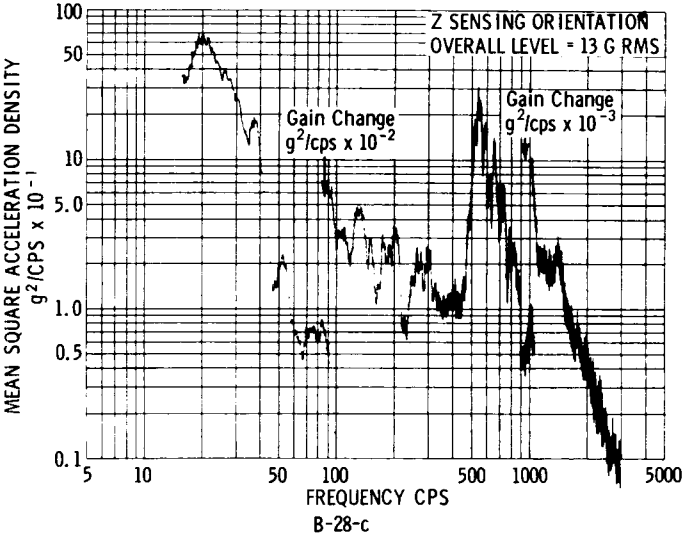

B-28-c

Figure B-28. –Z Subsystem Panel, Location I

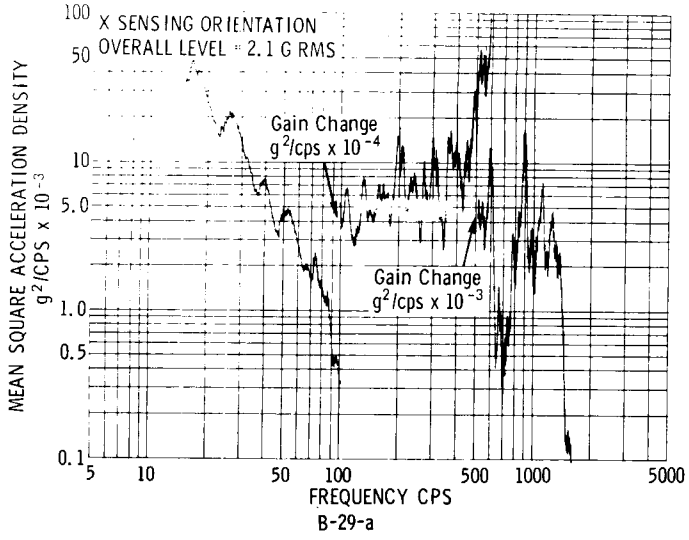

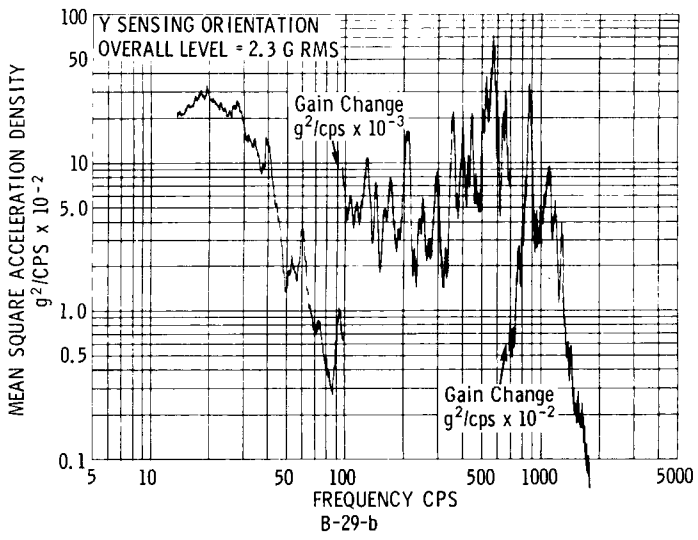

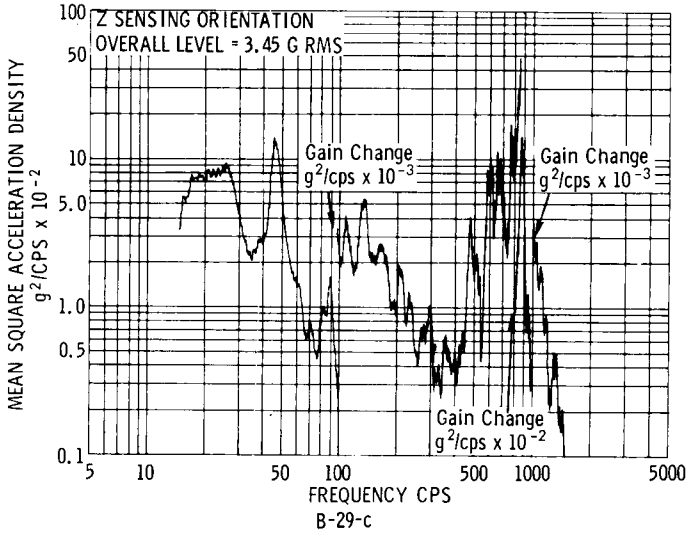

Figure B-29. +Z Experiment Panel, Location J

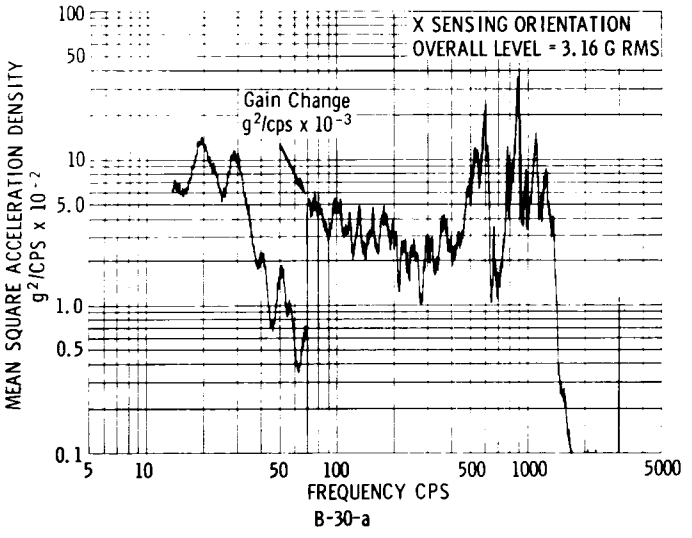

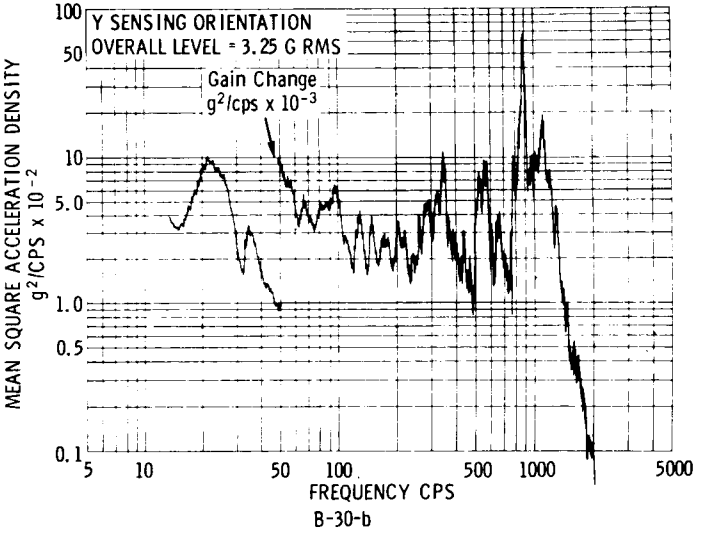

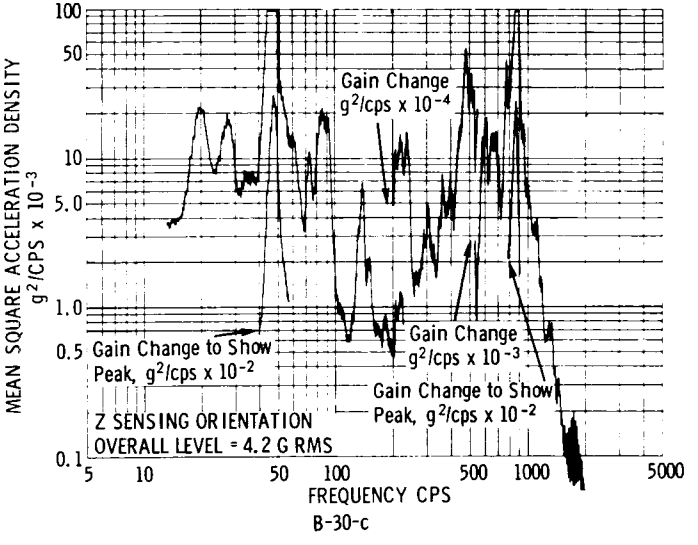

Figure B-30. High-Level Run on +Z Experiment Panel, Location J

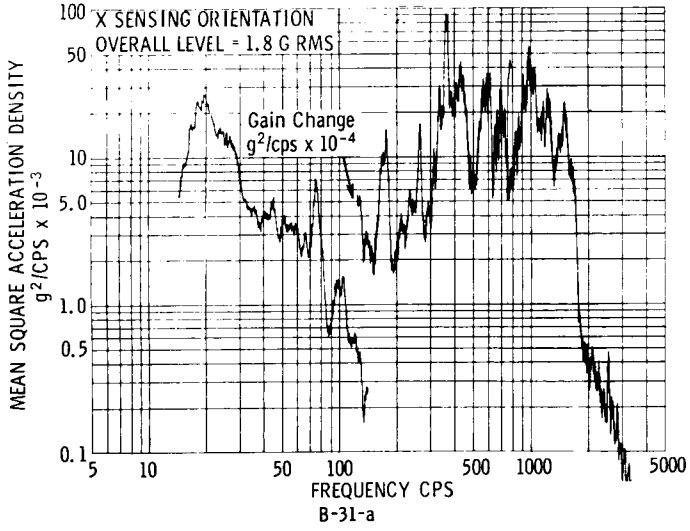

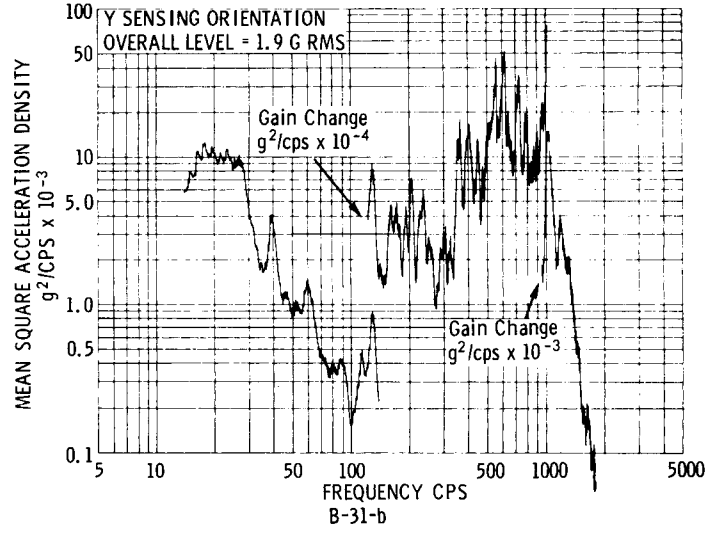

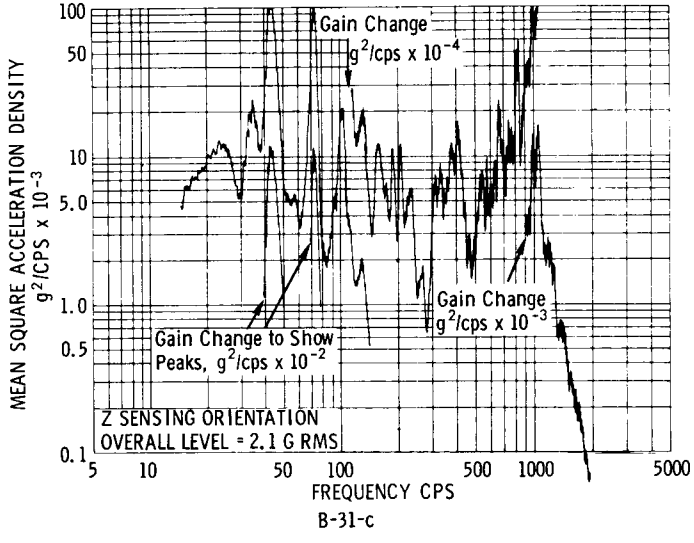

Figure B-31. +Z Experiment Panel, Location K

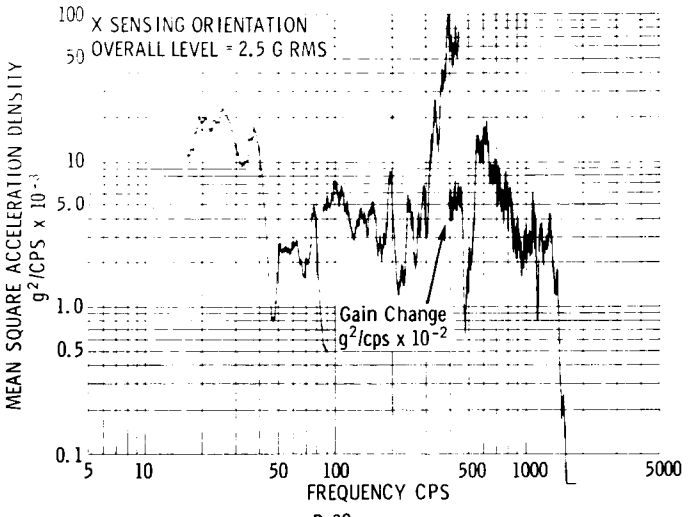

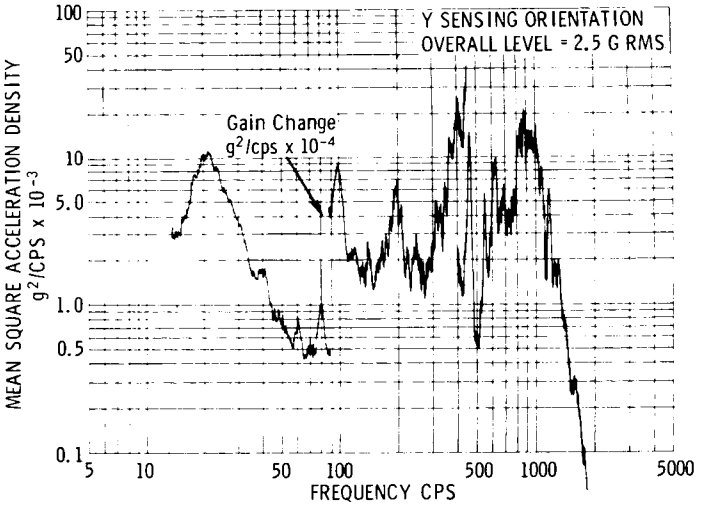

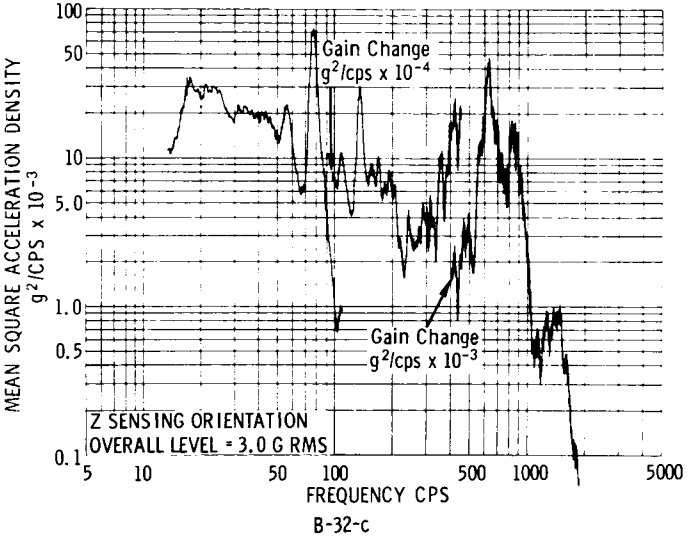

Figure B-32. –Z Experiment Panel, Location L

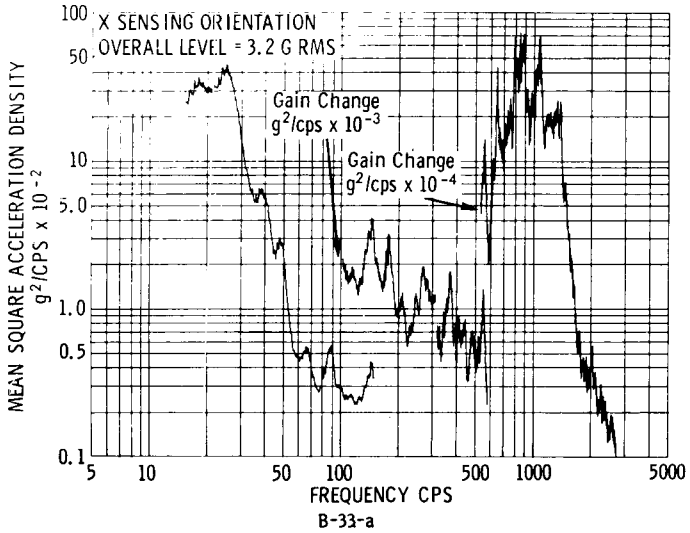

B-33-a

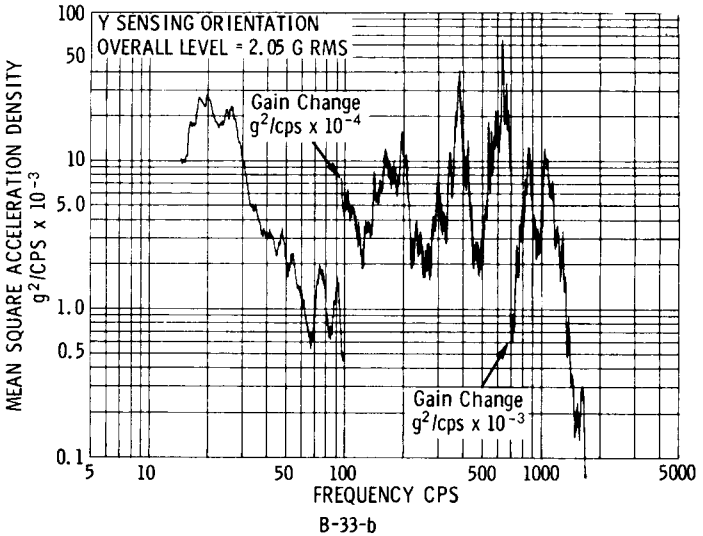

B-33-b

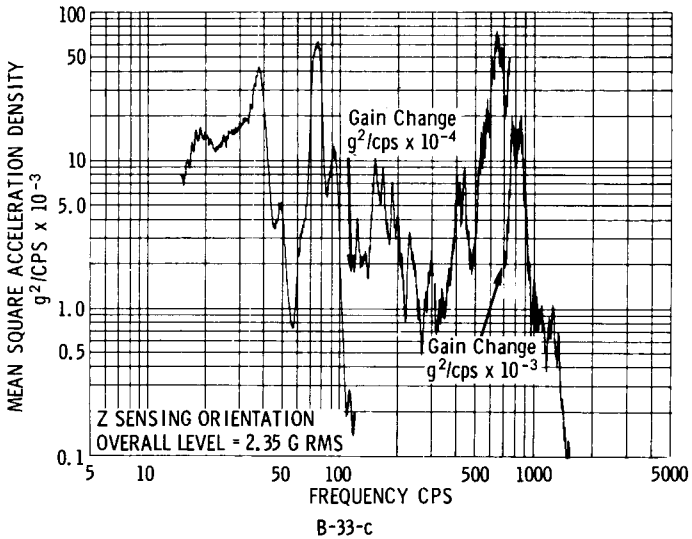

B-33-c

Figure B-33. –Z Experiment Panel, Location M

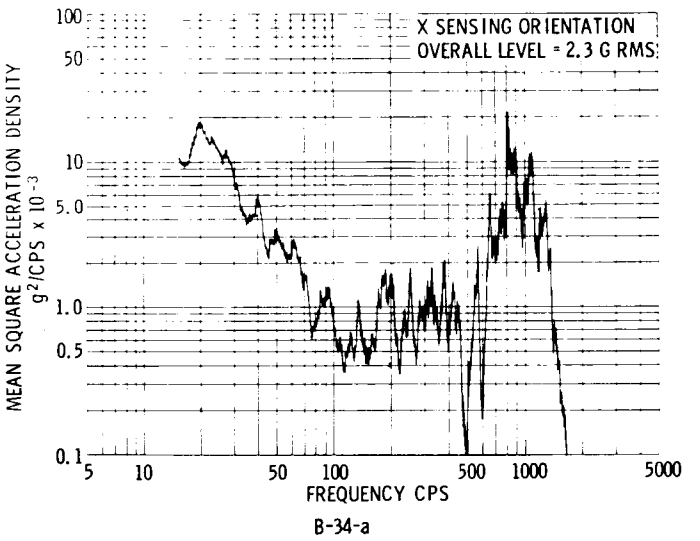

B-34-a

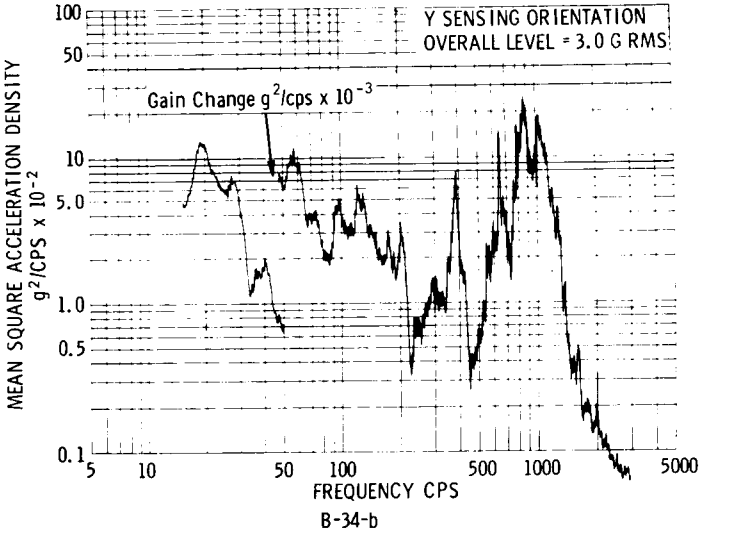

B-34-b

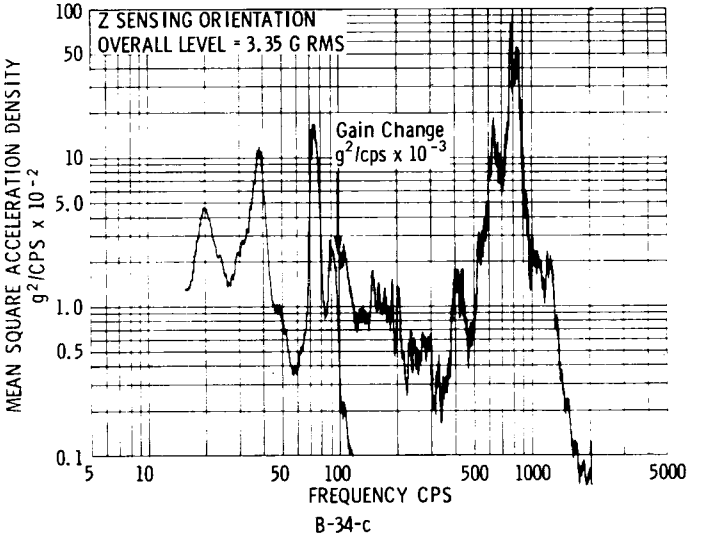

B-34-c

Figure B-34. High-Level Run on –Z Experiment Panel, Location M

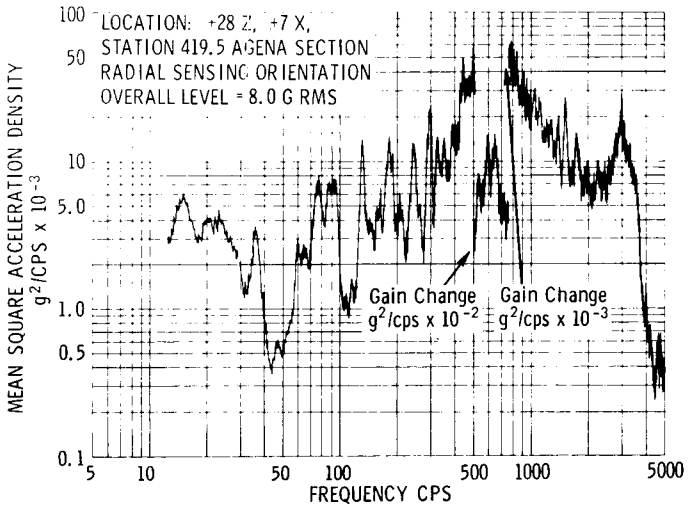

B-35-a

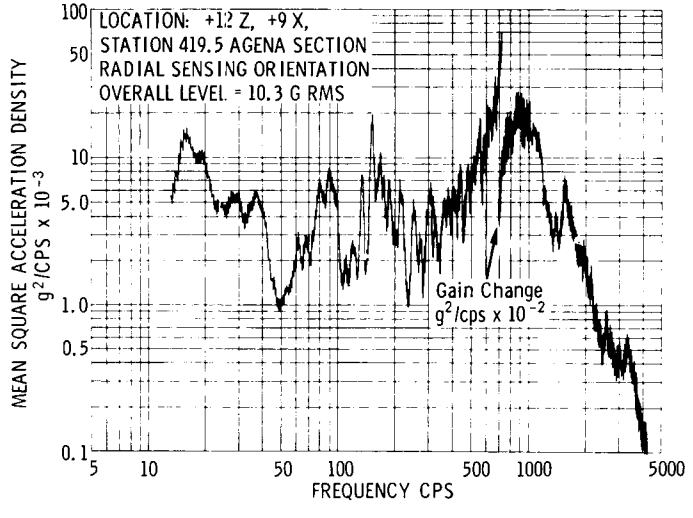

B-35-b

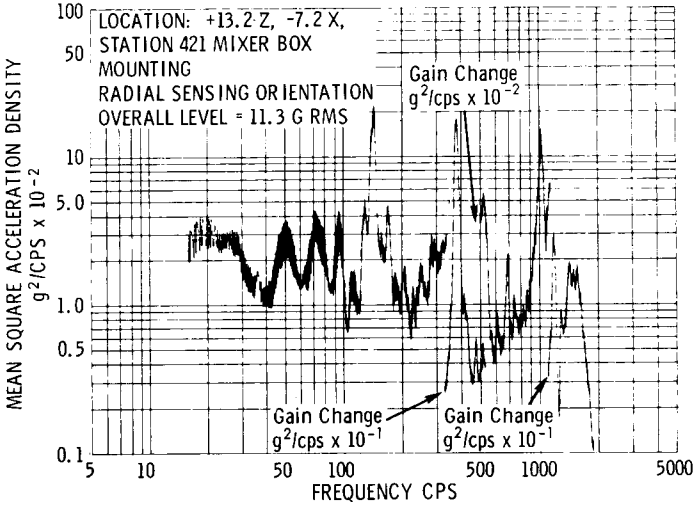

B-35-c

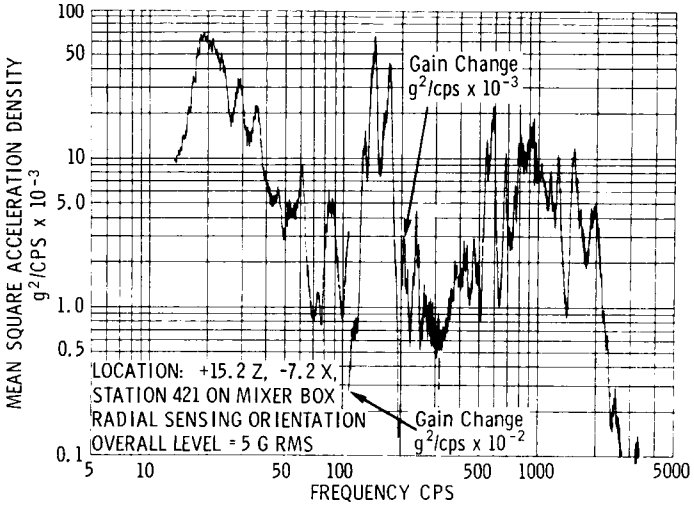

B-35-d

Figure B-35. Agena Sections and Mixer Box

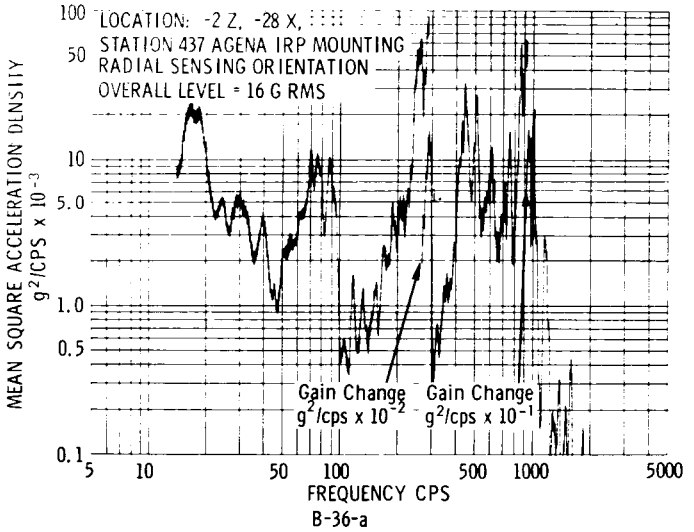

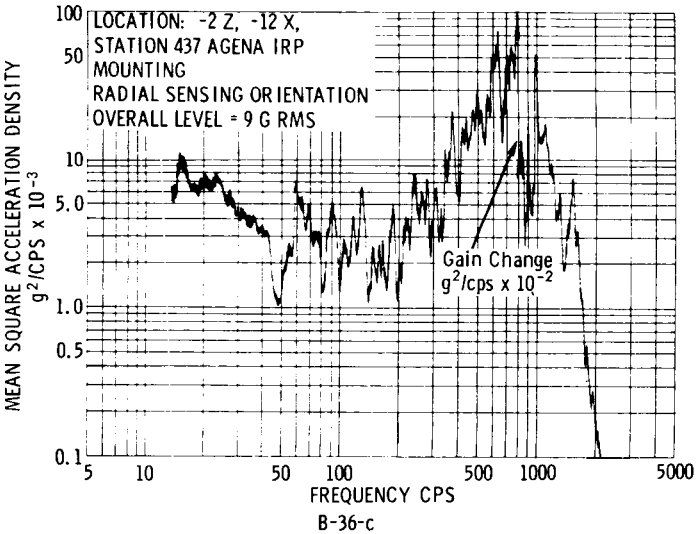

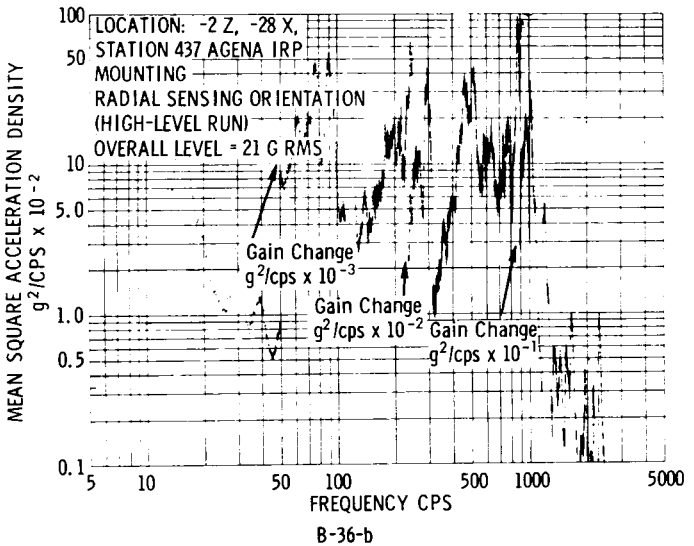

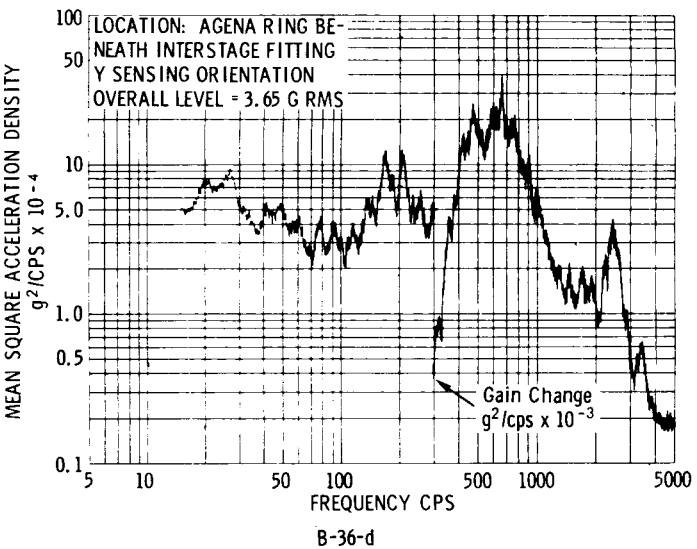

Figure B-36. Agena IRP Mounting and Ring Beneath Interstage Fitting

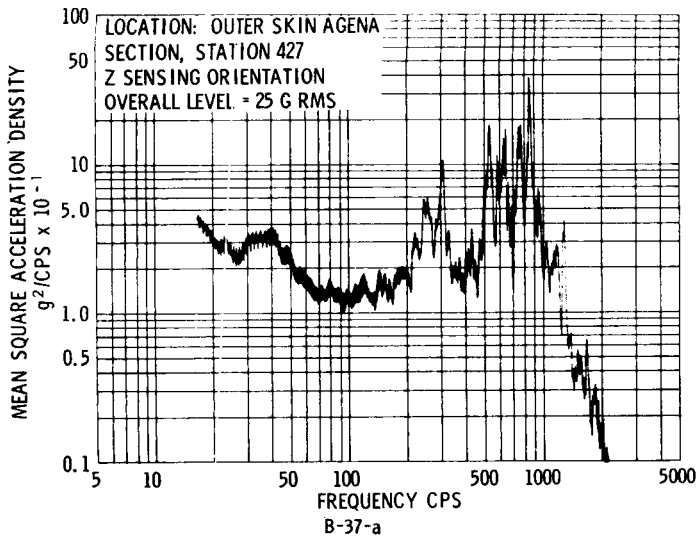

B-37-a

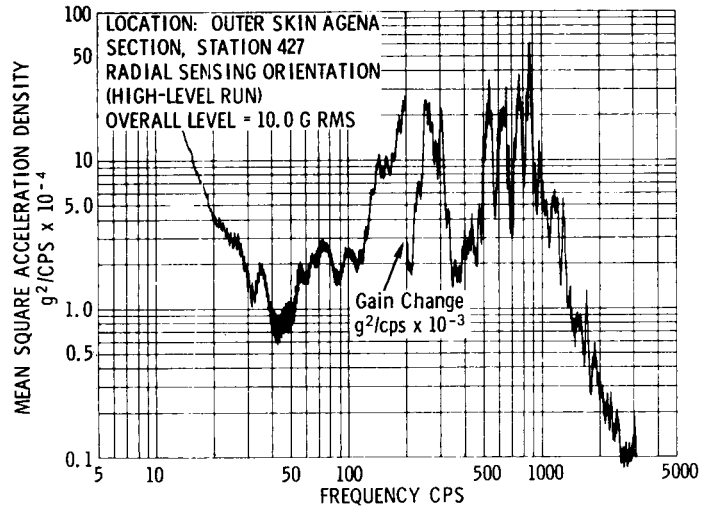

B-37-b

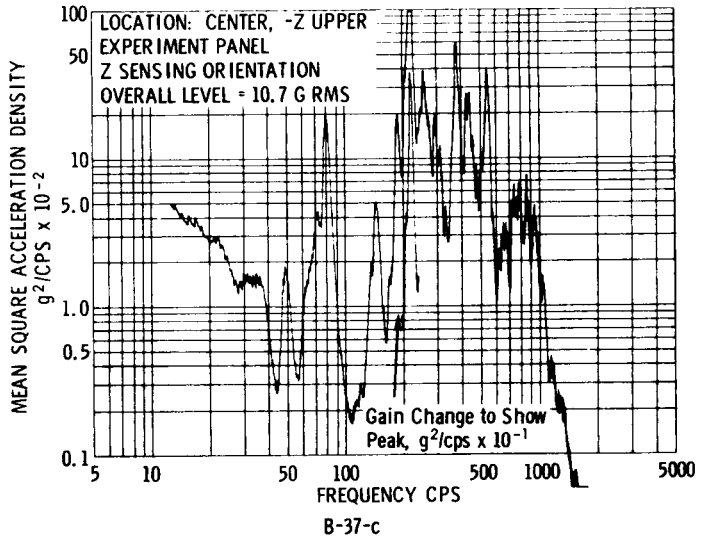

B-37-c

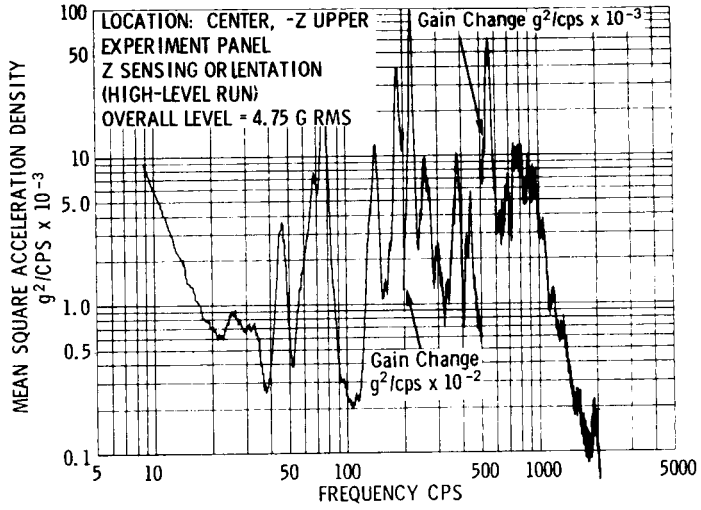

B-37-d

Figure B-37. Agena Outer Skin and –Z Upper Experiment Panel